MICROFLUIDICS-BASED MICROGEL SYNTHESIS FOR IMMUNOISOLATION AND IMMUNOMODULATION IN PANCREATIC ISLET TRANSPLANTATION

A Thesis
Presented to
The Academic Faculty

By

Devon Headen

In Partial Fulfillment
Of the Requirements for the Degree
Doctor of Philosophy in Bioengineering

Georgia Institute of Technology

May 2017

MICROFLUIDICS-BASED MICROGEL SYNTHESIS FOR IMMUNOISOLATION AND IMMUNOMODULATION IN PANCREATIC ISLET TRANSPLANTATION

Andrés García
Woodruff School of Mechanical Engineering
Petit Institute for Bioengineering and Bioscience
Georgia Institute of Technology

Peter Thulé
Department of Medicine
Emory University

W Robert Taylor
Department of Medicine
Emory University

Hang Lu
Chemical and Biomolecular Engineering
Georgia Institute of Technology

Krishnendu Roy
Coulter Department of Biomedical Engineering
Georgia Institute of Technology

Date approved: February 1, 2017

ACKNOWLEDGEMENTS

Foremostly, I must thank Dr. Andrés García for enabling any good science contained here. I always felt like I could try any crazy idea I had, and when I did, the resources I needed for those ideas were always close at hand: top notch training, reagents, connections, and equipment. But what makes you such a great manager is that you are a mentor first. The resources that I needed to develop professionally and as a scientist were also close at hand: advice, conference travel, even time off for a last minute internship at an inconvenient time. I am grateful for what you have allowed and empowered me to achieve, and I am humbled by your influence, knowing that I am only one of many people that feel the same.

Also, critical to this work was Dr. Jessica Weaver. Your expertise in islet research is impressive, and without it my PhD would have taken much longer. Thank you for shouldering a majority of the in vivo workload. We have had an enjoyable and productive collaboration, and I will miss days in the PRL that go smoothly without a word spoken about what is needed.

Next I would like to thank my thesis committee for their contributions to the evolution of this project. Dr. Hang Lu, not only was the microfluidic platform shown here a direct result of collaboration with Guillaume Aubry in your lab, but your microfluidics class was an extremely valuable practice in rough estimation that made me a better engineer. Dr. W. Robert Taylor, the parallelization of

encapsulation shown in Chapter 5 was a direct result of trying to make one of your crazy ideas work, and I still think we can make it happen. Thanks for giving me a challenge, and for providing unpredictable but always productive afternoons at T3 Labs. Dr. Peter Thulé, your outside perspective is always appreciated. Dr. Krish Roy, even though you have only seen my project discussed once, thank you for serving on my committee. I look forward to hearing your comments.

I would also like to thank past and present lairmates, not only for their creative ideas and advice on practical lab matters, but also for happy hour companionship. It does not suck to work with your friends every day. Ted Lee, Ed Phelps, Ashley Allen, Amy Clark, Jose Garcia, Efraín Cermeño, Brennan Torstrick, and Albert Cheng have been particularly helpful, enabling my success whenever possible and keeping my mental health in check, but the lair is crawling with quality people.

I have to acknowledge the IBB staff, PRL staff, and cleanroom staff as well. None of this research would be feasible without the outstanding facilities at Georgia Tech. Particularly, I have to thank Laura Paige for always making things I think will be a headache very easy. Your positive attitude is contagious.

I would also like to thank all my friends in Atlanta for nodding and smiling when I needed to vent about science, even if we were riding bikes in the woods so I could forget about science.

Finally I would like to thank my family for their support during this endeavor. Mom, thanks for always enabling my curiosity, even when it was annoying.

TABLE OF CONTENTS

LIST OF TABLES

LIST OF FIGURES

Figure 15. Viability, apoptosis and functional data are shown for rat islets after being cultured for 6 days encapsulated in bulk PEG-4MAL hydrogels, which were functionalized with RGD or RDG (non-adhesive scrambled peptide), and crosslinked either entirely with PEG-dithiol (PEG-DT) (nondegradable) or with ½ PEG-DT and ½ VPM (degradable peptide). Notably, the nondegradable crosslinker used is not DTT as used in previous experiments presented. Bare (unencapsulated) and alginate bulk gel controls are also included for comparison. (A) Representative live/dead images of islets which had been stained with calcein AM (green) and TOTO-3 iodide (cyan) are shown, along with images showing 2 markers of apoptosis: caspase 3,7 activation (CellEvent, green on transmitted light image) and DNA fragmentation (TUNEL, green and DAPI, blue). (B,C) Bulk alginate hydrogels and PEG-4MAL gels functionalized with RGD supported similar islet glucose stimulated insulin secretion, whether degradable peptide crosslinks were included or not when PEG-DT was used as the non-degradable component of crosslinker. All groups were glucose responsive (GSI>1) on day 6 after encapsulation, but islets in hydrogels functionalized with non-adhesive RDG had notably impaired function. Unencapsulated islet controls had improved glucose responsiveness and insulin secretion compared to any treatment groups tested. (n=4, 150 IEQ each). 79

SUMMARY

Encapsulation of islets in hydrogel microspheres (microgels) before transplantation into diabetic recipients can establish an adequate immuno-isolation barrier to mitigate allogeneic rejection. The synthetic hydrogel macromer PEG-4MAL (4-arm polyethylene glycol terminated with maleimides) is an ideal candidate polymer for immunoisolation applications, since it can be easily modified with thiolated bioactive molecules, allowing precise control of islet microenvironment. Alginate microencapsulation dominates in literature even though alginate provides limited control of islet microenvironment, because no technique exists for islet encapsulation in synthetic microgels. Therefore, a microfluidic platform for the encapsulation of islets in size-controlled PEG-4MAL microgels was developed, and hydrogel composition was optimized to support encapsulated islet function. Islets microencapsulated in optimized PEG-4MAL restored glycemic control better than islets microencapsulated in alginate and equally as well as unencapsulated islets when delivered to epididymal fat pads in diabetic syngeneic mice within bulk vasculogenic hydrogels. Improved function was partially attributed to decreased microgel size vs. alginate, and therefore reduced diffusional barrier. Immuno-isolation potential of this strategy is currently

being investigated in allogeneic recipients. In a separate scheme, PEG-4MAL microgels were designed which could capture and display the chimeric immunomodulatory protein SA-FasL in its bioactive form. Simple cotransplantation of SA-FasL presenting microgels with unmodified allogeneic islets under the kidney capsule of diabetic mice resulted in long term graft acceptance without long term immunosuppression. Regulatory T cells mediated this acceptance since their ablation on day 50 post-transplantation prompted rapid graft rejection. Effective control or mitigation of immune responses is critical for successful outcomes in islet transplantation, and this work presents the development of two novel strategies for achieving long term function of allogeneic islet grafts.

CHAPTER 1: INTRODUCTION

1.1 Type 1 Diabetes

Type 1 Diabetes (T1D) affects between 11-22 million people worldwide [1], and its incidence has been increasing at a rate of 3% per year [2, 3]. T1D is often referred to as juvenile diabetes because onset frequently occurs during childhood, and there was a dramatic 21% increase in prevalence from 2001-2009 in US youths under 20 [4]. Annual healthcare costs associated with T1D exceed $14 billion dollars per year in the United States alone [5]. The disease is characterized by persistent hyperglycemia due to loss of pancreatic β cells, cells that release insulin to control blood glucose and are located in the islets of Langerhans (islets). Islets are polyhormonal organoids comprised of β cells along with several other important endocrine cell types, which are organized in spheroids of around 100 μm diameter and are distributed throughout the pancreas (Figure 1).

1.2 Current Treatments

1.2.1 Exogenous Insulin injections

Because endogenous insulin production is no longer sufficient to control blood glucose, standard therapy for T1D patients consists of daily injections of exogenous insulin. Recombinant protein technology enables highly engineered

insulin with improved safety and tunable absorption rates. However, manual exogenous insulin therapy is burdensome and often succeeds only in delaying the onset of morbidity, such as kidney disease and retinopathy, because of large fluctuations in blood glucose. Recent decades have seen decreases in mortality, due in large part to improved blood glucose sensors and protein engineering technologies [6]. However, dangerous, and potentially fatal, hypoglycemic states are possible when too much insulin is administered. Bolus delivery of insulin results in large blood glucose concentration fluctuations, even when slow absorbing insulins are used. Insulin pumps with transdermal catheters can provide a slow infusion of insulin, minimizing frequency of large fluctuations in blood glucose. Strategies to enforce closed loop control of blood glucose by integrating glucose sensor with insulin pumps are becoming practical, and a recent commercially available insulin pump has semi-autonomous insulin delivery capabilities when integrated with a compatible transdermal blood glucose monitor (Medtronic MiniMed). Any viable cure for T1D must include closed loop regulation of blood glucose to avoid hypoglycemic episodes and prevent wild fluctuations in glucose levels. Transdermal systems are often painful for patients and cannot recapitulate endogenous insulin response kinetics, but the closed-loop control they control can improve blood glucose control.

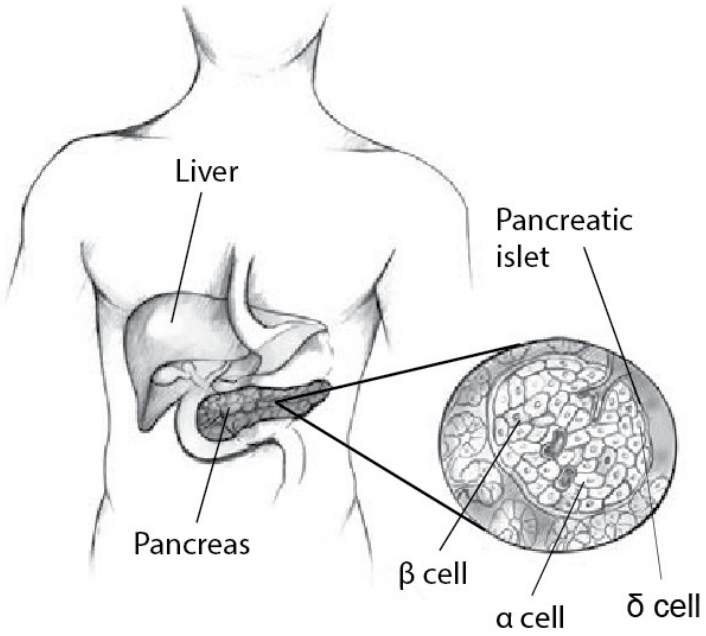

Figure 1. Pancreatic islets are endocrine organoids that regulate blood glucose by releasing insulin in the presence of glucose. Islets are composed of several cell types which are defined by the hormones they secrete, including insulin producing β cells, glucagon producing alpha cells, and somatostatin producing delta cells. Figure adapted from public domain material [7]

1.2.2 Transplantation

Transplantation of allogeneic islets can potentially provide such regulation, and can provide temporary independence from exogenous insulin therapy [8, 9]. In fact, both whole pancreata and purified islets have been transplanted to successfully reverse diabetes [10, 11]. While whole pancreas transplant is about as effective as islet transplant, limited supply of pancreata exclude this procedure as a widespread cure for diabetes.[12]

1.2.2.1 The Edmonton Protocol

The Edmonton Protocol [9], an optimized islet transplant procedure developed for humans, was put into use in 2000, and was the first demonstration of purified islets being used to reverse T1D in humans. In this procedure, islets isolated from multiple cadavers are infused into the liver through the hepatic portal vein, where they lodge and produce insulin in response to increasing blood glucose (Figure 2). This important proof of concept enabled seven patients to achieve 100% insulin independence initially. However, after 9 years, the same group had only 15% insulin independence, but 73% of transplanted subjects still had detectable C-peptide [13]. In a separate study of 36 patients that received islet transplants according to the Edmonton Protocol, 21 patients achieved insulin independence, and of these only 5 were still insulin independent after 2 years [13]. Although the optimized immunosuppressive prescribed by the Edmonton Protocol have resulted in little to no instance of opportunistic infections, cancer, or lymphoproliferative disease[13], long term immunosuppression does introduces a major source of potential morbidity for transplant recipients[14].

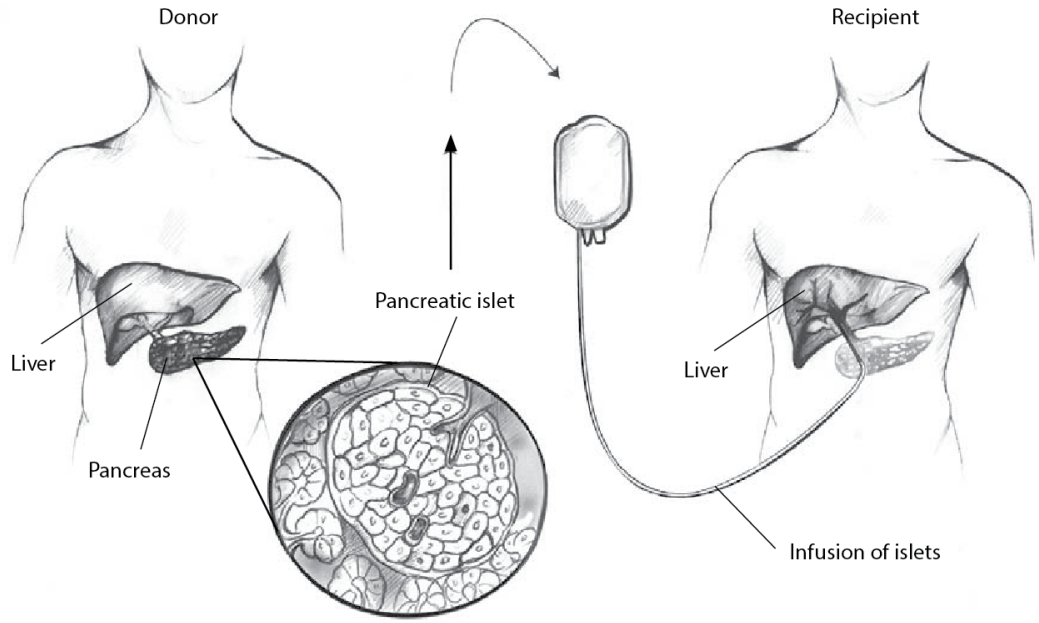

Figure 2. Schematic illustrating intra-hepatic islet transplantation in humans. Islets are purified from cadaveric pancreata and are infused into the hepatic portal drainage of recipients. Islets lodge in the liver and provide endocrine function. Figure adapted from public domain material [7].

1.2.2.2 Improved Protocols

Since the development of the Edmonton Protocol, intrahepatic transplantation of islets has expanded, with new protocols being developed, which overcome limitations of the Edmonton Protocol, particularly those associated with immunosuppression. Recently, the Collaborative Islet Transplant Registry released a report that compiled data from 864 islet allograft recipients

that received 1679 infusions of islets between 1999 and 2012. These data demonstrate a remarkable improvement in the rate of insulin independence of islet graft recipients during this period. Insulin independence after 3 years was 27% from 1999-2002, 37% from 2003-2006, and 44% from 2007-2010. Moreover, other indicators of islet graft function were better maintained in 2007-2010 when compared with earlier transplants, including resolution of severe hypoglycemic episodes, reduction of HbA1c, and stabilization of blood glucose [15]. Recent reports of successful transplantation from various European groups particularly demonstrate the efficacy of improvements over the Edmonton Protocol. In a study by the UK islet transplantation program, 80% of islet transplant recipients still maintained graft function after two years, and 70% maintained HbA1c less than 7% [16]. Even more excitingly, two other European studies reported insulin independence in 50% and 75% of patients a full 5 years after islet transplantation [17, 18]. The progress that has been made in improving islet transplantation in the last 15 years is due largely to improvements in both induction and maintenance immunosuppressive regimens, which improve islet engraftment and viability, both by possessing lower toxicity to islets and by protecting islets from allo- and auto- immune rejection [19].

1.3 T1D Disease Progression

Optimizing immunosuppression is particularly important in clinical islet transplantation because recipients have primed autoreactive responses against islet antigens in addition to the allogeneic antigens that necessitate immunosuppression in the context of solid organ transplantation [20]. Any strategies to mitigate immune responses to allografts must address both forms of rejection, so an understanding of their underlying mechanisms is important.

Onset of T1D begins with autoantibody production, followed by infiltration of innate and adaptive immune cells into islets, which form islet lesions and produce insulitis, or inflammation of the islets. Studies have indicated that autoimmune destruction of islets requires macrophages as well as CD4+ and CD8+ T cells [21-23], but when these cells are in islet lesions they are not destructive until an unknown triggering event occurs [24], which initiates the autoimmune destruction of β cells. Dominant autoantigens responsible for islet rejection are associated with β cell components, specifically insulin, glutamic acid decarboxylase 65 (GAD65), and islet-cell antigen-2 (IA-2) have been identified as primary players [25]. Insulin is the first target for autoantibodies detectable during the onset of T1D [26], but during the progression of disease, autoantigen epitope spreading occurs [27]. This process begins when the immune system recognizes and responds to an antigen with a single epitope, and spreads over time as the immune system recognizes new epitopes of the same antigen, as well as wholly new autoantigenic targets. In fact, increasing severity of the disease is correlated

with an increase in both autoantigens and in autoantibodies [25]. During the progression of T1D, macrophages invade islets and are activated to produce asymptotic inflammation via an unknown mechanism. Activated macrophages are required for the progression of T1D, because they secrete inflammatory cytokines and act as antigen-presenting cells (APCs), activating local effector T cell populations against β cell-specific antigens [24, 28]. Death of β cells in islet lesions results in a higher concentration of autoantigens for presentation, and exacerbates cell-mediated islet destruction in a feedback cycle [29].

Even without primed autoimmune responses, recipients of islet transplants would promptly reject the graft due to alloreactive immunity. Alloantigens may be recognized by T cells utilizing two mechanisms – direct and indirect alloantigen recognition. In direct recognition, donor tissue dendritic cells, expressing allogeneic MHC and costimulatory activity, migrate to lymph nodes and stimulate alloreactive T cells endogenous to the host [30]. In indirect recognition, host dendritic cells process allogeneic proteins from the graft, and trigger a T cell response by presenting processed antigens via MHC class I or MHC class II. The difference in these mechanisms lies solely in the source of the APCs, and both mechanisms require primed T cells to infiltrate the graft before destruction occurs.

1.4 Native Islet Microenvironment

During the process of pancreatic islet isolation, islets are removed from their native microenvironment. It is important to understand the critical facets of this environment that support islet function and health so that these aspects can be recapitulated when delivering purified islets in a transplantation setting.

1.4.1 Vascularization

Cumulatively, islets make up only about 1-2% of pancreas mass, but they receive about 15% of the blood supplying the pancreas [31, 32]. This disproportionate supply of blood suggests the importance of islets. In addition to receiving more blood, islets are themselves highly vascularized, containing fenestrated capillaries organized into a glomerular-like network, which make up 8-10% of islet volume [33, 34]. In fact, the number of fenestrae is approximately 10 times higher in islets that in exocrine pancreatic capillaries, islet capillaries have 20-30% larger diameter that exocrine pancreatic capillaries, and vascular density is higher for islets than the exocrine pancreas [35]. Capillary fenestrations and increased blood supply to islets facilitate rapid sensing of blood glucose as well as rapid release of insulin into circulation. In order to recapitulate healthy glucose kinetics in transplant recipients, rapid transport of glucose and insulin between islets and blood circulation is critical.

1.4.2 Innervation

Acetylcholine is necessary for pancreatic β cell function [36, 37], and until recently, prevailing wisdom suggested that the endocrine pancreas is highly innervated by the autonomic nervous system, directly stimulating insulin release. Requirements for innervation would place more hurdles in the path of successful islet transplantation. Preliminary studies of islet innervation did show extensive nerve networks forming throughout islets and demonstrated their direct cholinergenic action, but these studies were performed in mice. Similar studies in human islets showed that islets are only slightly innervated, but that the sympathetic nervous system innervates smooth muscle cells in blood vessels surrounding islets [38]. In 2011 it was shown that the required cholinergenic input to β cells is provided in a paracrine fashion by α cells in humans [39], eliminating a potentially difficult requirement for innervation of islet grafts. In fact, these studies not only show innervation is not critical in human islets, they further demonstrate the biological priority that is placed upon controlling blood supply to islets.

1.4.3 Cell-ECM Interactions

In the healthy pancreas, islets are each surrounded by a capsule of extracellular matrix. This capsule has been shown to have a composition consistent with basement membranes which function as barriers to infiltrating inflammatory cells in both mice and humans [40]. Several ECM components

which are known to bind to integrin receptors and facilitate adhesion and signaling make up the capsule, including several laminin isoforms (α1, β1, γ1, α2, β2), perlecan, and collagen type IV α1, but not including collagen type IV α3-6 [41, 42]. Studies have shown that for transplanted islets to survive, adhesive interaction with ECM is required, suggesting that the basement membrane provides important signaling cues to islets in addition to providing a barrier to infiltrating immune cells [43, 44]. Isolation of pancreatic islets is facilitated by enzymatic digestion, and thereby destruction, of the basement membrane which surrounds islets. Therefore, delivery strategies for islet transplantation should strive to restore important cell-ECM interactions that are lost during isolation in an effort to prolong islet survival and function. Motivated by this logic, several investigations have found that presentation of cell adhesive peptides on biomaterials can enhance islet viability and function [45, 46]. Several cell adhesive peptides, including RGD, GFOGER, and IKVAV [45] (derived from fibronectin, collagen and laminin, respectively) have been identified in these studies as useful for enhancing islet survival and/or function *in vitro*.

1.5 Transplant Site

1.5.1 Intrahepatic

Although the intra-hepatic site is the current clinical standard for islet transplantation, the efficacy of these interventions is limited by graft failure

resulting from instant blood-mediated inflammatory reaction (IBMIR) from platelet and complement activation. Therefore, to avoid this graft failure, new sites should be investigated for clinical islet transplantation. Clinical trials utilizing the Edmonton Protocol with intrahepatic allogeneic islet transplantation have demonstrated insulin independence in diabetic patients, but the median duration of insulin independence is only 35 months and requires multiple donor pancreata [47]. The intrahepatic site is accessible laproscopically for islet delivery, but the hepatic vasculature is an inhospitable transplant site, as evidenced by suboptimal performance of autoislet grafts [48, 49]. Rapid IBMIR to intraportally infused islets contributes to extensive graft deterioration [50-52], with approximately 50-60% of transplanted cells being lost immediately [53], and further islet destruction is mediated by both innate and adaptive immune responses, even when chronic immunosuppressive regimens are used[15]. Islets transplanted intrahepatically are also gradually deteriorated by fibrotic encapsulation, toxicity due to immunosuppressant drugs, and glucolipotoxicity [54-56]. Cumulatively, the stresses from intrahepatic islet delivery produce high rates of islet engraftment failure, so islets from 2 to 3 donors must be transplanted in each recipient to achieve insulin independence [57]. In addition to the hostile nature of the intravasculature site due to direct exposure of islets to blood, islet performance may be further decreased by a lack of cell adhesive protein binding sites in islet microenvironment, which have been shown to facilitate islet survival and function.

1.5.2 Alternative Transplant Sites

Various alternative transplant sites do not expose islets directly to circulating blood, and so have been explored to avoid IBMIR-instigated graft loss. These sites include the subcutaneous space [58-62] and intraperitoneal tissue that is laparoscopically-accessible such as the small bowel mesentery (SBM) [63, 64] or omentum [65-68]. These extrahepatic sites are appealing due to ready accessibility, but each of these tissues presents varying degrees of vascular supply and inflammatory responses, which are known to influence islet survival, engraftment, and function [69-71]. Preclinical models have demonstrated that re-establishment of blood flow to islets requires several days to weeks when using intraportal, renal subcapsular, or splenic subcapsular sites [72-74]. During this period, the local islet environment has reduced oxygen tension and a vascular bed with lower vessel density than the native pancreas [75, 76]. This slow, insufficient revascularization of transplanted islets is a major cause for reduced islet viability and function [77-79]. Delivery of pro-vascularization factors utilizing genetic manipulation of islets has improved vascularization and islet function [80-86], but thise strategy is limited by technical challenges and safety considerations.

1.6 Immunoisolation

1.6.1 Mechanism

While vascularization of transplanted islets improves their function and survival in syngeneic transplant scenarios, vascularization also facilitates exposure of islet grafts to the host immune system, possibly exacerbating rejection by auto- and allo-immune mechanisms, especially in the absence of systemic immunosuppression. With the ultimate goal of eliminating the requirement for systemic immunosuppression along with its associated side effects, it has been proposed that transplanted islets be protected from the host immune system using permselective (semi-permeable) membranes. This approach, known as immuno-isolation, requires membranes that have a pore size designed to simultaneously accomplish two tasks. First, the membrane pore size must be large enough to allow the relatively unhindered transport of small molecules and proteins, so that nutrients can be supplied to the islets while waste products and insulin rapidly diffuse away. Second, the membrane pore size should be small enough to exclude larger immune system components, including antibodies and immune cells (Figure 3). While there is no perfect cutoff size at which functional molecules transport easily and all immune components are excluded, preventing cell-cell contact of the islets with immune cells will undoubtedly mitigate damage to the graft, and may reduce immunosuppressive requirements for maintaining graft function.

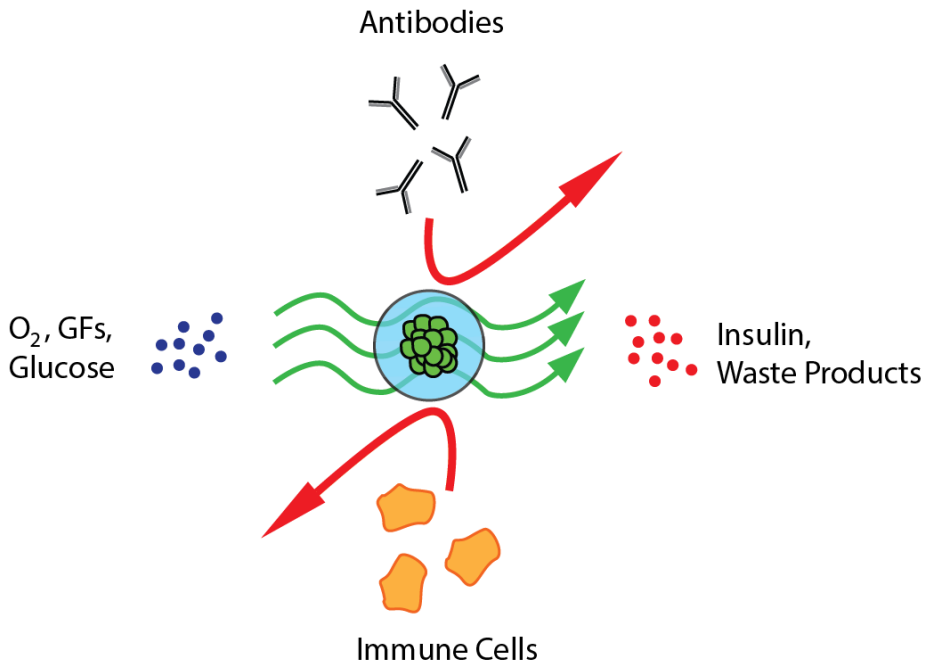

Figure 3. Microencapsulation of cells can provide an immunoprotective effect while facilitating cell function. By tuning pore size of the hydrogel network, antibodies and immune cells can be excluded from the microcapsule, while smaller nutrients and functional molecules can diffuse relatively freely through the hydrogel.

1.6.2 Immunoisolation Devices

1.6.2.1 Intravascular Macrodevices

Attempts at immuno-isolation over time have taken several form factors, each of which has inherent advantages and disadvantages. Early immuno-isolation devices were intravascular and were partially comprised of a tubular semi-permeable membrane that was required to be surgically implanted by vascular anastomoses so that blood circulated through its lumen [87, 88] (Figure 4). Excellent transport of nutrients and oxygen is achieved with these devices, but the risk associated with the surgical operation and likelihood of post-operative thrombosis are major practical limitations the the intravascular approach. Since the 1990s, immuno-isolation has focused on extravascular devices, which are not as risky and invasive as devices which contact the blood, but are more likely to suffer from hypoxia or nutrient deficiency due to transport limitations.

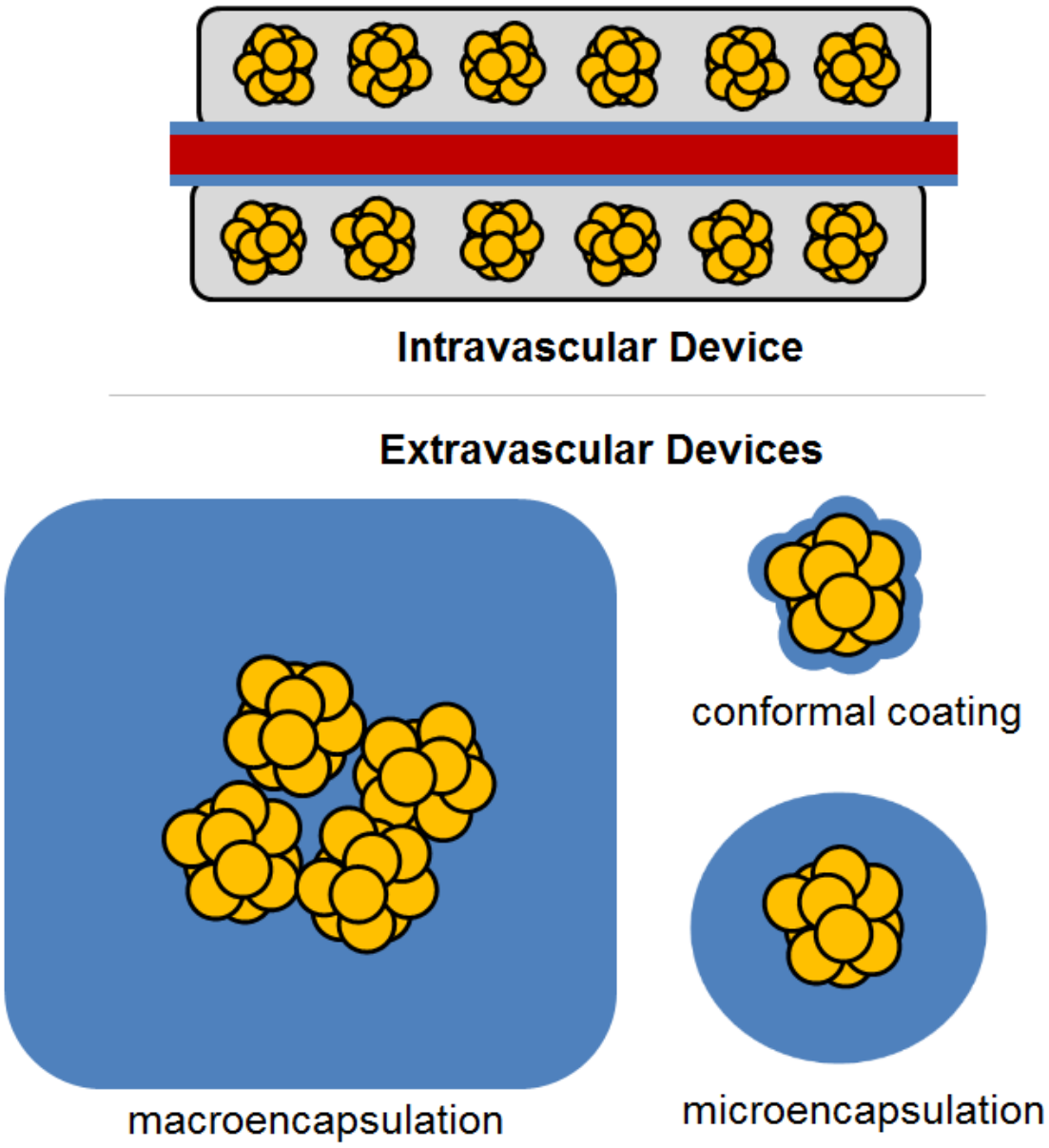

Figure 4. Immuno-isolation devices with various forms have been investigated. Early intravascular devices required invasive surgical implantation, and so were not clinically practical. Later, safer extravascular devices were explored, generally consisting of a polymer, usually a hydrogel, into which cells were embedded. By reducing thickness of membranes, diffusion of critical nutrients and oxygen can be increased.

1.6.2.2 Extravascular Macrodevices

Extravascular macrodevices comprise macrocapsules, as well as planar and tubular membranes with a variety of configurations. These devices are the most widely tested in the clinic because they are easily retrievable in case of complications. Unfortunately, because of a low surface area to volume ratio in these devices, poor diffusion of oxygen and nutrients usually lead to cell necrosis and loss of function. In the clinic, these effects are often exacerbated by the selection of poorly vascularized sites, with subcutaneous implantation. A benefit of subcutaneous implantation is that non-functional devices can be explanted and replaced in a minor operation. A promising insulin producing extravascular macrodevice is being developed by TheraCyte[89], who claim that their device functions for 6 months when implanted subcutaneously.

1.6.2.3 Extravascular Microcapsules

Extravascular microcapsules are generally comprised of hydrogel spheres with diameter less than 1mm which contain cells or cell clusters [90]. Microcapsules have drastically higher surface area to volume ratio than macrodevices and therefore improved transport kinetics of oxygen and nutrients, which promotes survival of encapsulated cells. The major downside to this approach is that microcapsules are difficult to retrieve in case of post-operative complications, which are likely in a transplant scenario. It is also very important to

ensure that microcapsules do not aggregate because this can result in necrosis and graft failure [91].

1.6.2.4 Conformal Coating

Finally, conformal coating of cells has been used to increase the surface area to volume ratio of grafts even more, facilitating even better mass transport than in microcapsules [92]. The smaller size of these constructs also enables the use of space-constrained transplant sites, including intra-hepatic. While many different approaches have been used to apply conformal coatings to cells, uniform coverage of all cells is usually questionable and most coatings are gone within a few days [93, 94]. For the most part, current efforts at conformal coating have been of limited use for long term immuno-isolation.

1.7 Polymers for Microencapsulation

Because of necrosis associated with hypoxic cores in macrodevices and because of limited persistence of conformal coating, microencapsulation is the most promising strategy for achieving immuno-isolation. While other classes of materials have been investigated for immuno-isolation, polymers, especially hydrogels, can also be designed to simultaneously recapitulate important aspects of native cell microenvironment. Polymers employed in this application must allow tunable permeability for optimization of immuno-isolation, must enable

gelation of microcapsules under cytocompatible conditions, and must retain mechanical integrity for the life of the graft, *in vivo*. Additionally, microcapsules should not elicit a strong foreign body response in the recipient, and they would ideally allow for recapitulation of the native islet microenvironment when possible.

Synthetic as well as naturally occurring hydrogels have been explored for immuno-isolation. Biologically derived hydrogels include gelatin, fibrin, hyaluronic acid, agarose, chitosan and alginate. Synthetic polymers which have been utilized include poly vinyl alcohol, poly lactic acid, poly glycolic acid, polypeptides, and polyethylene glycol, as well as a plethora of functional derivatives of these polymers [95-97]. While natural polymers are known to provide signals to cells that promote survival *in vivo*, the nature of these interactions is poorly defined, and they are difficult to modify. Conversely, synthetic polymers provide consistent, well defined compositions and their production is scalable. Additionally, synthetic polymers can be functionalized with a variety of reactive groups, including click chemistries which allows for functionalization and gelation in complex physiological milieu.

1.7.1 Alginate

Alginate has emerged as the dominant material reported for cell microencapsulation, largely due to its apparent biocompatibility and ease of gelation. Other natural materials investigated have not reached the level of performance which alginates have [98], but the performance of alginate

microcapsules is limited by several factors. Depending on the source of alginate, its composition, and thereby functional properties, vary significantly [99]. In addition to its source, the extraction and purification processes utilized for alginate can drastically alter many of the properties of alginate, including hydrophobicity, immunogenicity, viscosity [100], by altering the amount of contaminants present such as polyphenol, endotoxins, and proteins.

1.7.2 Alginate-PLL

Alginate does not inherently provide an easy mechanism for tuning permeability, as required in immuno-isolation applications. Negatively charged alginate microcapsules are generally coated with a polycation (usually poly-L-lysine) for stability and to control the molecular weight cut off of the membrane more precisely [101, 102]. While poly-L-lysine (PLL) coatings enable tuning of membrane permeability, they are also known to be immunogenic, which is counterproductive in immuno-isolation applications [103]. Microcapsules often undergo a final coating with alginate so that the final structure is alginate-PLL-alginate (APA), but studies suggest that external alginate is not sufficient to mask the immunogenicity of PLL. Indeed, APA microcapsules activate complement, induce cytokine production by macrophages, and elicit an exacerbated pericapsular response when compared to alginate-only microcapsules. Alginate microcapsule technology has been extensively developed, beginning more than 30 years ago, but still faces technical hurdles, especially relating to sourcing and quality control of the alginate used. These challenges have made widespread

clinical deployment unlikely. However, some alginate derivatives have recently been identified which elicit minimal foreign body response in vivo, and allogeneic stem cell-derived β cells delivered microencapsulated in these alginates could restore long term glycemic control in immune-competent diabetic mice [104, 105].

1.7.3 Synthetic Polymers

Scalable production of high-purity synthetic polymers can be accomplished with current technology, and some chemistries utilized enable stoichiometric incorporation of bioactive moieties and independent control of permeability. Polyethylene glycol (PEG), known for its low-protein adsorption and minimal inflammatory profile, is the gold standard synthetic hydrogels, and hydrogel properties can be altered by changing macromer structure, molecular weight, and end group functionalization. Bioactive hydrogels are usually crosslinked with either Michael-type addition reactions or acrylate polymerization [106]. Early synthetic hydrogels were largely based on PEG diacrylate chemistry, which are crosslinked via free-radical initiated polymerization of acrylate functional groups. Free radicals generated either through chemical activation or cleavage of photoinitiators with UV irradiation can rapidly crosslink hydrogels, but exposure of cells to free radicals decreases encapsulated cell viability. More recently, branched PEG macromers have been utilized, which contain 4- or 8-arms that are terminated with functional groups - acrylate[107, 108], vinyl-sulfone [109, 110], and maleimide[111] end groups have been investigated, among

others[112]. Each of these reactive end groups can be used to tether bioactive moieties, enabling covalent incorporation of cell adhesive peptides and growth factors into hydrogels. A comparison between 4 arm macromers terminated with these functional end groups showed that 4-arm PEG maleimide (PEG-4MAL) had improved cross-linking efficiency, bioligand incorporation, and encapsulated cell viability [113]. Reproducibility of hydrogel structure and properties, along with stoichiometric control of bioactive moiety presentation, are major advantages of synthetic hydrogels (particularly PEG-4MAL) over alginate. Alginate solutions have relatively high surface tension in water, and their crosslinking is accomplished through diffusion of very small cations, so it occurs rapidly enough that aqueous phase droplets can be crosslinked cytocompatible aqueous buffers. This method cannot be utilized to crosslink droplets of PEG-4MAL solutions, because they crosslink more slowly than alginate and disperse before gelation can occur. Therefore, new techniques must be developed for the fabrication of synthetic hydrogel microcapsules.

Incorporation of important biological molecules can be easily accomplished with some synthetic hydrogels, such as those containing vinylsulfones and maleimides, which react with thiol-containing molecules to form a covalent bond. Because the amino acid cysteine contains a thiol reactive group, peptides and proteins which contain cysteine residues can be covalently bonded to hydrogels. This is a major benefit over alginate because it enables a high level of control of the microenvironment of encapsulated cells, since cell

adhesive peptides and proteins can be incorporated stoichiometrically and presented to encapsulated cells. Many cell types require adhesive cues to survive and proliferate, and the effect of adhesive ligands on β-cell function and proliferation has been shown to be significant [45, 114]. Facile incorporation of adhesion molecules is only one benefit of synthetic hydrogel chemistry – another being the ability to control crosslinker size and stability. Dithiol molecules can be used to crosslink multi-arm PEG-MAL and PEG-VS, and by controlling the degradation mechanism and rates of these crosslinkers, tissue ingrowth and implant engraftment may be enhanced. In fact, several different dithiol peptide crosslinkers have been identified which are protease degradable, and crosslink synthetic hydrogels which have tunable degradation rates and MMP specific degradation [115, 116]. By allowing for host cell adhesion and infiltration, these synthetic hydrogels allow tissue ingrowth that cannot occur with alginate, which could result in better engraftment of implanted cells or tissues.

1.8 Droplet Templated Microgels

By definition, microencapsulation involves structures under 1 mm in size, so functional grafts must be comprised of many microcapsules. A high throughput method exists for the production of alginate microcapsules, in which droplets containing cells are produced by extrusion through a needle, and are subsequently crosslinked by an aqueous bath containing cations. Unfortunately,

this technique is not amenable to the production of hydrogel microspheres, or microgels, with different chemistries. Direct templating of microcapsules on a large scale, through microfabrication of molds into which gels can be cast, is a viable method that has been explored with some synthetic polymers, but throughput is severely limited by the size of molds and by handling considerations. Therefore, a scalable approach for the micro-encapsulation of cells and islets is required before modern synthetic polymers can be utilized for delivery of clinically relevant cell numbers in transplant scenarios.

Indirect templating of microcapsules in immiscible oil through droplet microfluidics could allow for continuous, rather than batch, production of microcapsules. In continuous droplet microfluidics, fluid flows cause the breakup of liquid droplets, and an immiscible carrier phase (liquid or gas) is used to separate and stabilize droplets. Droplet diameter can be controlled by varying channel geometry as well as fluid flow rates in these devices, and droplet populations are generally uniform in size, with low polydispersity [117-119]. This control can be utilized to minimize immune response and fibrous overgrowth of microcapsules, because microcapsule size has been correlated with host response *in vivo* [120].

Droplet microfluidics has enabled the production of crosslinked hydrogel spheroids (microgels) with varied chemistries and utilizing differing methods of crosslinking. Microfluidic droplet templating has been applied to alginate and other ionically crosslinking polymers by allowing diffusion of ions from the

continuous phase in order to utilize size control that is not possible with extrusion techniques [121]. Chemically crosslinked microgels have also been produced on microfluidics, by emulsifying aqueous solutions of monomers and subsequently inducing crosslinking in these compartmentalized droplets. This approach has been used to photopolymerize microgels made of various synthetic polymers, including PEG-DA [122], and acrylamide [123] among others [124, 125]. However, this approach limits production of microgels to polymers that can be photo-crosslinked, which disqualifies polymers which are more amenable for functionalization with bioactive moieties, such as PEG-4MAL. Moreover, UV radiation and free radicals are harmful to cells, and so are not ideal for crosslinking cell-laden microcapsules. Another mechanism that has been employed for droplet-templated microcapsule production is to first generate droplets containing either polymer precursor or crosslinker, and then to force coalescence of droplets and subsequent hydrogel formation [126]. Modifications of this approach might allow the production of microgels in modern synthetic polymers, but control of stoichiometry of droplets will be difficult if cell suspensions are being used.

1.9 Immunomodulation

The immuno-isolation potential of microcapsules is determined by the pore size cut off of the membrane formed by encapsulating hydrogels. Molecular weight cut off of PLL-alginate microcapsules can be controlled by changing PLL molecular weight and coating method [127], but even so, no alginate microcapsules have been demonstrated to reliably mitigate rejection in immune-competent animals. Therefore, some form of additional immuno-modulation will have to be deployed for long term graft acceptance. Microencapsulation has demonstrated synergistic effects with traditional immunosuppression, which could reduce the dose of immunosuppression as well as associated side effects. However, local immunomodulation at the site of the transplant could eliminate the requirement for systemic immunosuppression, and make transplantation a sensible therapy for a much larger number of patients. Several approaches have been investigated for local modulation of the immune response around tissue grafts, including co-transplantation of mesenchymal stem cells (MSCs), as well as presentation of various immune-regulatory proteins, either through direct display or genetic engineering of transplanted cells. Because graft acceptance is strongly correlated with FoxP3+ T reg cells in the graft microenvironment, these strategies strongly favor approaches which enhance T reg cell recruitment [128, 129].

1.9.1 MSC Co-Delivery

MSCs may improve graft acceptance through the modulatory effects they exert on various immune cell populations, and they may also improve islet function [130]. Immune-privileged status conferred by a lack of MHC class II and other costimulatory molecules allows allogeneic MSCs to be transplanted without being rejected, and MSCs effects on immune cells are powerful. MSCs inhibit T cell activation and proliferation [131, 132] through the induction of CD4+CD25+FoxP3+ regulatory T cells [133], and through the induction of regulatory APCs [134]. MSCs also alter the cytokine secretion profile of APCs, decreasing the production of inflammatory tumor necrosis factor α (TNF-α), while increasing the production of anti-inflammatory IL-10 [135]. B lymphocyte proliferation, differentiation, and antibody production are all impaired by co-culture with MSCs [136], demonstrating the various immunomodulatory effects of MSCs. In nonhuman primates, co-transplanted MSCs have been shown to increase the percentage and number of FoxP3+ T regulatory cells [137], suggesting that effects on immune cells that were observed *in vitro* are robust. However, more studies are needed to determine whether the immunomodulatory effects of MSCs are capable of mitigating the severe auto- and allo- reactive immune rejection of co-transplanted islets *in vivo*, as well as the ideal delivery vehicle for localized immunomodulation without systemic effects.

1.9.2 Protein and Gene Delivery

Another approach to immunomodulation is presentation of immunomodulatory proteins, such as transforming growth factor β (TGF-β) and fas ligand (FasL), either locally along with grafts, or systemically. TGF- β1 is an immune signaling molecule that plays an important role in maintenance of, and the induction of, Treg cells, because mice deficient for TGF-β1 consistently have reduced numbers of this important immune suppressor cell [138]. Ectopic TGF-β expression in allogenic heart grafts resulted in long term survival, demonstrating the *in vivo* efficacy of TGF-β therapy. Systemic TGF-β therapy is associated with increased fibrosis of transplants, but immobilization of TGF-β on transplanted tissue may potentially reduce this fibrosis. Although mechanistic studies suggest the promise of TGF-β as an immunomodulatory signal, effective allograft acceptance through TGF-β therapy remains to be demonstrated. Another protein which has been utilized for immunomodulation is FasL. FasL plays an important role in activation-induced cell death, which is a major mechanism of immune homeostatis [139, 140]. Ectopic expression of FasL has been successfully utilized to induce hyporesponsiveness to allogenic antigens *in vivo,* and transfusion of DCs ectopically expressing FasL prolonged survival of fully MHC-mismatched cardiac allografts [141]. Genetic transfer of FasL in renal allografts also resulted in prolonged graft survival in rats, suggesting the potential for localized FasL modulation that does not require systemic administration of this powerful immunomodulator [142]. While FasL studies demonstrate potential for

effective local immunomodulation, ectopic expression of proteins is technically challenging, and imposes severe safety concerns. Therefore, new delivery vehicles are needed to fully investigate the potential of immunomodulatory proteins for achieving allogenic graft acceptance.

1.10 Summary of early studies utilizing PEG-4MAL for islet delivery

Dr. Edward Phelps, a García lab alumnus, developed a hydrogel system for enhancing vascularization and function of implanted pancreatic islets utilizing PEG-4MAL macromer cross-linked with protease degradable peptides which delivered VEGF in response to cell activity at the transplant site [143]. The maleimide reactive group is extensively used in peptide bioconjugate chemistry because of its fast reaction kinetics and high specificity for thiols at physiological pH. Simple co-incubation of macromer with thiol - containing molecules at pH 7.4 results in a Michael-type addition reaction that forms a covalent bond (Figure 5). Maleimide-based cross-linking of PEG hydrogels has significant advantages over other cross-linking chemistries, namely well-defined hydrogel structure, stoichiometric incorporation of bioligands, increased cytocompatibility, improved cross-linking efficiency, and tunable reaction time scales appropriate for *in situ* gelation for *in vivo* applications [143]. Additionally, the base macromer exhibits minimal toxicity and inflammation *in vivo* and is rapidly excreted via the urine [63]. These are important considerations in establishing the safety and

translational potential of these hydrogels. Hydrogels cross-linked by protease-degradable cross-links have been engineered as protein delivery vehicles with controlled, on-demand release profiles for protein therapeutics, including the vasculogenic agent VEGF [63, 144, 145].

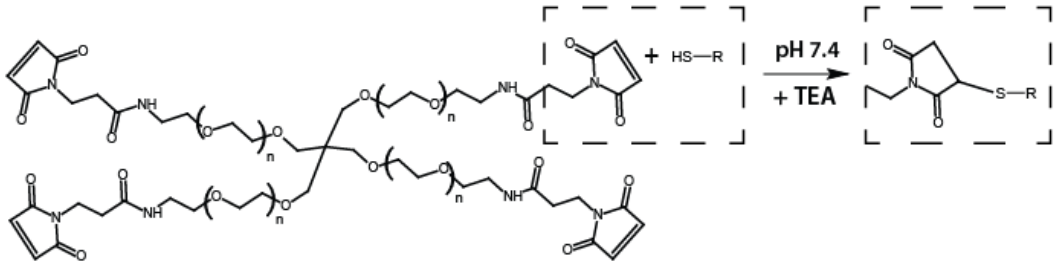

Figure 5. PEG-4MAL Macromer consists of a 4-arm branched PEG backbone that has been modified with a maleimide group terminating each arm. At physiological pH, free thiol-containing molecules undergo a Michael-type addition reaction with maleimides, forming a covalent bond to macromer. This reaction is facilitated by a nucleophilic buffer such as triethanolamine, and can be used to either functionalize the macromer or crosslink macromer into a hydrogel network.

While I was in a supporting role on this project, Dr. Phelps developed these vasculogenic hydrogels and utilized them to deliver islets to an alternative delivery site, the small bowel mesentery (SBM), successfully reversing diabetes in a syngeneic murine model [63]. The SBM is a thin tissue which connects the small bowel to the back wall of the abdomen, and it is highly vascularized,

allowing for the transplantation of islets very near existing vasculature. 400 bare islets were immobilized on the mesentery surface by suspending them in PEG-4MAL that had been functionalized with 2.0 mM RGD and 10 µg/mL VEGF, and subsequently adding 2.6 mM of a degradable peptide crosslinker (VPM) before pipetting mixture onto the mesentery. Within 5 minutes, a crosslinked gel had formed, adhering islets to the mesentery surface. After 4 weeks, animals were injected with lectin to label vasculature and were sacrificed. Figure 6B shows an image of a transplanted islet graft and the extensive vascularization that had occurred after 4 weeks in vivo. Vascularization of this graft, along with several controls, was quantified by vessel area (lectin positive) over total islet area (Figure 6C). While the PEG-4MAL + VEGF delivery system had less vascularization than native islets, there was a statistically significant improvement of vascularization over the hepatic portal vein control.

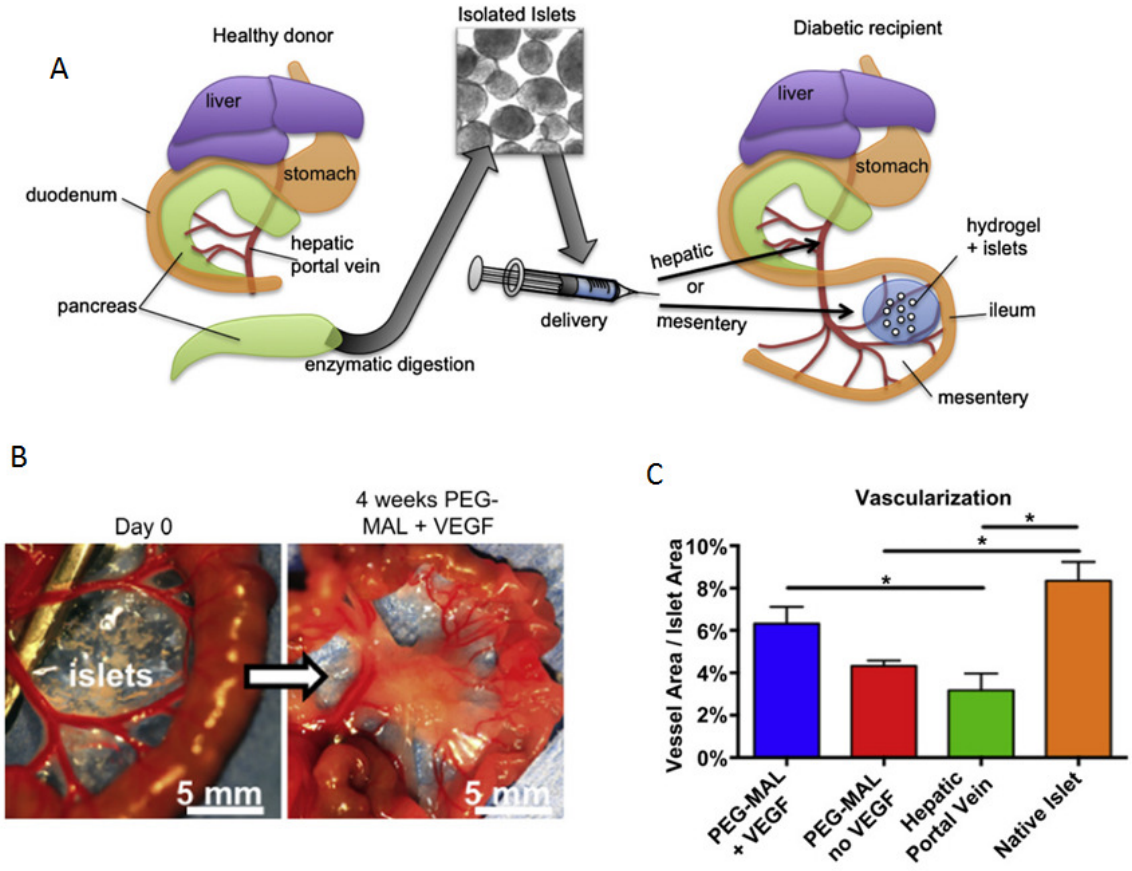

Figure 6. Rapid and extensive revascularization occurs in islets delivered to the SBM using our engineered vasculogenic hydrogel. (a) Islets are isolated from donors using standard methods, and are adhered to the SBM of diabetic recipients using PEG-MAL + VEGF. (b) Extensive engraftment of the transplant occurs in 28 days, (c) resulting in significantly more intraislet vessels than islets delivered through the hepatic portal vein (n=6, SEM bars shown). Adapted from [63].

Rapid revascularization is important for improving islet engraftment, but the restoration of euglycemia is the ultimate metric for islet transplant strategies. Therefore, blood glucose was monitored daily for the mice receiving 400 islets at various sites. All treatment groups received streptozotocin (STZ) injections 2 weeks prior to transplant, and all animals were stably diabetic (>250 mg/dL blood glucose) on day 0. Euglycemia was restored in the PEG-4MAL + VEGF animals on day 16 after receiving a 400 islet transplant, but transplants in the hepatic portal vein failed to reverse diabetes within 28 days (Figure 7). A peritoneal glucose challenge was performed on day 28, and again, only the healthy animals and those receiving SBM grafts with PEG-4MAL and VEGF had blood glucose levels below 250 mg/dL after 3 hours. Finally, serum C-peptide levels on day 28 measured using ELISA showed that more insulin was being produced in animals receiving a SBM graft than in those receiving an intrahepatic graft. Taken together, these results indicate that the SBM is a promising site for islet delivery, especially when transplants are delivered with biodegradable PEG-4MAL containing VEGF, a potent inducer of vascularization.

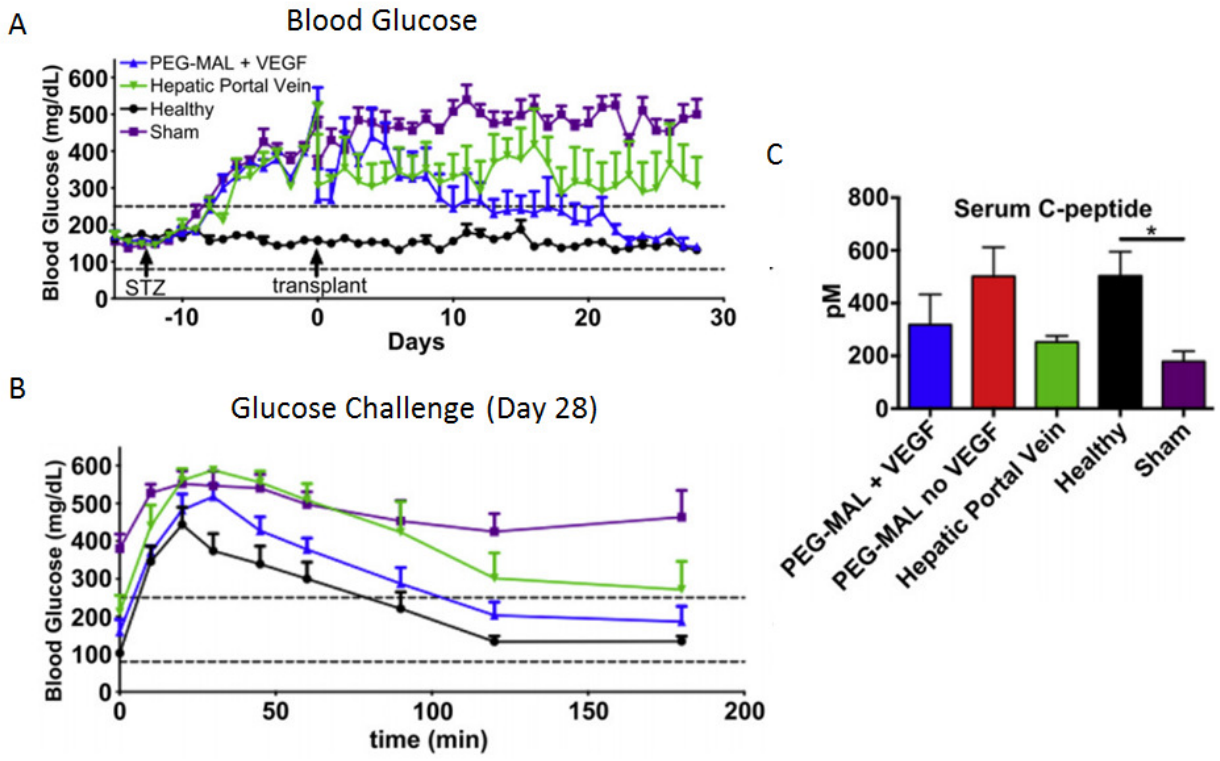

Figure 7. Delivery of pancreatic islets to the SBM in degradable PEG-4MAL gels, functionalized with VEGF and RGD, restores euglycemia in a syngeneic murine model. (a) 400 islets delivered to the SBM reverse diabetes, while 400 islets delivered through the hepatic portal vein were unable to restore euglycemia (n=4-6) in a streptozotocin diabetes model. (b,c) Serum C-peptide levels and IP glucose challenge response on day 28 after transplantation further demonstrate the superior function of islets delivered to the SBM with our vasculogenic hydrogel. Adapted from [63].

1.11 Research Summary

Permselectivity of microgels which encapsulate cells can provide immunoprotective effects as demonstrated by studies utilizing alginate-PLL coatings on pancreatic islets. Due to their high surface area to volume ratio, microgels also reduce mass transport limitations of encapsulation compared to bulk hydrogel encapsulation. Alginate microgels have controlled permselectivity, but synthetic hydrogels may additionally be covalently functionalized with bioactive molecules in order to support encapsulated cell survival and function, or to provide instructive cues to the host, functions not readily accomplished with alginate. Specifically, PEG-4MAL possesses versatile utility as a cell encapsulant, and can be used to instigate functional vascularization of encapsulated pancreatic islets when functionalized with VEGF. Permselectivity alone may not provide enough protection to eliminate immune rejection of encapsulated cells, so the ability to deliver bioactive moieties may enable active modulation of the immune response. Unfortunately, the extrusion fabrication method that has been used to produce alginate microgels for decades is not compatible with covalently crosslinked synthetic hydrogels, and is not well suited to producing cell-laden microgels below 250 μm diameter. Therefore, new methods are needed to microencapsulate cells in synthetic microgels, ideally with controlled size.

The work presented here describes an enabling tool for the encapsulation of cells and pancreatic islets in synthetic microgels, as well as applications and

refinements of this technology. The format of chapters may not be uniform, because each chapter is compiled from a separate manuscript intended for independent publication. Chapter 2 describes the development of a microfluidic platform capable of encapsulating cells and pancreatic islets, as well as generating monodispersed microgels. Chapter 3 describes the optimization of pancreatic islet microencapsulation in PEG-4MAL, and develops a unique strategy for in vivo delivery. Chapter 4 describes the development of a strategy for active immunomodulation by simple co-delivery of unmodified islets with microgels presenting an engineered FasL protein in diabetic mice. Chapter 5 breaks from the theme of diabetes and instead describes a two-layer elastomeric microfluidic device with parallelized encapsulators for increased throughput when encapsulating cells in small microgels. Together, these accomplishments both empower and demonstrate the utility of microfluidics for cell encapsulation in synthetic microgels.

CHAPTER 2: MICROFLUIDIC-BASED GENERATION OF SIZE-CONTROLLED, BIOFUNCTIONALIZED SYNTHETIC POLYMER MICROGELS FOR CELL ENCAPSULATION

Text as Published in *Advanced Materials* [146], U.S. Patent 9,381,217

Authors: Devon M. Headen, Guillaume Aubry , Hang Lu , and Andrés J. García

2.1 Abstract

Cell and islet microencapsulation in synthetic hydrogels provides an immunoprotective and cell-supportive microenvironment. A microfluidic strategy for the generation of biofunctionalized, synthetic microgel particles with precise control over particle size and molecular permeability for cell and protein delivery is presented. These engineered capsules support high cell viability and function of encapsulated human stem cells and islets.

2.2 Main Text

Hydrogel microencapsulation of cells is a promising strategy for immunoprotection after transplantation. Since the development of alginate-poly-L-lysine encapsulation by Lim and Sun in 1980 [101], their approach has remained the standard for cell encapsulation, although major efforts have led to significant improvements.[147] The ease of alginate microencapsulation, along

with alginate's inherent biotolerance *in vivo*, have led to its prevalence,[148] even though the ability to control local cellular environment via incorporation of bioactive molecules (e.g., adhesive peptides) is limited. Highly tunable, synthetic hydrogel encapsulation is attractive for various regenerative medicine applications,[149-151] not only for immunoisolation, but also for directing cell behavior and fate.[149] Several groups have developed more complex encapsulation configurations, such as cell encapsulation in natural hydrogel fibers,[152, 153] but the benefits of added geometric complexity remain to be established. Minimization of encapsulation volume is also important in many regenerative medicine scenarios, including pancreatic islet transplantation. In an effort to reduce the high polydispersity present in electrostatically generated alginate droplets with diameters <200 μm,[154] microfluidic droplet generation has been explored.[155-157] Microfluidic devices have also been used to generate synthetic hydrogel particles.[122, 158-161] Even for synthetic polymer encapsulation, control of cellular microenvironment by functionalization of polymers with bioactive molecules remains a significant challenge. Current synthetic polymer encapsulation strategies typically rely on cytotoxic crosslinking mechanisms such as UV- or thermal-based free radical polymerization. Here, we present a facile, modular microfluidics-based technology for the generation of microgels of controlled size and microencapsulation of clinically relevant cells, such as human pancreatic islets and human mesenchymal stem cells (hMSCs). Peptides and proteins are also easily incorporated into 4-arm PEG maleimide (PEG-4MAL) microgels, which allows for the presentation of a highly controlled

cellular microenvironment. The PEG-4MAL hydrogel system has significant advantages over other hydrogel chemistries, such as well-defined hydrogel structure, facile and stoichiometric incorporation of bioligands, increased cytocompatibility, improved crosslinking efficiency, and tunable reaction rates.[113] Additionally, the PEG-4MAL macromer exhibits minimal toxicity and inflammation *in vivo* and is rapidly excreted via the urine,[63] which are important considerations in translating this material to *in vivo* applications. The crosslinking scheme for this system utilizes a Michael-type addition reaction, is cytocompatible, and does not rely on free radical polymerization. By varying device geometry and fluid flow rates, monodisperse microgels with a wide range of diameters can be produced. Kinetic studies of the release of microgel-encapsulated biomolecules demonstrate not only the immunoisolation potential of the microgels, but also the capability of tuning critical network parameters that cannot be easily tuned in natural polymers, such as macromer molecular weight, for rate-controlled release of peptide therapeutics. Importantly, the microencapsulation process does not affect the viability or function of human pancreatic islets and mesenchymal stem cells (hMSCs).

Pioneering studies by Thorsen demonstrated controlled generation of emulsions using T-junctions in microfluidic devices,[162] and the work of Stone established the ability to generate droplets using flow focusing microfluidic geometries.[163, 164] Weitz established encapsulation of cells inside emulsions for high throughput cell-based assays.[165] Translating this work into covalently crosslinking of microgels within microfluidic devices adds significant complexity

because polymer precursors must be liquid while flowing through the focusing nozzle, but droplets must crosslink rapidly after being generated to prevent them from merging. Recently, synthetic polymer microgels have been generated, including cell-laden microgels.[122, 158-161, 166, 167] However, most of these schemes require crosslinking using UV-based free radical polymerization, resulting in potentially cytotoxic effects on encapsulated cells. Although cell encapsulation in synthetic microgels crosslinked without free radicals has been reported, the polymers utilized cannot easily be functionalized with bioactive molecules.[158, 166] This major limitation makes the maintenance of cells requiring adhesive ligands for viability and function difficult. Recently, Lutolf devised an elegant microfluidic scheme to generate surface-modifiable synthetic microgels that does not utilize free radical polymerization, but neither bulk modification with bioactive molecules nor cell encapsulation was shown.[160] Microfluidic encapsulation of large clusters of cells, such as human islets, is more challenging than single cell encapsulation, because the larger particles tend to clog microfluidic channels. For these reasons, synthetic polymer microencapsulation of islets using microfluidics has not been shown. To minimize encapsulation volume while avoiding microfluidics altogether, investigators have explored conformal coating of islets.[168, 169] Whereas conformal coating minimizes transplant volume, the immunoisolation potential of such thin polymer membranes remains unknown.

To address these limitations, we generated a strategy (Figure 8) to produce cell- and cell aggregate-laden synthetic PEG-4MAL-based microgels,

functionalized with cell adhesive peptides, by producing droplets using a flow focusing microfluidic device and subsequently covalently crosslinking the droplets with the small molecule dithiothreitol (DTT). Three independent flows of (1) mineral oil containing SPAN80 (a surfactant), (2) a crosslinker phase containing mineral oil and SPAN80 with an emulsion of aqueous DTT solution, and (3) PEG-4MAL macromer in aqueous physiological buffer were pumped into the microfluidic chip using syringe pumps. As the macromer phase approached the flow-focusing nozzle, a co-flowing continuous phase of oil shielded the macromer from contact with the crosslinker-laden oil phase. Because crosslinker could not reach the macromer before flow instability occurred, monodisperse, spherical droplets were formed. The crosslinker then rapidly diffused into droplets, covalently crosslinking the PEG-4MAL macromer into the hydrogel network via Michael-type addition reaction of the maleimide groups on the macromer and thiols on the crosslinker. The PEG-4MAL hydrogel platform used for this system is easily modified with thiol-containing molecules, including cysteine-containing adhesive ligands and growth factors, due to the high specificity of the maleimide groups for thiols at physiological pH. This Michael-type addition reaction requires no free radicals and is cytocompatible.[113] Furthermore, fast reaction kinetics render this hydrogel ideal for microfluidic encapsulation, allowing for short residence time on chip, and minimizing cell stress.

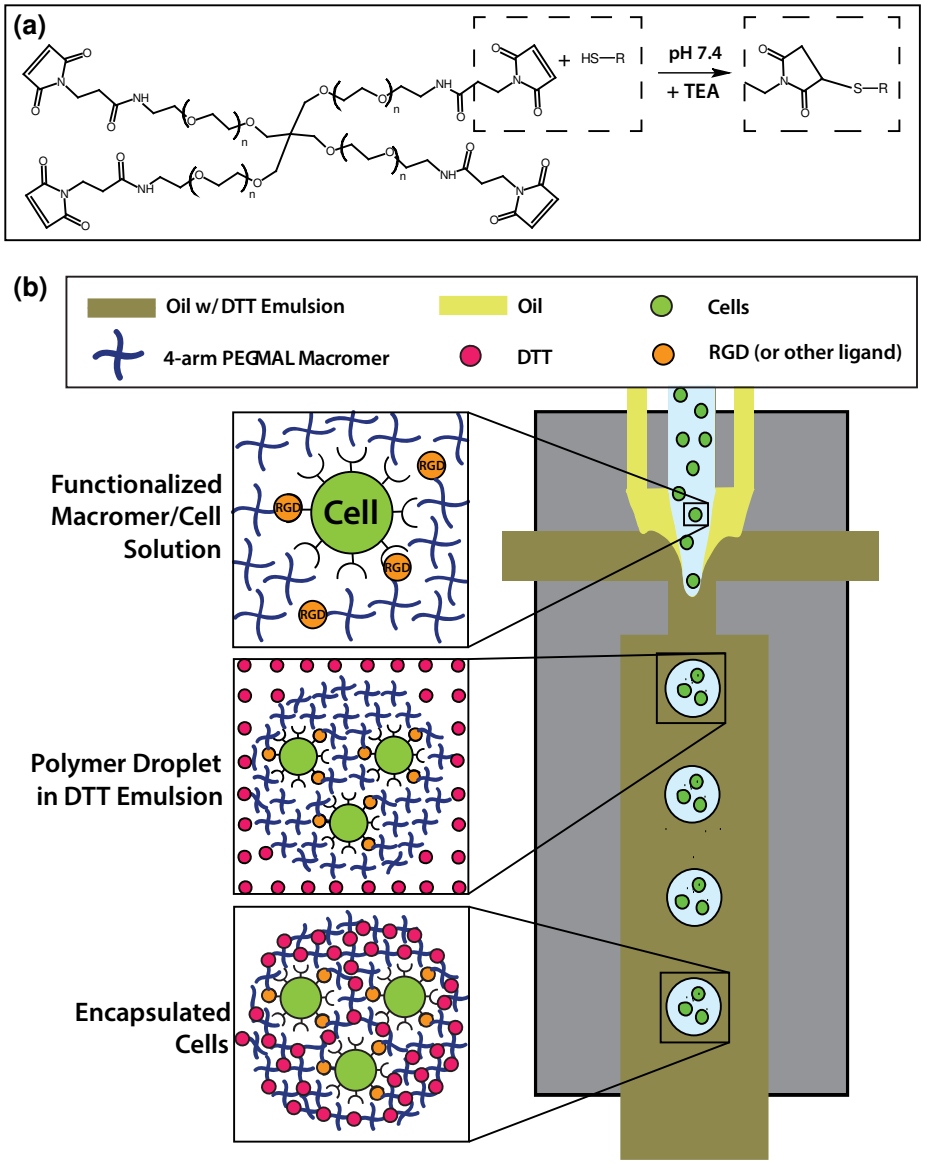

Figure 8. PEG-4MAL for microencapsulation of cells and proteins in a flow-focusing microfluidic chip using a cytocompatible crosslinking reaction. (a) PEG-4MAL macromer consists of a 4-arm branched PEG backbone modified with a maleimide group terminating each arm. At physiological pH, free thiol-containing molecules undergo a Michael-type addition reaction with maleimides, forming a covalent bond to macromer. This reaction is facilitated by nucleophilic buffers such as triethanolamine (TEA), and can be used to either functionalize the

macromer or crosslink macromer into a hydrogel network. (b) A microfluidic device with flow focusing geometry is utilized to produce microgels. A co-flowing oil phase shields an aqueous macromer solution, containing cells and/or proteins, from the crosslinker-containing oil phase as the macromer solution approaches the flow focusing nozzle. After droplet formation, the DTT emulsion rapidly crosslinks macromer solution into cell- or protein-laden microgels.

Precise control of particle size and monodispersity are critical for many applications of microgels, and the microfluidic platform affords this control over a wide range of particle sizes. We varied macromer solution and continuous phase flow rates for a device with a 300 μm nozzle, and measured the corresponding droplet size for each flow rate (Figure 9). No cells were encapsulated in this application. Microgels with a wide range of sizes, ranging from 20 to 400 μm, could be produced on the same device; however, several flow regimes produced microgels with undesirable polydisperse distributions (coefficient of variation, CV>10%). Importantly, flow rate combinations were identified that produced a range of microgel sizes from 135 – 325 μm with monodisperse populations (CV< 5%). An example of one of these flow rates is shown in figure 2, along with several other representative flow regimes, including one regime that does not produce droplets and one that produces a very polydisperse (CV = 22%) microgel population. Although a device with fixed geometry is capable of producing a wide range of particle sizes, droplets should be generated with diameters that are 50-100% of the nozzle width to obtain a monodisperse population. Even if polydisperse populations are acceptable, device throughout is

limited, because no droplets were formed for any PEG-4MAL macromer flow rates exceeding 50 µL min^{-1}. If monodisperse populations of microgels are required that are outside the 135 – 325 µm range, the microfluidic device nozzle can be scaled up or down so that nozzle is roughly equal to the desired microgel size.

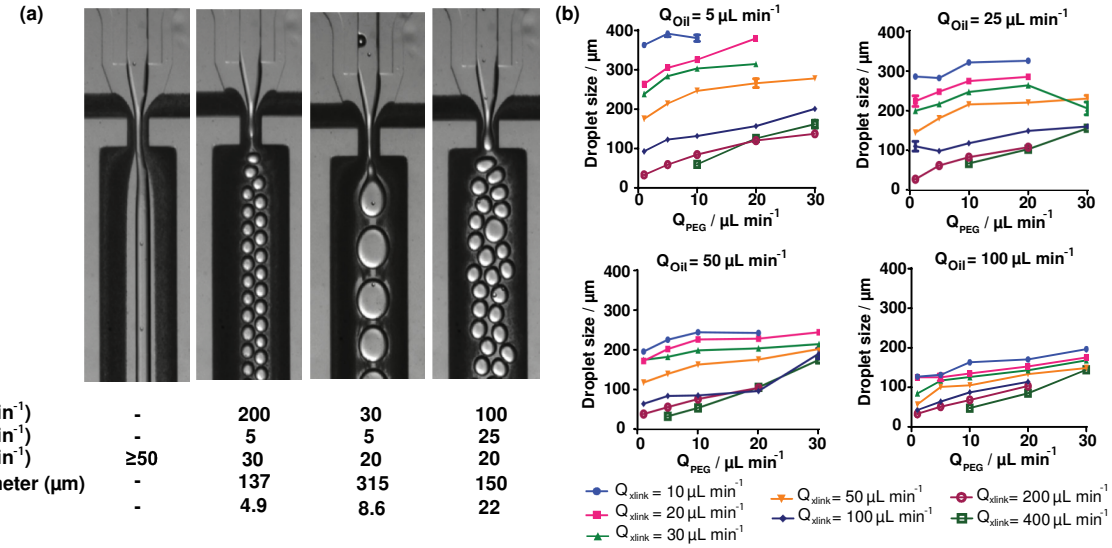

Q_{xlink}(µL min^{-1})	-	200	30	100
Q_{oil} (µL min^{-1})	-	5	5	25
Q_{PEG}(µL min^{-1})	≥50	30	20	20
Mean Diameter (µm)	-	137	315	150
CV (%)	-	4.9	8.6	22

Figure 9. Microgel size and polydispersity can be controlled by altering macromer solution and continuous phase flow rates. (a) Representative images and quantification of microgel diameters are shown for varied flow rates. (l-r) No droplets are produced for PEG-4MAL flow rates of 50 µL min^{-1} or greater. Monodisperse (CV < 5%) populations can be generated for a range of sizes, one of which is shown here. Polydispersity is driven by a complex combination of factors as seen in the final 2 images. (b) Microgel diameter was measured for fluid flow rates that were varied for all combinations of: Q_{PEG} (µL min^{-1}) = 1, 5, 10, 20, 30; Q_{oil} (µL min^{-1}) = 5, 25, 50, 100; Q_{xlink} (µL min^{-1}) = 10, 20, 30, 50, 100, 200,

400. Mean and standard error were plotted as calculated from a minimum of 30 measurements for each condition.

A tunable hydrogel network with selective permeability to biomolecules is essential for cell microencapsulation, because antibodies and immune cells (relatively large objects) must be prevented from reaching encapsulated cells, while nutrients, signaling molecules, and waste (relatively small molecules) must be easily transported across the microgel capsule. Therefore, we investigated the suitability of our microgels for biomolecule release and cell encapsulation by measuring their permeability to relevant molecules of various sizes that were labeled with fluorescent tags. These molecules were encapsulated within microgels generated from a 20 kDa PEG-4MAL macromer, and the rate of their release into buffer was used as a metric of permeability (Figure 10a). 2-NBD-glucose (342 Da) was rapidly released from the gels, fully equilibrating concentration with the buffer by the first fluorescence measurement, 5 minutes after swelling. Similarly, insulin-AlexaFluor488 (5.8 kDa) was rapidly released from the microgels upon swelling, indicating that relevant functional molecules diffuse quickly through the microgel. In contrast, encapsulated IgG-AF488 (~160 kDa) was released from the microgels at a slow rate, suggesting that the microgel capsules are capable of preventing transport and binding of antibodies to encapsulated cells. Release kinetics for BSA (66.5 kDa) fell between IgG and insulin, suggesting that physical molecular entanglement due to the network structure is the determining factor for permeability in our hydrogel network. These

results show nearly 100% release for the smaller molecules glucose and insulin. For the larger proteins BSA and IgG, the release did not reach 50% of the incorporated amount because these larger molecules remain trapped within the tight network structure of the PEG hydrogel. These results for reduced transport and entrapment of IgG support the use of these materials for immuno-encapsulation applications.

As a demonstration of the ability to tune network structure for protein release applications, we encapsulated IgG in microgels made with PEG macromers of different (10 kDa vs. 20 kDa) molecular weights (Figure 10b). As expected, the tighter network mesh of the microgels based on 10 kDa macromers slowed the release of IgG compared to microgels made with 20 kDa macromer. Because altering macromer size results in drastic changes in release kinetics, we expect that other parameters that influence network structure as related to the hydrogel correlation length, such as polymer weight % and crosslinking density, can be systematically varied to obtain desired release kinetics. Flexibility in protein encapsulation, as well as the ability to simultaneously control therapeutic release kinetics and particle size, render this encapsulation platform ideal for a wide range of protein delivery applications

Having shown the ability to exclude high molecular weight proteins such as IgG with minimal impact on the transport of critical molecules such as glucose and insulin, we next examined cell encapsulation applications of this microgel system using clinically relevant cell types. Human pancreatic islets were encapsulated with high efficiency (>99% of islets loaded into microfluidic device

were encapsulated, and 80% of microgels produced contain at least one islet), in microgels made from PEG-4MAL, a polymer that has been shown to support islet engraftment and function.[63] Encapsulated islets were maintained in culture for 8 days with no decrease in viability (Figure 10c,d), demonstrating the capacity of this synthetic hydrogel network to support high viability of these sensitive human cells. This result also shows that any potentially cytotoxic effects of hydrogel precursor constituents (e.g., DTT) prior to network formation are mitigated by the short residence time of cells in crosslinker emulsion. The device used for islet encapsulation was scaled to have a 600 µm nozzle, and produced microgels from 300–800 µm in diameter. As a further demonstration of the versatility of this platform, human mesenchymal stem cells (hMSCs), currently under investigation for various biomedical applications due to their regenerative and immunomodulatory properties, were encapsulated in PEG-4MAL microgels of either 400 µm or 90 µm diameter. These microgels were precisely functionalized with a cell adhesive RGD peptide (2.0 mM) by simply reacting maleimide groups in the macromer with this peptide prior to cell encapsulation and hydrogel crosslinking. This RGD peptide supports cell adhesion, survival and function when incorporated into the PEG-4MAL network.[113] After encapsulation, hMSCs encapsulated in both microgel sizes exhibited high viability (Figure 10e), and hMSCs in 400 µm diameter microgels were maintained in suspension culture for 7 days with no loss in viability (Figure 10f). Therefore, controlled presentation of adhesive peptides to cells encapsulated using a cytocompatible crosslinking reaction provides an environment amenable to long-term cell viability. Such a

microenvironment presenting defined bioactive peptides may be suitable not only for cell encapsulation and delivery,[170] but also for directing stem cell behavior and fate.[171, 172] Additionally, control of microgel size facilitates optimization for cell delivery applications.

A crucial consideration in the engineering of microgels for cell encapsulation is that critical cell functions are not negatively impacted following encapsulation. To this end, we performed a glucose-stimulated insulin secretion (GSIS) assay to evaluate the function of encapsulated human islets. Bare or encapsulated islets were challenged with either 1.67 mM or 16.7 mM glucose for 30 minutes, and the normalized insulin content from each group was assayed using ELISA. The stimulation index (SI), or ratio of normalized insulin secreted in high glucose group to that of low glucose group, was calculated for both bare and encapsulated islets. No significant difference was found between the groups (Figure 10f), demonstrating that microfluidic-based encapsulation in PEG-4MAL has no deleterious effects on human islet function or viability, and that mass transfer of molecules relevant to islet function is not significantly affected by microencapsulation.

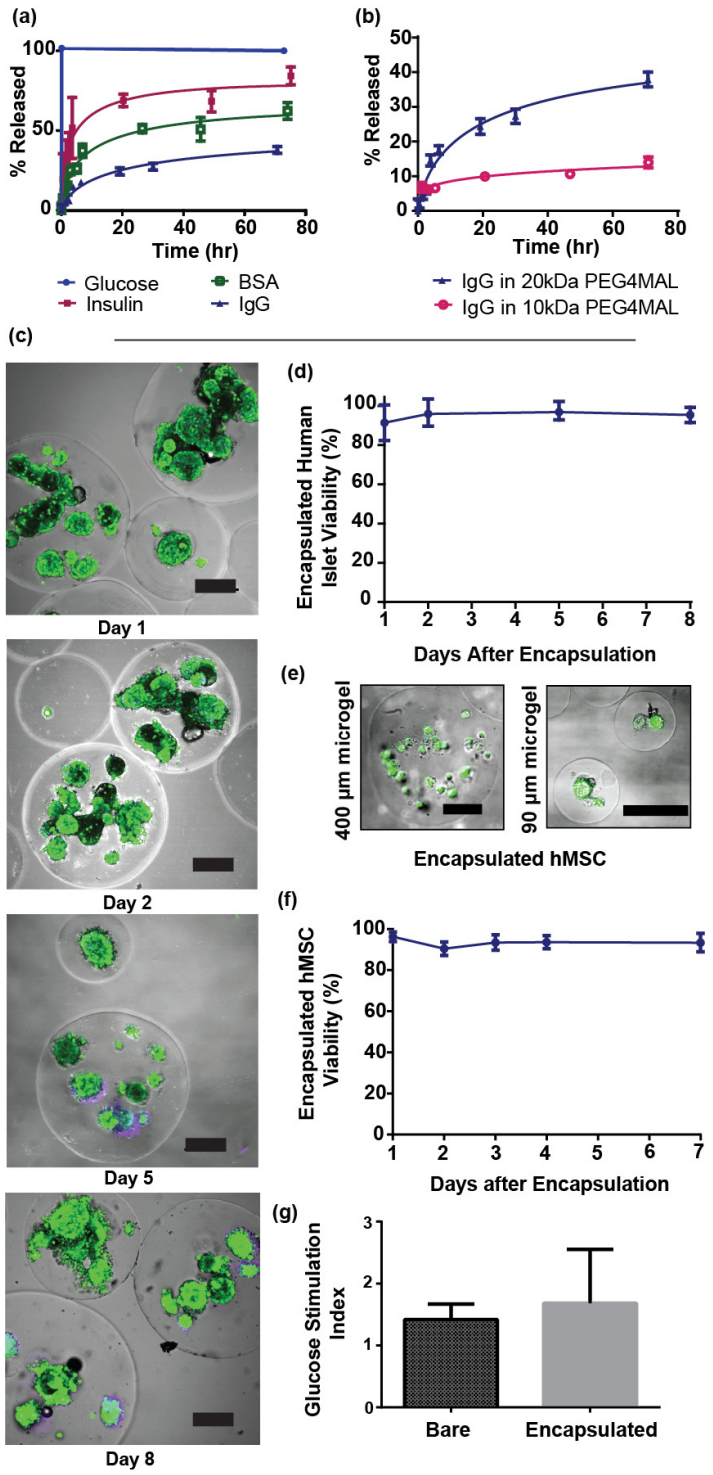

Figure 10. PEG-4MAL microgels exhibit selective permeability to biomolecules and retain viability and function of encapsulated cells. (a) Release kinetics for biomolecules of varying size from microgels (made with 20 kDa macromers)

demonstrate selective permeability. IgG was released from microgels slowly and incompletely. Conversely, glucose and insulin were rapidly released, indicating that mass transport of these smaller, function-preserving molecules is not grossly limited. (b) IgG was encapsulated in PEG-4MAL prepared from macromers of 10 kDa or 20 kDa, and the tighter network structure generated with smaller macromer decreased permeability of microgel to IgG. (c) Human islets maintain high viability in culture after encapsulation. On days 1, 2, 5, and 8 after microencapsulation, viability of human pancreatic islets was imaged (c) (scale bars = 200μm) and quantified (d) using fluorescent area ratios between TOTO-3 iodide (dead, purple) and calcein AM (live, green). (e) Human MSCs were encapsulated in microgels of various sizes (scale bars = 100 μm), and viability of hMSCs encapsulated in 400 μm microgels was quantified for 7 days post encapsulation. (f) No significant loss in viability was noted for hMSCs. (g) A glucose-stimulated insulin secretion assay, performed one day after human islet encapsulation, shows no significant difference between bare and encapsulated islets, demonstrating no functional losses in microencapsulated cells.

The high potential of synthetic hydrogel microencapsulation for cell and protein therapeutics has been limited by the lack of synthetic polymer systems with tunable capsule size, cytocompatible crosslinking reactions, rapid crosslinking rates, adequate biomolecule permeability, and ease of functionalization with bioactive molecules (e.g., adhesive peptides). Using a synthetic hydrogel system with tunable network and crosslinking characteristics and a microfluidics encapsulation platform, we have created an integrated and

robust strategy for microencapsulation of cells in which we can control capsule size and local cellular microenvironment. Additionally, microgel network structure can be tuned to optimize permeability of the capsule to molecules of various sizes. We have demonstrated proof of concept with two different clinically relevant human cell types, but the versatility of this strategy will allow it to be tailored to fit diverse engineering applications.

2.3 Experimental Section

2.3.1 Microfluidic device preparation

PDMS microfluidic flow focusing devices were cast using soft lithography from silicon and SU8 masters that were fabricated by the Stanford Microfluidics Foundry. Devices with 300 µm nozzles were bonded directly to glass slides after treatment with air plasma. 600 µm nozzle devices were manufactured by first bonding mirror-image PDMS channels, each with 300 µm depth, together to create a channel with 600 µm depth.

2.3.2 PEG-4MAL microgel formation and particle encapsulation

Flow-focusing microfluidic geometry was utilized to form polymer droplets. Both shielding and crosslinker phases consisted of light mineral oil (Sigma) with 2% SPAN80 (Sigma). The crosslinker phase also contained an emulsion, at a ratio of 1:15, of 20 mg/mL dithiothreitol (DTT) (Sigma) in PBS. A co-flowing shielding phase protected the macromer solution – a 5% PEG-4MAL (10 kDa or 20 kDa, Laysan Bio) solution containing molecules or cells to be encapsulated – from the crosslinker phase until droplets of the macromer solution were formed. DTT

rapidly diffused into macromer droplets, forming crosslinked microgels. To functionalize hydrogel with GRGDSPC ('RGD', AAPPTec), macromer was reacted for 20 minutes before encapsulation with 2.0 mM RGD in buffer solution containing 4 mM triethanolamine (Sigma). After formation, microgels were washed 5 times by centrifugation to remove mineral oil and excess DTT.

2.3.3 Microgel size control

To characterize the relationship between microgel size and the various macromer solution and continuous phase flow rates, hydrogel droplets were generated using computer-controlled syringe pumps, and were measured while still in the microfluidic chip. Harvard Apparatus Elite syringe pumps were computer controlled using FlowControl software to pump inlet solutions at various flow rates. Video was recorded during droplet generation using a Hammamatsu ORCA-ERA 1394 camera connected to a Nikon TE300 microscope. Droplet diameter was measured using ImageJ analysis software. The coefficient of variation (CV) was calculated for each flow rate combination by dividing the standard deviation of the sample by its mean. At least 30 microgels were measured for each flow rate combination.

2.3.4 Protein encapsulation and release

AlexaFluor488-labeled IgG (goat anti-rabbit IgG, Life Technologies), bovine serum albumin-AlexaFluor488 conjugate (Life Technologies), 2-NBD-glucose (Life Technologies) or insulin (Sigma) tagged with AlexaFluor488 was dissolved in a 5% PEG-4MAL (10 kDa or 20 kDa) solution before being microencapsulated

by macromer droplet gelation. To prevent proteins from being crosslinked by the macromer, thiols were capped using aminoethylate reagent (Thermo Scientific) according to product instructions. Particles were washed and resuspended in PBS and divided into 5 replicates containing 2 mL total volume. 50 µL samples were taken of supernatant alone, as well as of supernatant containing well-mixed, protein-laden microgels. These samples were placed in a 96 well plate, and their fluorescent intensity was measured using a Perkin Elmer HTS 7000 plate reader. To generate release curves, supernatant samples were collected over the course of 3 days, and their fluorescent intensity was measured. Protein release was normalized by setting fluorescent intensity of the supernatant alone correspond to 0% protein released, and fluorescent intensity of the buffer/microgel mixture correspond to 100% protein released. This data was plotted using GraphPad Prism, and exponential best fit curves were calculated from normalized data.

2.3.5 Human MSC encapsulation and viability assay

Passage 3 hMSCs (Texas A&M Health Science Center College of Medicine) were trypsinized and washed 3 times with PBS before being suspended in RGD-functionalized macromer solution (5% wt macromer) at a concentration of 5×10^6 cells/mL. Generation and subsequent gelation of cell-laden macromer solution droplets, using a microfluidic device with a 300 µm nozzle, resulted in microencapsulated hMSCs. These cells were maintained under static culture conditions in chemically defined MSC media (Lonza) for 7 days, with media changes every 2 days. On days 1, 2, 3, 4, and 7, microencapsulated cells were

removed from culture, stained with Calcein AM and TOTO-3 iodide (Life Technologies) for 15 minutes, washed, and resuspended in fresh media. At least 200 cells were imaged each day using a Nikon Eclipse Ti microscope, and their viabilities were assessed based on fluorescent signal. ANOVA analysis was performed using GraphPad Prism software. The percent viability was calculated by taking the ratio of live cells to total cells. Viability data was plotted using GraphPad Prism. ANOVA analysis between the groups found no significant difference in viability, and a student's t-test between days 1 and 7 also found no significant difference in viability.

2.3.6 Human islet encapsulation and in vitro characterization

Human pancreatic islets (PRODO Laboratories and the Integrated Islet Distribution Program) were suspended at a concentration of 2 x 10^4 IEQ/mL in culture media containing 5% (w/v) macromer. A microfluidic device with a 600 µm nozzle was used for droplet generation and subsequent crosslinking of the macromer solution, resulting in microencapsulated islets. After microencapsulation, islets were washed 5 times with media (PRODO labs PIM(S)), placed in fresh media, and allowed to recover overnight. On days 1, 2, 5, and 8 after encapsulation, islets were stained with Calcein AM and TOTO-3 iodide (Life Technologies) for 15 minutes, washed, and resuspended in fresh media. At least 74 islets were imaged each day using a Nikon Eclipse Ti microscope, and their viabilities were assessed based on fluorescent signal. For each islet, dead cell area to total islet area was computed, and this fraction was subtracted from 100% to obtain percent viability. ANOVA analysis was performed

using GraphPad Prism software, and no significant difference in viability was found. On day 1 following encapsulation, a glucose-stimulated insulin secretion assay was performed. Islets were washed and were equilibrated using 1.67 mM glucose in Hanks Buffered Salt Solution for 30 minutes. Two groups, containing 5 replicates of approximately 10 islets each, were collected from both microencapsulated and bare islets. One group from each treatment was incubated with high (16.7 mM) glucose HBSS, and the other group was incubated with low (1.67 mM) glucose HBSS for one hour. Supernatant from each sample was collected, and insulin content was quantified using human insulin ELISA (Sigma). DNA from each sample was then quantified using a Quant-iT PicoGreen kit (Invitrogen). Insulin secretion was normalized to DNA content for each well. The Stimulation Index for each replicate was calculated by taking the ratio of normalized high glucose insulin secretion to normalized low glucose insulin secretion (n=5). Groups were compared using a student's t-test in GraphPad Prism. Human islets and MSCs were obtained by third party distributors, and consent was provided by donors or next of kin.

CHAPTER 3: TRANSPLANTATION OF MICROENCAPSULATED ISLETS IN PEG-4MAL HYDROGELS WITH OPTIMIZED CELL-MATRIX INTERACTIONS FOR TREATING TYPE 1 DIABETES

3.1 Abstract

Encapsulation of islets in alginate hydrogel microspheres (microgels) can provide a sufficient immuno-isolation barrier to mitigate allogeneic rejection when delivered intraperitoneally (IP) to diabetic recipients. However, due to their fabrication method, alginate microgels are large relative to islets and the IP space has low vascular density, so diffusional limitations contribute to gradual graft destruction. Additionally alginate does not allow for recapitulation of native islet microenvironment through adhesive signaling. We previously developed a microfluidic platform for the size-controlled microencapsulation of islets in 4-arm poly(ethylene glycol) terminated with maleimides (PEG-4MAL), which is a hydrogel can be readily functionalized with thiolated bioactive molecules. Here, we optimize the composition of PEG-4MAL hydrogels to support islet function in vitro, and compare the ability of PEG-4MAL and alginate microencapsulated islets to support islet health in vivo.

3.2 Introduction

Islet transplantation can restore glycemic control in patients with Type 1 diabetes. However, transplantation of islets from multiple donors is required to restore recipient insulin independence, which exacerbates demand on limited donor

tissue, and islet grafts are prone to gradual destruction due to allo- and auto-immune reactivity, even with improved immuno-suppression regimes [47]. The current clinical standard for islet transplantation involves intrahepatic infusion of islets, which contributes even further to graft destruction by exposing directly to host blood and thereby to instant blood-mediated inflammatory reaction (IBMIR) instigated by platelet and complement activation, resulting in immediate loss of 50-60% of transplanted cells [51, 53]. Because this transplantation strategy requires long-term immunosuppression and results in islet destruction, significant efforts have been exerted to identify alternative delivery strategies.

Encapsulation of islets in alginate microspheres (microgels) before transplantation into diabetic recipients can establish an adequate immuno-isolation barrier to mitigate allogeneic rejection. However these microgels are typically large compared to islet size due to limitations electrostatic droplet extrusion with alginate, and therefore constitute a significant diffusional barrier—not only to immune cells, but also to insulin, glucose, oxygen, and other molecules critical to cellular function. Furthermore, alginate is not easily modified for presentation of bioactive molecules, and so cannot recapitulate important aspect of the native islet microenvironment such cell adhesion binding sites, which have been shown to be important for islet survival and function. The synthetic hydrogel PEG-4MAL (4 arm polyethylene glycol terminated with maleimides) can be easily modified with thiolated bioactive molecules, allowing precise control of islet microenvironment, and has tunable permeability. Therefore PEG-4MAL is an ideal candidate polymer for immunoisolation

applications. We have developed a microfluidic device for the size controlled microencapsulation of islets in PEG-4MAL microgels that simultaneously enables reduction in microgel diameter and recapitulation of adhesive signaling in the islet microenvironment[146], but microgel composition has not been optimized.

Islet encapsulated in alginate microgels are usually transplanted into the IP space, which abrogates IBMIR mediated islet loss, but this site provides poor access of islets to host circulation. Rapid transport of oxygen, insulin, and glucose between transplanted islets and host circulation is required to maintain effective glycemic control. To enable this rapid transport, islets must be immobilized within a confined location near a dense vascular bed. We have previously developed a vasculogenic PEG-4MAL hydrogel that releases VEGF as it is degraded by invading cells, resulting in increased vascularization and function of transplanted allogeneic islets delivered to the small bowel mesentery (SBM)[63]. We have since identified a transplant sites that results in better vascularization and function than the SBM--the epididymal fat pad (EFP), a highly vascularized membranous tissue that is the murine equivalent of the human omentum[publication under review]. While immuno-isolation precludes direct vascularization of islets, the diffusional barrier between islets and host circulation can be minimized by decreasing encapsulating microgel diameter and simultaneously instigating new vascularization around microgels.

Here, we optimized PEG-4MAL hydrogel composition for supporting islet health and function by testing an array of adhesive ligands as well as different

crosslinkers in vitro. Subsequently, we compared the ability of single donor islet mass to restore euglycemia in syngeneic recipients, when islets were unencapsulated, or were microencapsulated using optimized PEG-4MAL or alginate. Microencapsulated islets are compared in two different transplant sites, the EFP and IP space. Islets microencapsulated in optimized PEG-4MAL restored glycemic control better than islets microencapsulated in alginate and equally as well as unencapsulated islets when delivered to epididymal fat pads in diabetic syngeneic mice within bulk vasculogenic hydrogels. Lectin staining of functional vasculature confirmed that microencapsulated islets were not directly vascularized, but that vessels grew in close proximity to microgels, which supported islet graft function.

3.3 Experimental

Animals. Animal experiments were performed with the approval of the Georgia Tech Animal Care and Use Committee with veterinary supervision and within the guidelines of the Guide for the Care and Use of Laboratory Animals. In syngeneic studies, C57BL/6J male mice (10-14 weeks) were used as recipients and diabetes was induced by single dose streptozotocin i.p. injection (200 mg/kg) at pre-operative day 5. C57BL/6J female mice (10-14 weeks) were used as islet donors in transplant studies and for microgel in vitro characterization. Lewis rats (11-15 weeks) were used as donors for all bulk gel *in vitro* studies.

Islet isolation. Islets were isolated by pancreatic perfusion with Liberase TL (Roche), 10 min of digestion at 37^0C with gentle shaking, and ultra-pure (80-90%) islet separation from acinar using standard Ficoll gradients (Mercodia: 1.108, 1.096, 1.069, 1.037). Islets were counted using the standard islet equivalent method and dithizone staining. Islets were cultured in CMRL-1066 complete medium (0.1 g/L L-glutamine, 25mM HEPES, 1% Pen/Strep, 10% FBS).

Synthetic hydrogel optimization. To optimize hydrogel composition for islet delivery, a series of experiments was performed in which islets were bulk encapsulated in 50µL hydrogel constructs with varied chemistry and were cultured for 6 or 7 days before islet health and function were characterized. All synthetic gels consisted of 6% (w/v) PEG-4MAL (Laysan Bio) functionalized with 2mM ligand density for all adhesive ligands tested. These hydrogels were crosslinked with varied dithiol molecules between experiments. Groups labelled 'nondegradable' are crosslinked with entirely DTT (Sigma) or PEG dithiol (PEG-DT, 226Da, Sigma). Groups labelled 'degradable' contain ½ nondegradable crosslinks (as specified per experiment) and ½ degradable crosslinks supplied by the peptide GCRDVPMSMRGGDRCG (VPM), which can be cleaved by MMPs. Bulk alginate hydrogels were made by first suspending islets in 50µL 1.6% Ultra-Pure Low Viscosity Mannuronic (UP-LVM) alginate (Novomatrix) dissolved in PBS -/- (Gibco). Alginate-islet mixture was pipetted into a silicone mold which was submerged in 1.5% BaCl2-MOPS crosslinking solution (50 mM BaCl2,

10mM MOPS, 140mM D-Mannitol, 0.025% vol/vol Tween-20, pH 7.4) for 10 minutes. After crosslinking, construct was washed in complete CMRL-1066 medium twice before culture. After encapsulation, all islets were cultured in complete CMRL-1066 with media changes every 2 days. On day 6 or 7 after encapsulation, glucose stimulated insulin secretion was measured for all encapsulated islets.

To test glucose stimulated insulin secretion (GSIS), islets were first equilibrated for 1 hour in low glucose (1.67mM) solution dissolved in DMEM containing 1%BSA. After equilibration buffer was discarded, 800µL of the same solution was added to each sample and was removed after one hour. Subsequently, a high glucose (16.7mM) solution was added to islets for an hour to stimulate insulin secretion. After collecting buffer containing high glucose sample, low glucose buffer was added again for one hour and then was collected for analysis. Insulin from all collected buffer samples was quantified by ELISA. Glucose Stimulation Index was calculated as the ratio of insulin secreted during high glucose incubation to the insulin secreted during initial low glucose incubation, and acts as a measure of glucose responsiveness.

Following GSIS, various staining and imaging protocols were used to characterize islet health. To image live and dead cells, islets were stained with calcein AM and TOTO-3 iodide, respectively (Thermo Fisher), and maximum intensity projections are shown for z-stacks of representative islets obtained on Nikon Eclipse confocal microscope. Some samples were stained for caspase 3/7

activation using CellEvent kit (Thermo Fisher) as a marker of apoptosis and are presented superimposed on transmitted light images. Some samples were imaged using TUNEL assay (Click-iT green, Thermo Fisher) for DNA fragmentation, a more definitive marker of apoptosis. DAPI was used to counterstain nuclei blue on all TUNEL samples. Phase microscopy images were captured on an EVOS XL cell imaging system.

PEG-4MAL microencapsulation. Islets were microencapsulated in PEG-4MAL using a scheme similar to one reported previously [146]. One day after isolation, islets were dispersed in 6% PEG-4MAL with 2mM RGD made in a buffer of 1 part OptiPrep density gradient (Sigma):4 parts PBS +/+ to reduce islet settling. Droplets were formed from this dispersion in Mineral Oil (Sigma) containing 2% Span80 (Sigma) utilizing flow focusing microfluidics, and then droplets were crosslinked by a DTT emulsified into the mineral oil continuous phase (Figure 11). After crosslinking, encapsulated islets were washed with complete CMRL 1066 medium 4 times by centrifugation to remove mineral oil, and were resuspended in complete CMRL-1066 medium for overnight culture.

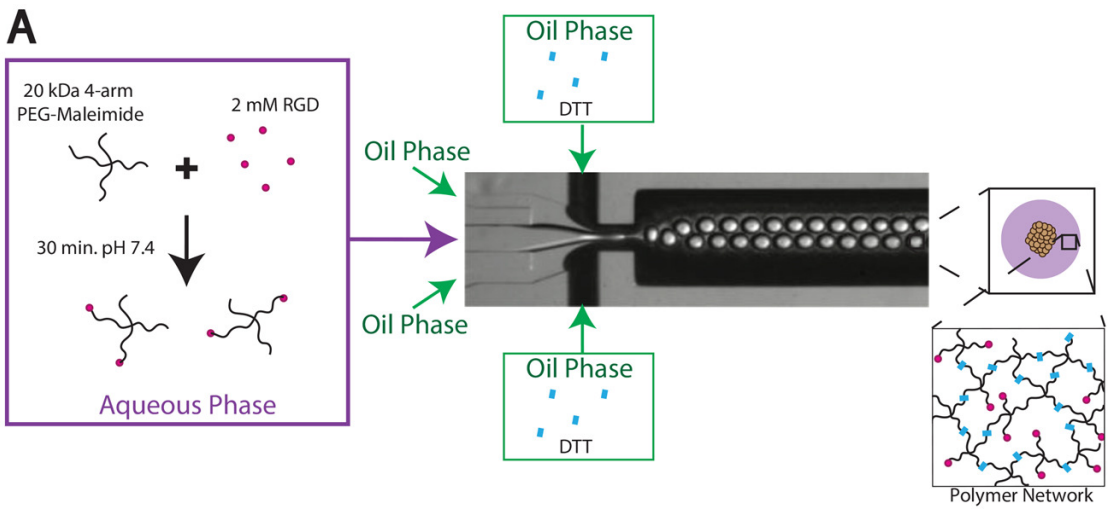

Figure 11. This schematic illustrates microfluidic encapsulation of pancreatic islets in PEG-4MAL microgels, which support islet function and may function as immunoisolation barriers.

Alginate microencapsulation. One day after isolation, islets were dispersed in 1.6% Ultra-Pure Low Viscosity Mannuronic (UP-LVM) alginate (Novomatrix) dissolved in PBS -/- (Gibco). Alginate-islet mixture was extruded through a 0.5 mm diameter needle into a 1.5% BaCl2-MOPS crosslinking solution (50 mM BaCl2, 10mM MOPS, 140mM D-Mannitol, 0.025% vol/vol Tween-20, pH 7.4) using an electrostatic droplet generator (Nisco Engineering, Zurich, Switzerland). Capsules were allowed to crosslink 10 minutes, washed 3 times with PBS -/-, and resuspended in complete CMRL-1066 medium for overnight culture.

Islet viability in microgels. Islet viability was assessed after 48 hours encapsulation or unmodified culture. Metabolic activity was assessed via Alamar Blue (Invitrogen) incubation (6 hours) (n=3), and fluorescence was normalized to

results from unencapsulated islets. Islet health was also assessed by Live/Dead Imaging (Invitrogen; Live: Calcein, Dead: Toto-3-Iodide).

Modified GSIS studies with microgels. 48 hours post encapsulation, islets were suspended in KREBs buffer (99mM $NaCl_2$, 5mM KCl, 1.2mM KH_2PO_4, 1.2 $MgSO_4$, 2.6mM $CaCl_2$, 26mM $NaHCO_3$, and 0.2% BSA) for static incubation. Unmodified or encapsulated islets were exposed to sequential D-glucose challenge in 30 minute intervals (3.3 mM, 6.6 mM, 9 mM, 13.2 mM, 16mM, 13.2 mM, 9mM, 6.6 mM, 3.3 mM) to evaluate insulin secretion and diffusional delays due to encapsulation. 1 mL buffer was collected at each interval for evaluation by insulin ELISA (Mercodia). Insulin secretion was normalized to aliquot DNA content by Picogreen DNA kit (Invitrogen). (n=3, 200IEQ/n)

Intraperitoneal (IP) encapsulated islet delivery. PEG-4MAL or alginate microgels containing islets were delivered by pipette in sterile saline (500 uL) to the peritoneal cavity through a 1 cm midline incision through the peritoneum. Peritoneum was closed via sutures and skin secured via surgical staples. Transplant recipients were monitored for nonfasting blood glucose levels for 75-120 days. Grafts were retrieved after euthanasia by a peritoneal flush with saline.

Epididymal Fat Pad (EFP) islet transplant via vasculogenic hydrogel delivery vehicle. One day post-encapsulation, 500 IEQ unmodified or encapsulated islets were dispersed within vasculogenic hydrogels (50 uL) to form two equal volume gels (25 uL each) for delivery to two EFP per animal. Gels were fabricated as follows: a sterile 5% (final, w/v) solution of 4-arm polyethylene

glycol (PEG)-maleimide monomer (20 kDa , Laysan Bio) was functionalized with 1.0 mM RGD peptide and 10 µg/mL VEGF (where applicable) at 37º C for a minimum of 15 min in gel buffer (PBS, 25 mM HEPES (Cellgro)). A separate crosslinking solution of VPM peptide was prepared in gel buffer. The pH for all solutions was adjusted to 7.0-7.5. To generate gels, functional macromers were mixed with unmodified or encapsulated islets and rapidly mixed with VPM crosslinker on a sterile paraffin surface, and swelled in complete CMRL-1066 for a minimum of 30 minutes prior to transplant. Peptide sequences: VPM (GCRDVPMSMRGGDRCG); RGD (GRGDSPC).

Mice were anesthetized with 2% isoflurane prior to surgery. A midline incision was made through the peritoneum and both EFPs exposed and spread on sterile gauze via manipulation with forceps and saline wash. One 25 uL islet-containing vasculogenic construct was deposited on each EFP surface (total of ~500 IEQ per recipient), and the EFP gently wrapped around the construct. To seal the EFP, a 30 uL gel (10% 10 kDa PEG, 1mM RGD, VPM crosslinker) was deposited on the surface of the enclosed EFP graft prior to gentle return to the IP space, peritoneal suturing, and surgical staples to secure the skin. Transplant recipients were monitored for nonfasting blood glucose levels for 75-120 days.

For lectin perfusion at experimental endpoint, anesthetized mice were given an intravenous lectin injection (DyLight 488-labeled lectin, 200 µL, Vector Labs) and sacrificed after 15 min, the vasculature flushed with saline prior to graft removal and fixation in 10% buffered formalin. Grafts were stabilized between

glass slides prior to whole-mount imaging on a confocal microscope. Z-stacks of each sample were acquired.

3.4 Results and Discussion

3.4.1 Synthetic hydrogel optimization

Because PEG-4MAL hydrogels can be covalently functionalized with bioactive molecules, encapsulated islet microenvironment can be controlled precisely. Recapitulation of some aspects of native islet microenvironment, such as adhesive cell-matrix interactions, could lead to improved islet health and function. A series of experiments were conducted in order to optimize gel composition for optimal islet function, testing effect of adhesive ligands as well as crosslinkers on function of rat islets encapsulated in bulk hydrogels. Preliminary studies to establish experimental parameters indicated that variability would be high and that islets should be cultured in hydrogels long enough for differences would become apparent. Islet viability was consistently impaired by day 7 post encapsulation, so this time point was selected for end point assays.

In the first of these experiments, islets were encapsulated in PEG-4MAL hydrogels which had been functionalized with an array of ECM derived peptide sequences with reported adhesive function. Hydrogels in this experiment were crosslinked with ½ degradable VPM and ½ nondegradable DTT crosslinks. After 7 days in culture, islets functionalized with all adhesive ligands had comparable viability by visual inspection, with the exceptions of YIGSR, AG73 and

scrambled, non-adhesive RDG which led to widespread cell death (Figure 12A). Cells imaged in these groups appeared to remain rounded, forming minimal adhesive interactions with surrounding hydrogel when contrasted with cells in hydrogels with the other adhesive peptides tested. All treatment groups had reduced viability compared to the unencapsulated control, but this could be due to the inability of dead cells to evacuate microgels. Results of glucose stimulated insulin secretion (GSIS) show impaired glucose responsiveness (GSI<1) of islets encapsulated in RDG and YIGSR, consistent with reduced viability in these groups (Figure 12B,C). However, islets encapsulated in hydrogels containing AG73 were glucose responsive even though they had impaired viability and did not appear to form adhesive interactions. Islets encapsulated in hydrogels containing the peptides IKVAV, C16, and A2G10 appeared to form cell adhesive interactions, maintained acceptable viability until day 7, and maintained glucose responsiveness (GSI>1), producing similar levels of insulin in GSIS assay. Although these adhesive peptides supported islet function, none were as effective as RGD, which maintained islet performance at comparable levels to the unencapsulated islet control. Because of these findings, only the adhesive peptide RGD and the scrambled non-adhesive peptide RDG were used in subsequent experiments.

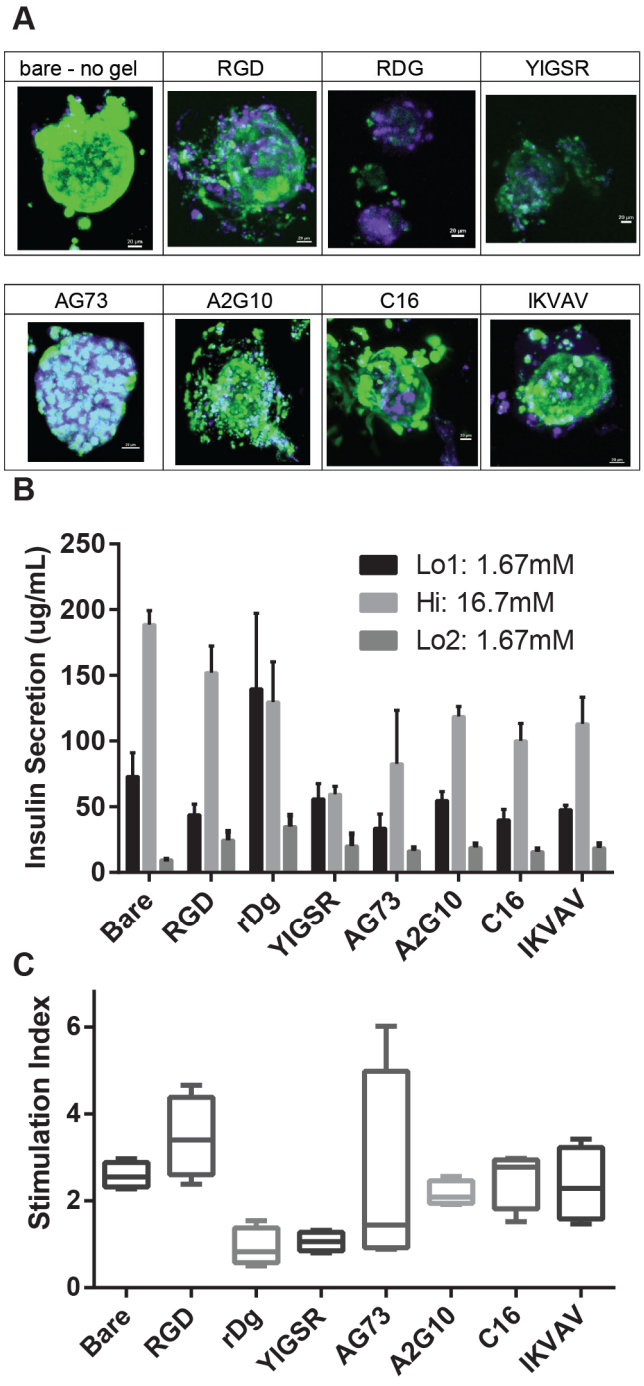

Figure 12. Viability and functional data are shown for rat islets encapsulated in bulk hydrogel constructs containing various adhesive ligands, and cultured for 7 days. (A) Representative live/dead images of islets encapsulated in each

adhesive demonstrate varied cell-matrix interactions and cell responses, as discussed in the text. (B,C) Support of glucose responsiveness and insulin secretion also varied between adhesive ligands, as seen by in raw insulin, as well as glucose stimulation index plots. Hydrogels functionalized with RGD supported the best glucose responsiveness and greatest magnitude of insulin secretion on high glucose stimulation, comparable to unencapsulated islets (n=4, 150IEQ each). Hydrogels were crosslinked with ½ DTT (nondegradable) and ½ VPM (degradable peptide) crosslinks.

RGD was identified as the best available adhesive peptide for supporting islet function; however, this experiment was performed using hydrogels containing protease degradable crosslinkers, because their increased gelation times facilitated handling. Hydrogels with degradable crosslinks eventually lose integrity, so hydrogels with only nondegradable crosslinks were investigated for use as effective long term immuno-isolation barriers, in a follow up experiment (Figure 13). For these experiments, DTT was utilized as the non-degradable crosslinker. Additionally, alginate bulk gels were included as a control, because alginate is the current standard for islet encapsulation. Imaging of cells stained to indicate live and dead cells, as well as samples stained for caspase 3/7 activation revealed comparable health of islets in RGD functionalized degradable hydrogels (Figure 13A). Alginate islets stained to indicate live and dead cells looked as healthy as bare controls as well, but notable caspase 3/7 activation was seen in these samples, which suggests declining cell health. Islets in

degradable gels functionalized with RDG and in nondegradable gels with either adhesive ligand had similar, somewhat reduced islet health compared to other groups. Response to glucose challenge was dysregulated in hydrogels functionalized with the scrambled nonadhesive peptide RDG, whichever crosslinker was used (Figure 13B,C). In contrast, RGD functionalized hydrogels supported glucose responsiveness with both crosslinkers, and islets in degradable, RGD functionalized hydrogels had insulin secretion and glucose responsiveness similar to unencapsulated islets. Islets encapsulated in alginate also had similar function to bare islets even though minimal cell-matrix interactions were evident morphologically.

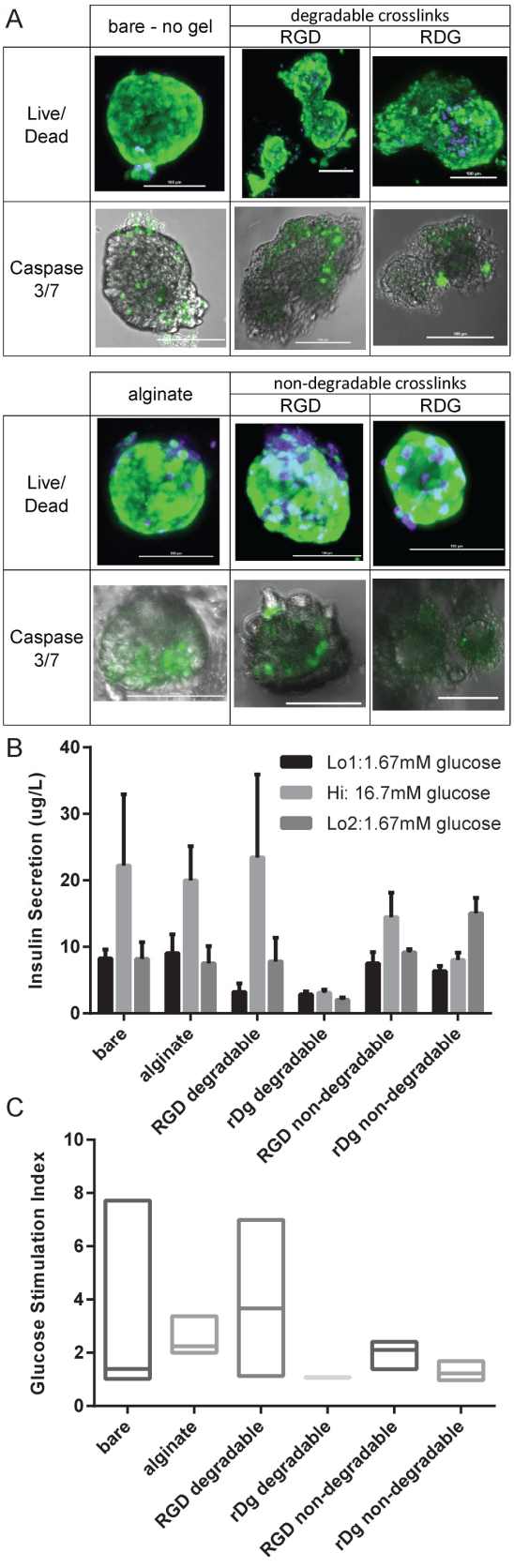
A
bare - no gel
degradable crosslinks
RGD
RDG
Live/ Dead
Caspase 3/7
alginate
non-degradable crosslinks
RGD
RDG
Live/ Dead
Caspase 3/7
B
Insulin Secretion (ug/L)
40
30
20
10
0
Lo1:1.67mM glucose
Hi: 16.7mM glucose
Lo2:1.67mM glucose
bare
alginate
RGD degradable
rDg degradable
RGD non-degradable
rDg non-degradable
C
Glucose Stimulation Index
10
8
6
4
2
0
bare
alginate
RGD degradable
rDg degradable
RGD non-degradable
rDg non-degradable

Figure 13. Viability, apoptosis and functional data are shown for rat islets after being cultured for 7 days encapsulated in bulk PEG-4MAL hydrogels, which were functionalized with RGD or RDG (non-adhesive scrambled peptide), and crosslinked either entirely with DTT (nondegradable) or with ½ DTT and ½ VPM (degradable peptide). Bare (unencapsulated) and alginate bulk gel controls are also included for comparison. (A) Representative live/dead [stained with calcein AM (green) and TOTO-3 iodide (cyan), respectively], and apoptosis [CellEvent caspase 3,7] images of islets encapsulated in each adhesive demonstrate varied cell-matrix interactions and cell responses. (B,C) Support of glucose responsiveness and insulin secretion also varied between adhesive ligands, as seen by in raw insulin, as well as glucose stimulation index plots. Degradable PEG-4MAL hydrogels functionalized with RGD and bulk alginate hydrogels both supported similar glucose stimulated insulin release similar to unencapsulated controls. RGD functionalized hydrogels with nondegradable crosslinks also supported glucose responsiveness at an impaired level. (n=4, 40IEQ each).

Because experiments with islets tend to have high variability, this experiment was repeated a second time. Hydrogels with only nondegradable crosslinks were poorly formed due to inadequate mixing resulting from rapid gelation, and results from these groups are unreliable, but the entireties of data collected are presented in Figure 14. Qualitative assessment of cell-matrix interactions can be seen in images, but in most nondegradable samples, it was difficult to find many islets on day 6 post-encapsulation, prompting early take down of this experiment.

Hydrogels crosslinked with degradable crosslinks were well formed, and results obtained with these samples are consistent with the experiment from Figure 13. Hydrogels functionalized with nonadhesive peptide RDG did not support islet function, but those functionalized with RGD enhanced insulin secretion compared to unencapsulated islet controls. Islets encapsulated in alginate were also glucose responsive, but secreted less insulin than islets encapsulated in synthetic hydrogels with RGD.

Impaired islet health and function were noted when nondegradable DTT crosslinks were exclusively used, as outlined in Figure 13. This potential DTT associated toxicity, along with the marked difficulty of casting uniform nondegradable hydrogels with DTT, motivated us to try using a different non-degradable crosslinker, PEG dithiol (PEG-DT), which had slightly slower crosslinking kinetics compared to DTT. Therefore, rat islets were isolated and encapsulated in bulk gels with identical composition as described before, except with equimolar PEG-DT in place of DTT. Islets in RGD functionalized hydrogels containing degradable crosslinks had similar health to unencapsulated control islets as indicated by live/dead and caspase 3/7 activation and additionally confirmed by the addition of a TUNEL assay for DNA fragmentation (Figure 15A). The TUNEL assay stained cells green, and cells were counterstained with DAPI in blue, but no notable differences were seen by this metric for any samples. Islets encapsulated in hydrogels other than RGD functionalized degradable gels appeared to have impaired viability; especially those in RDG functionalized degradable hydrogels. Functionally, RGD functionalized degradable hydrogels

supported the highest GSI and greatest insulin secretion of any composition tested (Figure 15B,C). Alginate and nondegradable PEG-DT crosslinked PEG-4MAL supported similar, slightly reduced function of encapsulated islets. This finding is consistent between both nondegradable crosslinkers tested, DTT and PEG-DT. It appears, then, that decreased islet function may be associated with the inability of cells to remodel their microenvironment, and is not the result of DTT specific toxicity.

The series of experiments shown here was meant to optimize microgel composition for supporting microencapsulated islet function in immuno-isolation applications. Islet function is best supported in degradable RGD functionalized hydrogels, but degradable crosslinks would result in an eventual break down of the immuno-isolation barrier. PEG-4MAL hydrogels with nondegradable crosslinks persist for months *in vivo*, and, when functionalized with RGD, can support islet function at similar levels to alginate *in vitro*. Because relative islet function did not improve notably when PEG-DT was used rather than DTT, DTT was selected as the nondegradable crosslinker for subsequent studies. A microfluidic scheme has been established for the encapsulation of islets in DTT crosslinked PEG-4MAL microgels, and permeability of these microgels appears promising for immuno-isolation applications [146].

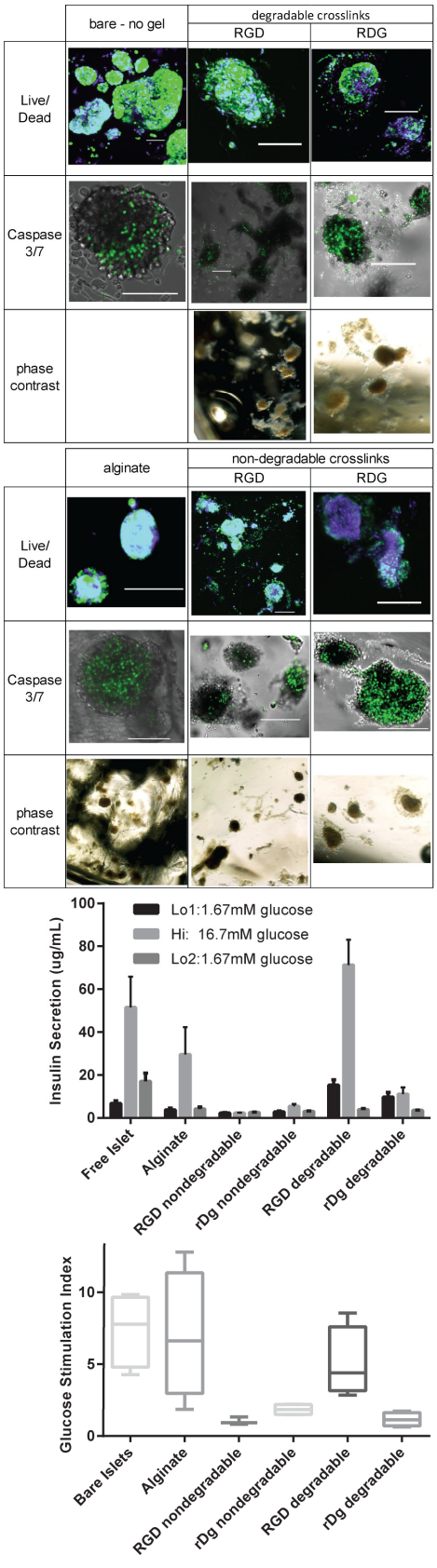
bare - no gel
degradable crosslinks
RGD
RDG
Live/ Dead
Caspase 3/7
phase contrast
alginate
non-degradable crosslinks
RGD
RDG
Live/ Dead
Caspase 3/7
phase contrast
Lo1:1.67mM glucose
Hi: 16.7mM glucose
Lo2:1.67mM glucose
Insulin Secretion (ug/mL)
100
80
60
40
20
0
Free Islet
Alginate
RGD nondegradable
rDg nondegradable
RGD degradable
rDg degradable
Glucose Stimulation Index
10
5
0
Bare Islets
Alginate
RGD nondegradable
rDg nondegradable
RGD degradable
rDg degradable

Figure 14. Viability, apoptosis and functional data are shown along with phase contrast images for rat islets after being cultured for 6 days encapsulated in bulk PEG-4MAL hydrogels, which were functionalized with RGD or RDG (non-adhesive scrambled peptide), and crosslinked either entirely with DTT (nondegradable) or with ½ DTT and ½ VPM (degradable peptide). Bare (unencapsulated) and alginate bulk gel controls are also included for comparison. (A) Representative phase contrast microscopy, live/dead [stained with calcein AM (green) and TOTO-3 iodide (cyan), respectively], and apoptosis [CellEvent caspase 3,7] images of islets encapsulated in each adhesive demonstrate varied cell-matrix interactions and cell responses. (B,C) Support of glucose responsiveness and insulin secretion also varied between adhesive ligands, as seen by in raw insulin, as well as glucose stimulation index plots. Degradable PEG-4MAL hydrogels functionalized with RGD supported glucose stimulated insulin release similar to unencapsulated controls. Bulk alginate hydrogels also supported glucose responsiveness, but at an impaired level. (n=4, 40IEQ each).

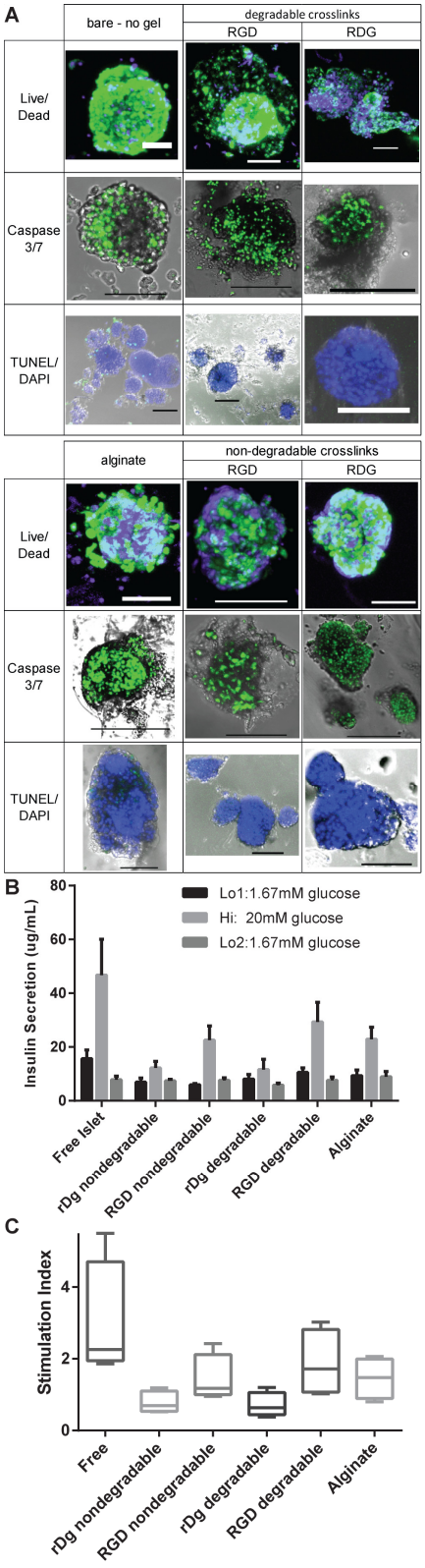
A
bare - no gel
degradable crosslinks
RGD
RDG
Live/ Dead
Caspase 3/7
TUNEL/ DAPI
alginate
non-degradable crosslinks
RGD
RDG
Live/ Dead
Caspase 3/7
TUNEL/ DAPI
B
Lo1:1.67mM glucose
Hi: 20mM glucose
Lo2:1.67mM glucose
Insulin Secretion (ug/mL)
80
60
40
20
0
Free Islet
rDg nondegradable
RGD nondegradable
rDg degradable
RGD degradable
Alginate
C
Stimulation Index
4
2
0
Free
rDg nondegradable
RGD nondegradable
rDg degradable
RGD degradable
Alginate

Figure 15. Viability, apoptosis and functional data are shown for rat islets after being cultured for 6 days encapsulated in bulk PEG-4MAL hydrogels, which were functionalized with RGD or RDG (non-adhesive scrambled peptide), and crosslinked either entirely with PEG-dithiol (PEG-DT) (nondegradable) or with ½ PEG-DT and ½ VPM (degradable peptide). Notably, the nondegradable crosslinker used is not DTT as used in previous experiments presented. Bare (unencapsulated) and alginate bulk gel controls are also included for comparison. (A) Representative live/dead images of islets which had been stained with calcein AM (green) and TOTO-3 iodide (cyan) are shown, along with images showing 2 markers of apoptosis: caspase 3,7 activation (CellEvent, green on transmitted light image) and DNA fragmentation (TUNEL, green and DAPI, blue). (B,C) Bulk alginate hydrogels and PEG-4MAL gels functionalized with RGD supported similar islet glucose stimulated insulin secretion, whether degradable peptide crosslinks were included or not when PEG-DT was used as the non-degradable component of crosslinker. All groups were glucose responsive (GSI>1) on day 6 after encapsulation, but islets in hydrogels functionalized with non-adhesive RDG had notably impaired function. Unencapsulated islet controls had improved glucose responsiveness and insulin secretion compared to any treatment groups tested. (n=4, 150 IEQ each).

3.4.2 Microgel encapsulated islet characterization

Islets were encapsulated in PEG-4MAL microgels with chemical compositions identified in preliminary experiments (2mM RGD, DTT crosslinked), using a flow focusing microfluidic device that was previously reported [146]. 48 hours after encapsulation, islet viability was compared with unencapsulated control islets using Alamar Blue (Figure 16A) or live/dead imaging with calcein AM (green) and TOTO-3 iodide (magenta) (Figure 16C,D). In both comparisons, some minimal reduction in viability was noted in microencapsulated islets. Also 48 hours after encapsulation, kinetics of islet glucose responsiveness were roughly characterized with a modified GSIS experiment. In this experiment, buffer was exchanged every 30 minutes with varying glucose concentration, so any gross impairment of insulin diffusion would manifest as lag time in insulin response. No major lags in insulin release were seen in microencapsulated islets, and glucose responsiveness was at least as good as in unencapsulated control islets (Figure 16B). Taken together, these results indicate that PEG-4MAL microgels functionalized with 2mM RGD and crosslinked with DTT can support encapsulated islet viability and function for 48 hours at comparable levels to unencapsulated control islets, without grossly impairing insulin release kinetics.

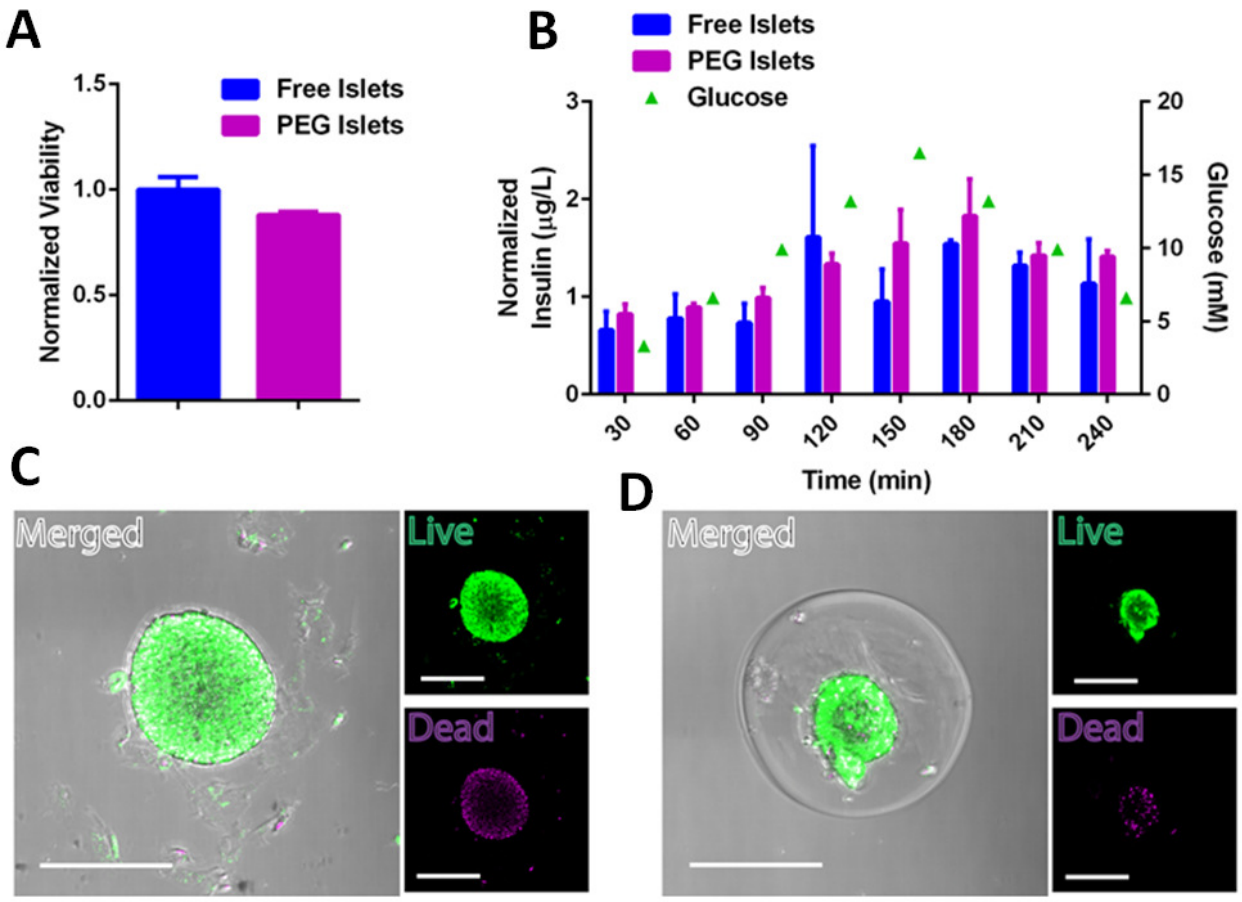

Figure 16. Islets microencapsulated in PEG-4MAL microgels, functionalized with RGD, maintain their viability and function. (A) Islet viability is not significantly reduced by encapsulation as assessed by Alamar Blue. (B) Islets in PEG microgels increase insulin secretion in response to glucose fluctuations with no major capsule associated lag time.

3.4.3 In vivo function of microencapsulated islets

Enhancing vascularization of transplanted islets drastically improves their function in syngeneic models, but encouraging direct vascularization will

simultaneously quicken immune rejection of transplants when immunogenicity is a concern. Immuno-isolation and enhancement of direct islet vascularization are inherently incompatible strategies. However, by decreasing microgel diameter and increasing local vascular density, diffusional lag times caused by immuno-isolating barriers can be minimized. Vasculogenic PEG-4MAL hydrogels that release VEGF on demand can enhance local vascular density at transplanted islets, resulting in improved blood glucose control in a syngeneic murine model of diabetes [63]. Since effective immuno-isolation eliminates direct islet vascularization, we tested whether increasing overall graft vascular supply enhanced function of microencapsulated islets by transplanting microencapsulated islets to diabetic recipients using two different transplant sites, the intraperitoneal (IP) cavity, and the epididymal fat pad (EFP). The IP space has been the most common site of transplantation for microencapsulated islets, but this site has a poor vascular supply. Conversely, the EFP is highly vascularized and microencapsulated islets were delivered to this site in vasculogenic degradable hydrogels, which further improved proximity of microencapsulated islets to host circulation. Islets microencapsulated in either nondegradable PEG-4MAL or the current standard material, alginate, were transplanted to each site in chemically diabetic mice, so the ability of these materials to support *in vivo* islet function could be compared. Islets which were not microencapsulated were also delivered to the EFP in vasculogenic bulk hydrogels as a control. A minimal islet mass of 500IEQ was transplanted per recipient, comparable to single donor human islet transplant. This minimal islet

mass does not always restore euglycemia, but it makes differences in graft function more obvious than in transplants with higher islet loading.

Results of transplant experiment are summarized in a persistence graph of diabetes in islet recipients (Figure 17A). Recipients were no longer considered diabetic when blood glucose stably dropped below 250 mg/dL. Between 20 and 55 days post transplantation, 5/7 recipients receiving PEG-4MAL microencapsulated islets delivered to the EFP in vasculogenic hydrogels became stably euglycemic. Bare islets that were delivered to the EFP in a vasculogenic bulk gel restored euglycemia at similar rate and extent to PEG-4MAL microencapsulated islets, suggesting that nondegradable PEG-4MAL microencapsulation does not impair islet function *in vivo*. Loss of glycemic control upon explant of functional EFP grafts (marked by arrows near day 100), confirmed that euglycemia was maintained by islet graft, and was not due to recovered host function. Conversely, alginate microencapsulated islets delivered to the EFP in vasculogenic hydrogels did not restore euglycemia within 100 days for any of 5 recipients. This could be attributable to increased mass transport limitations introduced by larger alginate microgels, which could instigate hypoxic cell death. All diabetic mice receiving alginate microencapsulated islets in their IP cavity show rapid, promising recovery of glycemic control, but subsequent, gradual reduction of graft function was evidenced by increasing fluctuations in daily blood glucose measurements (Figure 17B). This gradual reduction of function may also be due to the increased diffusional barrier associated with alginate microgels, either by direct means or indirectly by induction of hypoxic

cell death. PEG-4MAL microgels did not support islet function in the IP cavity, with only 1/3 recipients becoming euglycemic around day 30.

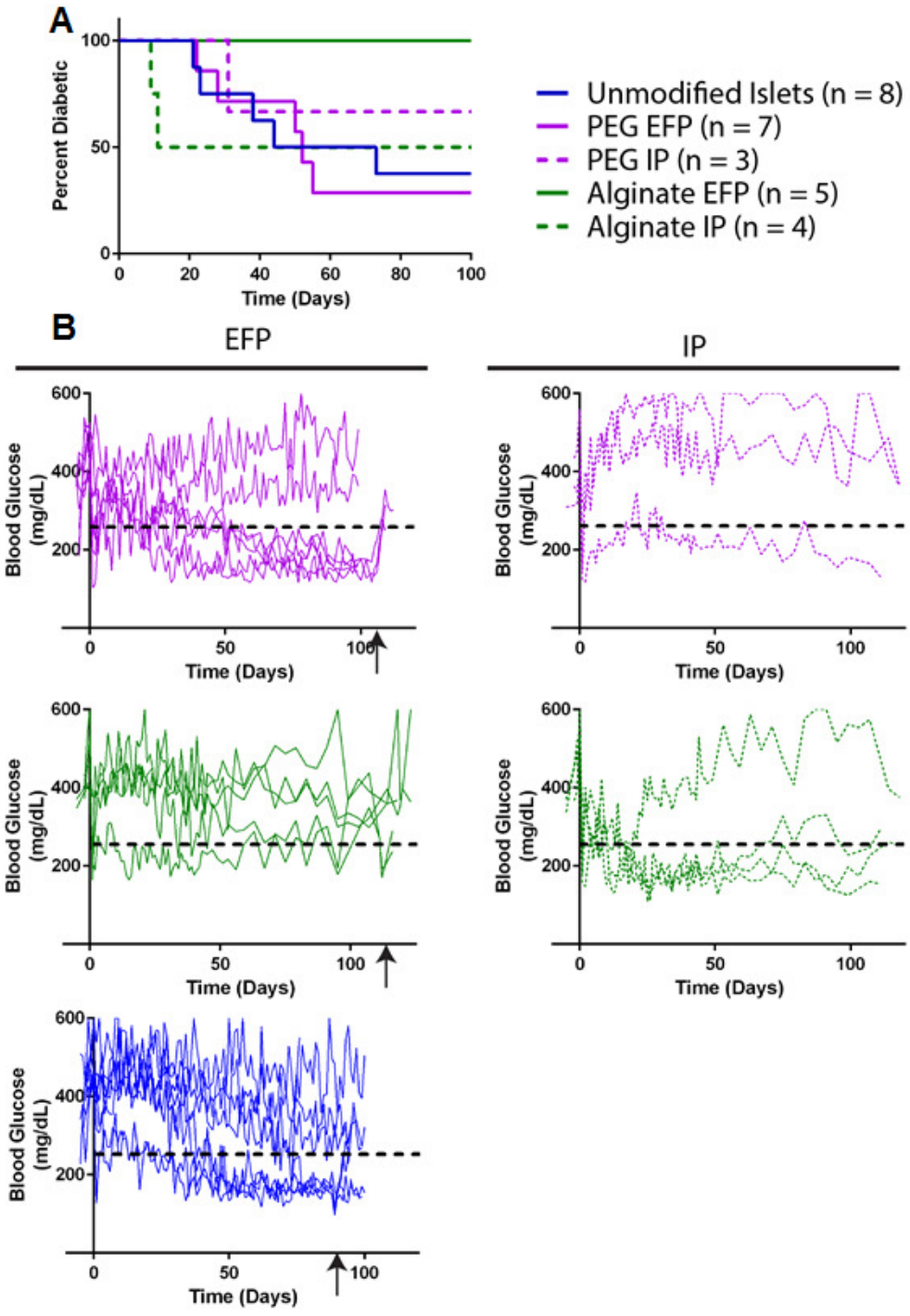

Figure 17. In vivo functional performance of islets microencapsulated using either PEG-4MAL and microfluidic techniques, or alginate and electrostatic droplet extrusion. Data are shown for two separate transplant sites. (A) Persistence of diabetes over after transplantation is summarized for syngeneic, diabetic murine recipients. (B) Daily blood glucose measurements used for production of summary plot are plotted for individual murine recipients. Islets transplanted to the IP space within alginate microgels reversed diabetes more rapidly than any other treatment, but resulted in unstable reversal of diabetes when compared with islets transplanted in microgels to the epididymal fat pad.

3.4.4 Vascularization of microencapsulated islets

Islets transplanted to the EFP were delivered in a vasculogenic bulk hydrogel that served as a substrate for invasion by host vasculature, and released bioactive VEGF as it was degraded. To assess the extent of vascularization, we labelled vasculature by perfusion with lectin in recipients of functional EFP grafts at the experimental end point. Lectin stained EFPs were explanted and functional blood vessels were fluorescently imaged with confocal microscopy. Representative images showing of ingrowth of host vasculature (green) superimposed on transmitted light photos are presented in Figure 18. Islets that were not microencapsulated were highly vascularized and were integrated into host vasculature. Islets microencapsulated in PEG-4MAL or alginate did not integrate with host vasculature because nondegradable microgels prevented invasion of host tissue. New host vasculature was often observed in close proximity to microgels, though; since microgels were delivered in vasculogenic

hydrogels (Figure 18). Because a dense vascular bed penetrated into packed microgels, decreasing microgel diameter reduced the distance required for diffusion between transplanted islets and host circulation. PEG-4MAL microgels had reduced diameter compared to alginate microgels, and the closer proximity of islets to host vasculature may partially explain improved functional performance seen in PEG-4MAL microencapsulated islets delivered to the EFP.

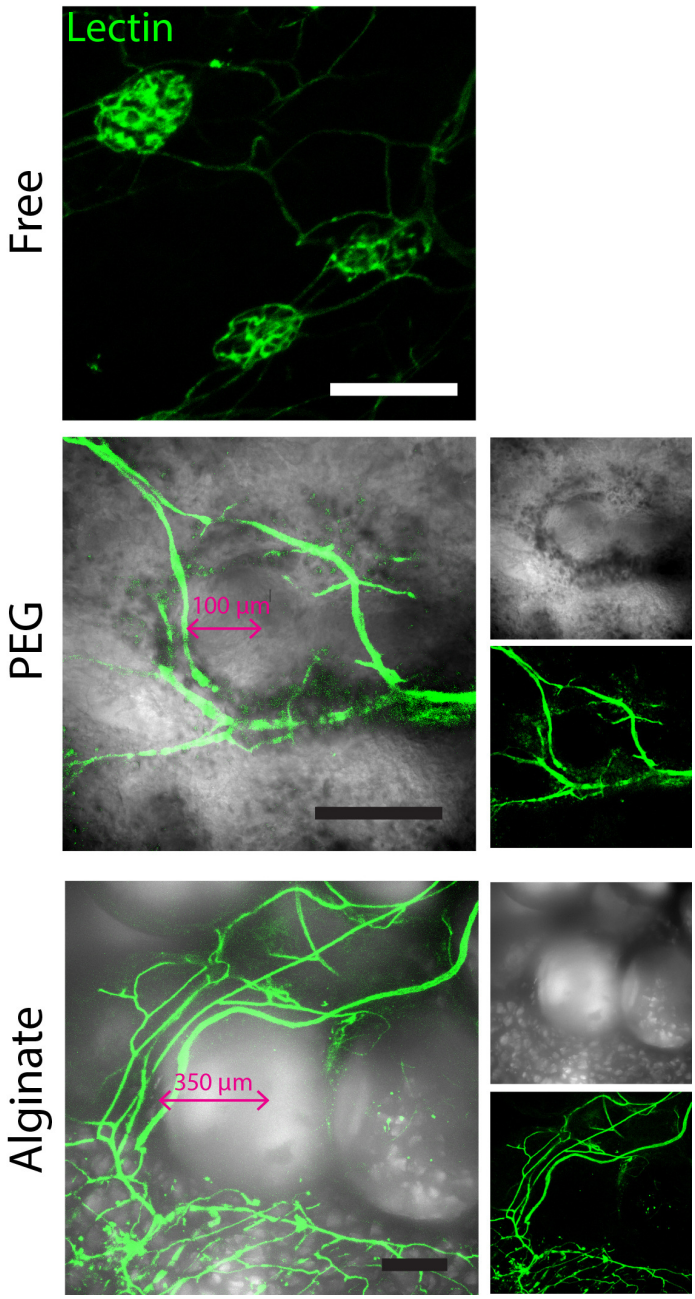

Figure 18. Functional vasculature labelled with lectin in green is show superimposed over transmitted light images, for islets transplanted to the EFP within bulk vasculogenic VEGF hydrogels. Islets were transplanted in bulk gel only, or were first microencapsulated in PEG-4MAL or alginate. Bare islets formed dense capillary networks, integrating with host vasculature. In contrast,

blood vessels grow up to microcapsules but could not penetrate them. Smaller PEG-4MAL microgels had decreased distance of diffusion between islets and host circulation compared to larger alginate microgels. (Scale bar = 200μm)

3.5 Conclusions

Permeability of synthetic hydrogels can be tuned, similarly to alginate, for immuno-isolation applications, but synthetic hydrogels also enable simultaneous control of microencapsulated islet microenvironment, which is not easily accomplished with alginate. Therefore, six different peptide sequences were tested in PEG-4MAL hydrogels for their abilities to support islet health and function. RGD was determined to support the best islet function, and the effect of crosslinker on encapsulated islets was investigated in RGD functionalized hydrogels. Hydrogels with non-degradable crosslinks supported slightly impaired function compared to hydrogels containing degradable crosslinks, whether DTT or PEG-DT were used as nondegradable crosslinking components. Although degradable hydrogels supported better islet function, their immuno-isolation potential is dubious. Therefore, non-degradable DTT crosslinked PEG-4MAL hydrogels were selected for further investigation, since they are more promising for immunoisolation and support similar islet function to alginate.

Enhancing vascularization of islets improves their function in syngeneic diabetic recipients, but direct vascularization cannot occur when effective immuno-isolation barriers surround islets. Therefore, droplet microfluidics were utilized to

encapsulate islets in PEG-4MAL microgels with diameters between 200-400μm, significantly smaller than typical alginate microgels produced by electrostatic extrusion which have diameters between 600-800μm. Islets microencapsulated in PEG-4MAL microgels with 2mM RGD and crosslinked with DTT showed only minimal reduction in viability and function after 48 hours when compared to unencapsulated controls, and did not show significant lag times in glucose responsiveness due to limited mass transport through microgels.

Our delivery system for islets *in vivo,* was further optimized by transplanting PEG-4MAL microencapsulated to the EFP within vasculogenic bulk hydrogels, which secrete VEGF as they degrade, prompting dense vascular ingrowth. This strategy is preferred to typical IP delivery of microencapsulated islets, because it improves the proximity of islets to host circulation and allows for graft retrieval. Islets delivered with this 2 layered PEG-4MAL delivery system are capable of restoring euglycemia at comparable rates and extents to bare islets delivered in vasculogenic hydrogels, but alginate microencapsulated islets have impaired function in the EFP, even when delivered in vasculogenic hydrogels. Because of the reduced size of PEG-4MAL microgels compared to extruded alginate microgels, induced vasculature grows closer to encapsulated islets, minimizing the mass transport limitations resulting from microencapsulation. This difference in mass transport limitations could explain the functional differences noted between groups, although differences in material composition may also contribute. Whatever the cause, islets in PEG-4MAL microgels delivered to the EFP in vasculogenic hydrogels restore more stable glycemic control than the

current standard material (alginate) and site (IP), and should be investigated for immuno-isolation applications.

CHAPTER 4: LOCALIZED IMMUNOMODULATION WITH BIOMATERIALS PRESENTING SA-FASL ACHIEVES ALLOGENEIC ISLET GRAFT ACCEPTANCE WITHOUT CHRONIC IMMUNOSUPPRESSION

Authors: Devon M. Headen, Kyle B. Woodward, Jessica D. Weaver, Hong Zhao, Pradeep Shastra, William S. Bowen, Christopher T. Johnson, Lonnie Shea, Esma Yolcu, Andrés J. García, and Haval Shirwan

4.1 Abstract

Islet transplantation is a promising therapy for type 1 diabetes. However, chronic immunosuppression to control rejection of allogeneic islets induces morbidities and impairs islet function. T-effector cells are responsible for islet allograft rejection and express Fas death receptor following activation, becoming sensitive to Fas-mediated apoptosis. Here, we report that localized immunomodulation using microgels presenting an apoptotic form of Fas ligand (SA-FasL) results in prolonged survival of allogeneic islet grafts in diabetic mice. A short course of rapamycin treatment boosted the immunomodulatory efficacy of SA-FasL-microgels, resulting in acceptance and function of all allografts over 200 days. Survivors generated normal systemic responses to donor antigens, implying immune privilege of the graft, and had increased $CD4^+CD25^+FoxP3^+$ T-

regulatory cells in the graft and draining lymph nodes. Deletion of T-regulatory cells resulted in acute rejection of established islet allografts. This localized immunomodulatory biomaterial-enabled approach may provide an alternative to chronic immunosuppression for clinical islet transplantation.

4.2 Main Text

Type 1 diabetes (T1D) is an autoimmune disease characterized by loss of insulin-producing β-cell mass, and thereby glycemic control, due to a coordinated immune response against β-cell specific antigens requiring $CD4^+$ T cells [173-175]. Restoration of β-cell mass through allogeneic islet transplantation is the current preferred clinical intervention to improve glycemic control [11, 13, 176]. However, longevity of allogeneic grafts is limited by host immune responses as well as secondary graft failure due to toxic effects of chronic immunosuppression required to control rejection [177, 178]. Pathogenic T effector (Teff) cells are the major culprit of islet allograft destruction [179, 180]. Therefore, a promising strategy to increase the functional longevity of islet allografts without the need for long-term immunosuppression comprises novel therapies that target Teff cells for elimination, mitigating their pathogenic function [181].

Upon activation, T cells upregulate Fas and become sensitive to FasL-mediated apoptosis, a process that plays a critical role in activation-induced cell death (AICD) and tolerance to self-antigens [182]. Deficiency in Fas or FasL results in massive lymphoproliferation and autoimmune pathologies in rodents and humans, demonstrating the importance of this pathway for immune

regulation [183]. Recognizing the immunomodulatory potential of this pathway, several groups have successfully used FasL gene therapy to mitigate allogeneic immune responses for graft acceptance in experimental animal models [184-188]. Although these interventions show efficacy, the unknown safety profile of sustained ectopic expression of FasL in target tissues, as well as technical and regulatory challenges of gene therapy, limit their clinical potential. Additionally, FasL only contributes to AICD in its membrane-bound, oligomeric form [189]. Matrix metalloproteinases (MMP) can cleave FasL into an extracellular soluble form that inhibits apoptosis and acts as a chemoattractant for neutrophils, accelerating the destruction of allografts [190]. To use FasL as an effective immunomodulatory agent, we have previously reported the construction of a chimeric form of FasL with streptavidin (SA), SA-FasL, in which the extracellular domain of FasL, lacking MMP sensitive sites, was cloned C-terminal to SA [191]. This protein exists as tetramers and oligomers with robust apoptotic activity on Fas-expressing cells. Importantly, pancreatic islets, modified with biotin attached to the cell surface followed by engineering with SA-FasL, acquired an immune privileged status and survived indefinitely in the absence of chronic immunosuppression in an allogeneic transplant murine model [192].

Here, we engineered a novel biomaterial for the sustained presentation of SA-FasL within the islet graft microenvironment, eliminating the need for islet modification, to establish a translatable, effective immunomodulatory strategy without chronic immunosuppression. Hydrogel microparticles (microgels) were synthesized from maleimide-terminated 4-arm poly(ethylene) glycol (PEG-4MAL)

macromers using microfluidics polymerization [146]. The PEG-4MAL platform enables stoichiometric, covalent incorporation of thiol-containing molecules, and provides improved crosslinking efficiency for formation of structurally defined hydrogels [143]. PEG-4MAL exhibits minimal toxicity *in vivo*, and it is rapidly excreted in the urine [63], important considerations for clinical applications. Biotinylated microgels were produced by reacting biotin-PEG-thiol with PEG-4MAL macromer, and generating 150 μm diameter microgels crosslinked with dithiothreitol (DTT) via microfluidics polymerization (Figure 19A). The resulting microgels displayed covalently-tethered biotin capable of capturing SA with high affinity (Figure 19B). Moreover, biotin-specific capture of SA on microgels varied linearly with concentration of SA in the tethering solution up to a saturating concentration of 150 μg/mL (Figure 19C), demonstrating dose-dependent control of SA presentation on the microgel surface. As expected, capture of SA-FasL on biotinylated microgels obeyed a similar dose-dependent relationship (Figure 23). Importantly, display of SA-FasL on microgels induced dose-dependent apoptosis in A20 cells (Figure 19D), which are sensitive to FasL-mediated apoptosis. In contrast, direct covalent coupling of SA-FasL to the PEG-4MAL macromer eliminated SA-FasL apoptotic activity (Figure 24), demonstrating the importance of biotin immobilization for presentation of bioactive SA-FasL. These results show that SA-FasL tethered to biotinylated microgels retains potent apoptotic activity, and that the quantity of bioactive SA-FasL delivered can be easily controlled using this approach.

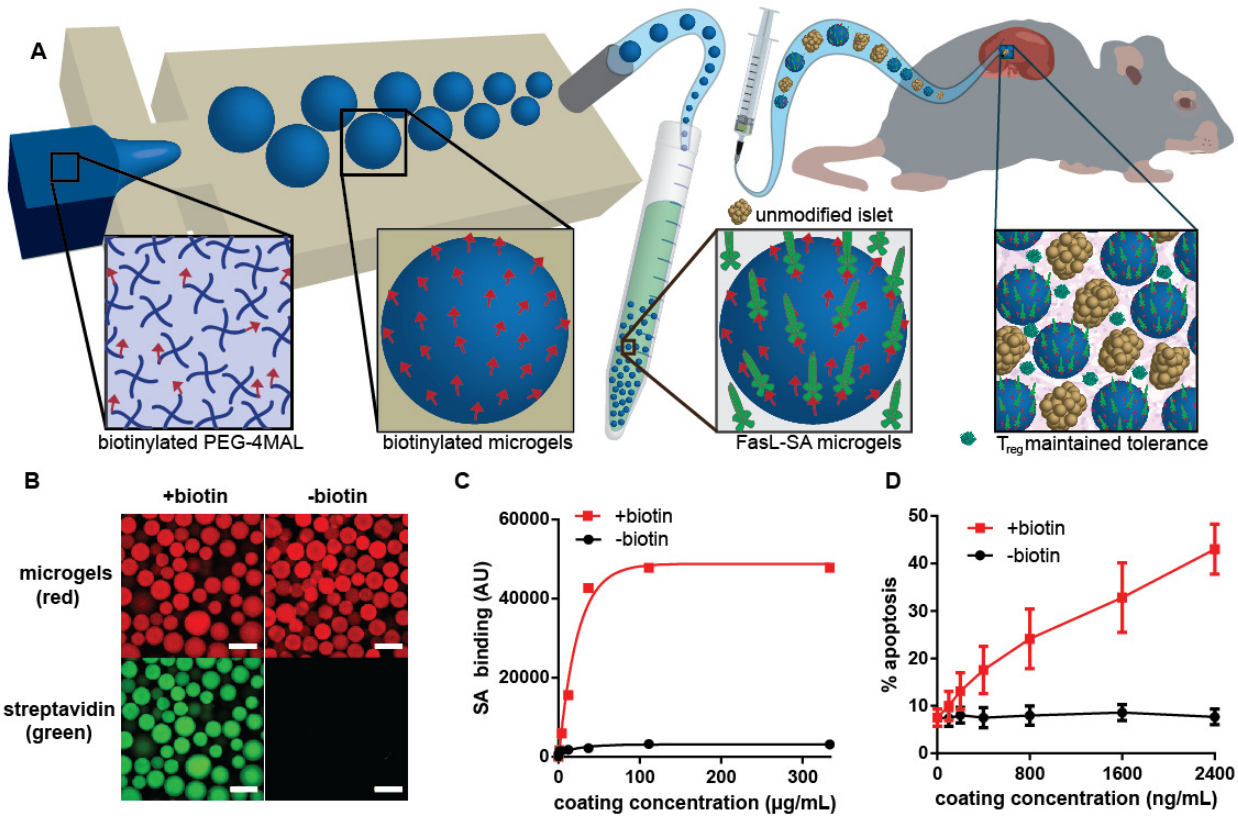

Figure 19. Microgels for controlled presentation of immunomodulatory proteins. (A) Flow focusing microfluidics were used to generate biotinylated microgels from biotin-functionalized PEG-4MAL macromers. SA-FasL was immobilized on microgels and these immunomodulatory microgels were co-transplanted with islets under the kidney capsule of diabetic mice, inducing graft acceptance. (B,C) Biotinylated microgels capture and display SA in a dose-dependent manner until reaching saturation. (D) SA-FasL presented on microgels maintains bioactivity and induces dose-dependent apoptosis in FasL-sensitive cells.

We next investigated the retention of SA-FasL presented on microgels *in vivo.* SA-FasL that had been labelled with a near-infrared fluorescent dye was immobilized on biotinylated microgels, which were implanted under the kidney capsule of mice. Longitudinal tracking of labelled SA-FasL was performed on an *in vivo* imaging system for 21 days. Images for fluorescent signal show concentrated signal localized to the area around the kidneys in mice receiving labelled SA-FasL-presenting microgels, whereas the fluorescent signal is diffuse for mice receiving labelled free SA-FasL without the microgel carrier (Figure 20A). In mice receiving only labelled SA-FasL, without the microgel delivery vehicle, the protein was rapidly cleared from the transplant site, with a 60% reduction in signal by day 4 post-implantation and negligible signal by day 11 after implantation (Figure 20B). In contrast, mice receiving SA-FasL-presenting microgels displayed significantly higher levels of SA-FasL over time with elevated levels comparable to day 0 signal at the site of implantation over 7 days post-transplantation. Analysis of retention profiles showed significantly longer retention times for SA-FasL-presenting microgels compared to free SA-FasL (9.6 ± 2.8 days vs. 3.2 ± 1.3 days, $p < 0.038$). Furthermore, area-under-the-curve calculations demonstrated increased retention of SA-FasL for microgel-tethered vs. free protein (4.25 ± 0.82 vs. 2.07 ± 0.21, $p < 0.034$). We expect that this biomaterial strategy for extended SA-FasL delivery in graft sites significantly enhances the local effects while minimizing risks of systemic effects of this potent immunomodulatory protein.

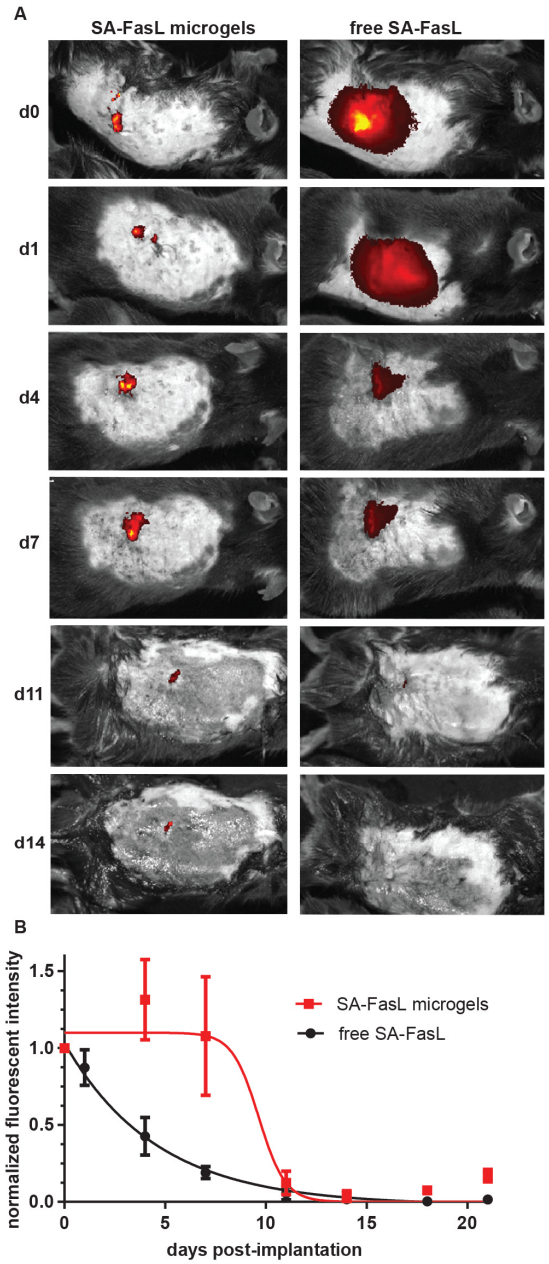

Figure 20. Microgels prolong SA-FasL retention *in vivo*. SA-FasL was labelled with a near-IR dye and implanted under the kidney capsule of mice and imaged *in vivo*. (A) Representative images show localization of SA-FasL to graft site when presented on microgels, in contrast to diffuse signal measured in animals receiving free SA-FasL. Heat maps are consistent across animals in the same

treatment group. Images are not shown for days 18 and 21 because signal was negligible. (B) Quantification of in vivo fluorescence demonstrates that microgels presenting SA-FasL prolong protein retention compared to free SA-FasL ($p<0.038$; $n=8$).

The immunomodulatory efficacy of microgels presenting SA-FasL was tested in an allogeneic islet transplantation setting. Unmodified allogeneic (BALB/c) islets were mixed with microgels, and the resulting mixture was transplanted under the kidney capsule of streptozotocin-diabetic C57BL/6 mice. Mice receiving unmodified islets and control biotinylated microgels acutely rejected all grafts [median survival time (MST) = 14.6 ± 1.7 days; Figure 21A). Islets co-transplanted with SA-FasL-engineered microgels had significantly prolonged survival (MST = 37.6 ± 9.0 days). The presentation of SA-FasL on both microgels and biotinylated islets further delayed rejection with four grafts rejecting within 59 days and one graft surviving for the 200-day observation period. The improved performance of this group suggests a dose-dependent immunomodulatory effect for SA-FasL. This was confirmed in mice receiving microgels engineered with 10 times more SA-FasL protein which further improved graft survival as 2/5 unmodified islet grafts did not show signs of rejection by the 200-day experimental end-point (Figure 21A, B). Notably, all grafts (n=5) functioned and survived for the entire 200-day observation window in mice co-transplanted with unmodified islets and SA-FasL-presenting microgels when subjects were treated with a short course of rapamycin (0.2 mg/kg daily

initiated on day 0 post-transplantation for 15 doses; Figure 21A,Figure 25). Intraperitoneal glucose tolerance tests demonstrated equivalent function of these long-term grafts compared with naïve mice (Figure 21C). In marked contrast, the same protocol with rapamycin injections but without SA-FasL-engineered microgels resulted in acute rejection (MST = 20.6 ± 3.9 days) (Figure 21A). Taken together, these results show that simple co-transplantation of allogeneic islets and SA-FasL-engineered microgels restores long-term glycemic control without the use of chronic immunosuppression or islet modification.

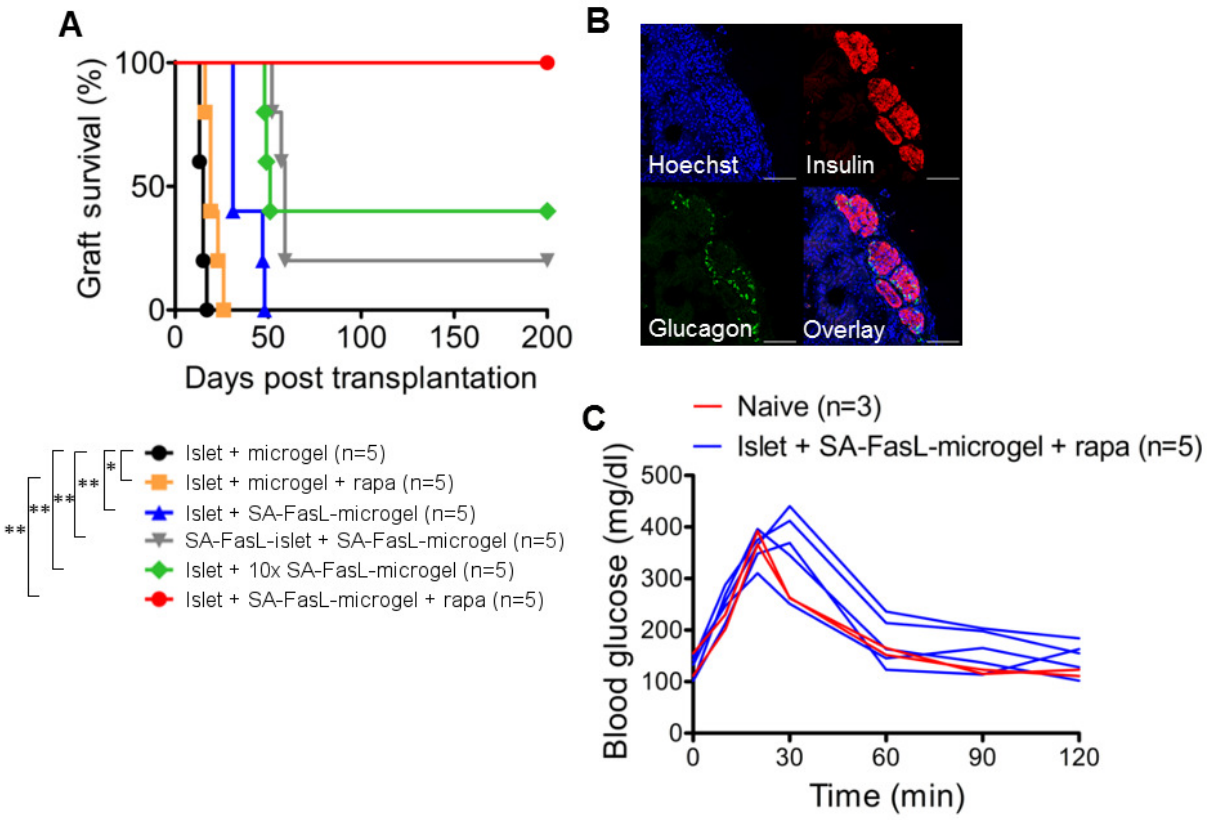

Figure 21. Survival of allogeneic islet grafts co-transplanted with SA-FasL-presenting microgels. (A) Islet graft survival. Biotinylated microgels were engineered with SA-FasL (1 µg protein/1000 microgels, unless otherwise noted) and co-transplanted with unmodified or SA-FasL-engineered BALB/c islets (500/transplant) under the kidney capsule of chemically diabetic C57BL/6 recipients. Rapamycin was used at 0.2 mg/kg daily i.p. injection for 15 doses starting the day of transplantation in the indicated groups. Animals were monitored for blood glucose levels and two consecutive daily readings of ≥ 250 mg/dL were considered to be diabetic (rejection). (B) Immunostaining of a long-term graft (> 200 days) from recipient receiving microgels presenting 10 µg of

SA-FasL showing insulin (red) and glucagon (green) positive cells as well as DNA (blue). (C) Intraperitoneal glucose tolerance test showing long-term islet grafts with normal function. (Data generated by Shirwan laboratory in collaboration with our group)

Because of the localized nature of immunomodulation, we assessed the systemic response of graft recipients to donor antigens in an *in vitro* proliferation assay. Both $CD4^+$ and $CD8^+$ T cells from long-term (> 200 days) islet graft recipients treated with SA-FasL-engineered microgels showed proliferative responses to donor as well as third party antigens (Figure 22A). The observed responses were at similar magnitudes to those obtained using T cells from rejecting mice receiving unmodified microgels plus rapamycin. This result indicates that mice receiving SA-FasL-engineered microgels maintain systemic immune competence, and that the protection afforded by SA-FasL-engineered microgels remains localized to the graft, as reported previously in two transplant settings using FasL as an immunomodulatory molecule [192, 193].

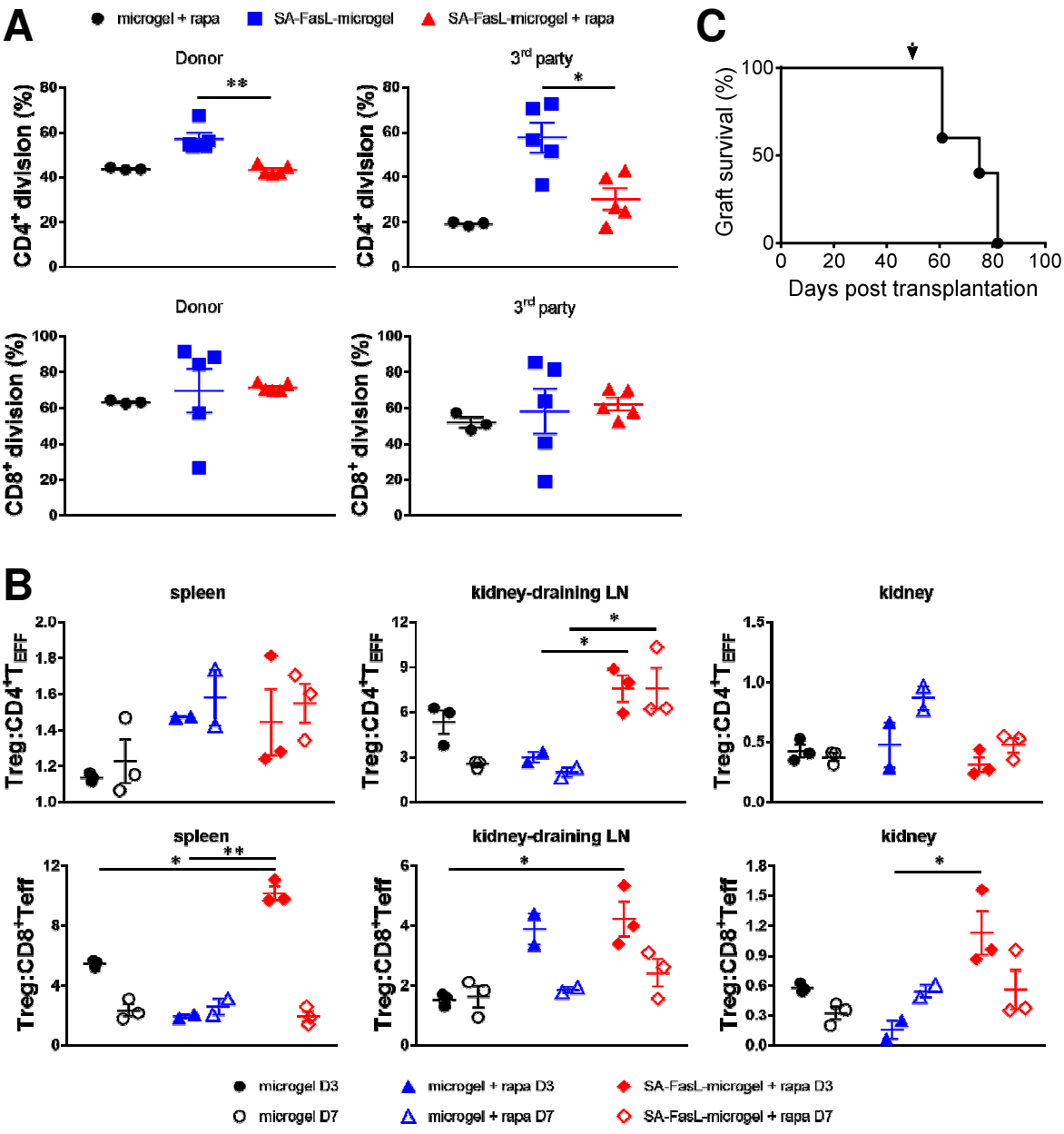

Figure 22. Immune monitoring and the role of $CD4^+CD25^+FoxP3^+$ Treg cells in islet graft acceptance. (A) Systemic response of long-term graft survivors to donor antigens. Splenocytes from the indicated groups were labeled with carboxyfluorescein succinimidyl ester (CFSE) and used as responders to irradiated BALB/c donor and C3H third party stimulators in an *ex vivo* mixed lymphocyte reaction assay. The dilution of CFSE dye in $CD4^+$ and $CD8^+$ T cells

was assessed using antibodies to CD4 and CD8 molecules in flow cytometry and plotted as percent division for each cell population. (B) Time course analysis of immune cell types. Single cells prepared from the spleen, kidney, and kidney-draining lymph nodes of the indicated groups on day 3 and 7 post-islet transplantation were stained with fluorescence-labelled antibodies to cell surface molecules that define $CD4^+$ Teff ($CD4^+CD44^{hi}CD62L^{lo}$), $CD8^+$ Teff ($CD8^+CD44^{hi}CD62L^{lo}$), and Treg ($CD4^+CD25^+FoxP3^+$) populations and analyzed using flow cytometry. The ratios of Treg to $CD4^+$ Teff and $CD8^+$ Teff are plotted (mean ± SEM, $*p < 0.05$, $**p < 0.005$). (C) Depletion of Treg cells results in acute rejection of established islet grafts. C57BL/6.$FoxP3^{EGFP/DTR}$ mice (n=5) were transplanted with BALB/c islet grafts and SA-FasL-presenting microgels under transient cover of rapamycin (administered i.p. daily at 0.2 mg/kg for 15 doses). These mice were then injected i.p. with 50 µg/kg diphtheria toxin on day 50 post-transplantation (arrow) to deplete Treg cells. (Data generated by Shirwan laboratory in collaboration with our group)

To further elucidate the mechanism of graft acceptance, immune cell populations harvested from the spleen, graft draining lymph nodes (LNs), and the graft were analyzed using flow cytometry in a time-course study, with particular focus on Teff and T-regulatory (Treg) cells as targets of FasL-mediated immunomodulation. We observed a trend towards an increased ratio of Treg to $CD4^+$ and $CD8^+$ Teff cells in the graft ($p < 0.05$ for Treg:$CD8^+$ Teff) and graft

draining LNs ($p < 0.05$ for both Treg:Teff populations) in groups receiving SA-FasL-engineered microgels and rapamycin compared to control groups receiving unmodified microgels alone or in combination with rapamycin (Figure 22B). Treg cells, similar to Teff cells, follow the inflammatory cues and infiltrate into rejecting grafts without a functional consequence [194, 195]. As such, we conducted a depletion study to directly assess the role of Treg cells in the observed graft acceptance in our model. For these studies, BALB/c allogeneic islets were transplanted into transgenic C57BL/6 mice expressing simian diphtheria toxin receptor under the control of Foxp3. Chemically diabetic transgenic mice transplanted with allogeneic islets and SA-FasL-engineered microgels under the transient cover of rapamycin established graft acceptance, as seen previously in C57BL/6 recipients, with all mice maintaining graft function at day 50 post-transplantation. Depletion of Treg cells by administration of DT on day 50 resulted in rejection of all grafts by day 82 (Figure 22C, S3; MST = 72.2 ± 10.2 days), demonstrating the dominant role of this cell type in graft acceptance.

These results are consistent with the established role of FasL in physiological immune privilege for selected tissues, such as the anterior chamber of the eye and the testes [196-198]. The observed protection against rejection required Treg cells and was localized to the graft, as long-term recipients generated a normal systemic response to the donor antigens, implying immune privilege. This is consistent with a study demonstrating that primary myoblasts transfected to express FasL conferred immune privilege to co-transplanted allogeneic islets [193]. Furthermore, we have previously demonstrated that

allogeneic islets engineered to display SA-FasL protein on their surface under a short cover of rapamycin overcame rejection by inducing graft-localized tolerance and immune privilege, maintained by Treg cells [199].

Engineering microgels with SA-FasL allows controlled loading, presentation, and retention of SA-FasL protein within the graft microenvironment for immunomodulation. This is a unique advantage over gene therapy, because uncontrolled, continuous expression of FasL, which possesses pleiotropic functions and different modes of expression that may be differentially regulated by the target tissues (membrane bound or soluble), may have unintended consequences. Indeed, ectopic expression of FasL using gene therapy for immunomodulation in transplantation settings has resulted in mixed and opposing outcomes with some studies showing detrimental impact of FasL expression on graft survival [200]. The localized and sustained presentation of SA-FasL with robust apoptotic function using microgels overcomes complications associated with ectopic expression of wild-type FasL in target tissues using gene therapy. This localized immunomodulation concept also limits potential toxicities associated with agonistic antibodies against Fas for immunomodulation [201]. Lastly, SA-FasL-engineered microgels provide the flexibility of an off-the-shelf product for wider clinical applications, as these immunomodulatory materials can be prepared at the time of transplantation and simply co-mixed with islets for delivery without the need of encapsulating islets or manipulating islets to present proteins. Further studies in large animal or humanized mouse models will be necessary for further proof-of-efficacy and translation to the clinic.

4.3 Methods

Microgel synthesis and characterization. A microgel precursor solution containing 5% w/v PEG-4MAL (20kDa, Laysan Bio) and 1.0 mM biotin-PEG-thiol (1 kDa, Nanocs) was reacted for 15 min in PBS. This precursor was dispersed into droplets and subsequently was crosslinked within mineral oil (Sigma) containing 2% SPAN80 (Sigma) and a 1:15 emulsion of 30 mg/mL dithiothreitol (Sigma) on a microfluidic chip, as described previously [146]. Control microgels which did not contain biotin-PEG-thiol were also synthesized using this protocol. After washing microgels 5 times by centrifugation in 1% bovine serum albumin (Sigma) in PBS, 10^4 microgels were incubated with varying concentrations of a streptavidin-AlexaFluor488 conjugate for 30 min in 500 µL PBS, and were washed 5 times by centrifugation to remove unbound SA. Microgels from each sample were placed in a 96-well plate and fluorescence was measured on a plate reader (Perkin Elmer HTS 7000). Biotin and control microgels were also synthesized with a covalently bound peptide (GRGDSPC)-AlexaFluor594 conjugate for capsule visualization, and were fluorescently imaged to confirm biotin-specific SA immobilization.

***In vitro* bioactivity.** 10^4 microgels, with or without biotin, were co-incubated for 30 min in 500 µL PBS with 1% bovine serum albumin containing varying concentrations of SA-FasL. Microgels were washed 8 times by centrifugation to remove unbound SA-FasL, and were incubated with 10^6 A20 cells in 1.0 mL media. After 18 h, cells were stained with markers of early and late apoptosis

(annexin V-APC and propidium iodide, BD Biosciences). Samples were analyzed by flow cytometry (Accuri C6 flow cytometer) and cells staining positive for either marker were considered apoptotic. 3 independent replicates of this experiment were performed.

***In vivo* SA-FasL tracking.** SA-FasL was labelled with AlexaFluor750 NHS Ester (Thermo Fisher), and free dye was removed by desalting in Zeba column (7k MWCO, Thermo Fisher) three times. 3.0 µg of labelled SA-FasL was immobilized onto 2000 biotin microgels by incubation for 30 minutes followed by 5 wash steps. Microgels presenting SA-FasL or free SA-FasL were implanted under the kidney capsule of C57Bl/6 recipients (n=8 mice/group), and signal intensity and distribution were monitored longitudinally using an IVIS SpectrumCT imaging system. Intensity measurements were normalized to day 0 values. Non-linear curve fits were performed in GraphPad Prism and retention time was compared using a t-test. Additionally, area under the curve was calculated for each group, and a Welch's t-test was used to compare groups.

Islet transplantation. BALB/c pancreatic islets were isolated using Liberase TL as a digestive enzyme (Roche Life Science) and purified by a Ficoll density gradient as previously published [191]. To biotinylated islets, overnight cultured islets were incubated in 5 µM EZ-Link Sulfo-NHS-LC-Biotin (Thermo Scientific) for 30 min at room temperature, washed extensively with PBS to remove unbound biotin solution. Biotinylated islets and microgels were engineered with SA-FasL (~150 ng/500 islets and 1-10 µg/1000 microgels). Five hundred islets were co-transplanted with 1000 microgels into streptozotocin diabetic (> 250

mg/dL) C57BL/6 recipients. Selected groups were also treated i.p. with rapamycin at 0.2 mg/kg daily for 15 doses starting the day of transplantation. Unmodified BALB/c islets co-transplanted with unmodified PEG gels were used as controls. Animals were monitored for blood glucose and ≥ 250 mg/dL blood glucose levels for two consecutive daily measurements were considered rejected.

Immune monitoring. Spleen, kidney, and kidney draining lymph nodes were harvested from rejecting and long-term mice (> 200 days). Single cells were prepared from the spleen and lymph nodes by gentle mechanical dispersion and from islet harboring kidney by collagenase digestion. Cells were stained using antibodies to cell surface markers (Alexa 700-CD4 Ab, APC-Cy7-CD8 Ab, PE-Cy7-CD25 Ab from Pharmingen, BD, and eFlour 450-CD44 Ab and PerCP-Cy5.5-CD62L Ab from eBioscience). Intracellular FoxP3 staining was carried out on fixed/permeablized cells using FoxP3 Transcription Factor Staining Buffer set (eBioscience). Data was collected using BD LSR II and analyzed using Diva software.

Proliferation assay. Splenocytes harvested from selected group of transplant recipients were labeled with CFSE and used as responders to irradiated (200 cGy) splenocytes from donor or third party C3H mice in a standard *in vitro* proliferation assay [192]. After 4 days in culture, cells were stained with fluorescence-conjugated Abs against CD4 and CD8, and analyzed for CFSE dilution by gating on live cells using BD LSR II. Data was analyzed using Diva software.

Confocal Microscopy. After the observation period of 200 days, long-term islet bearing kidneys were snap frozen in OCT compound (Sakura Tissue-Tek) by submerging in methyl butane (Sigma) on dry ice. Tissues were cut in 10 µm-thick slices using a Bright OTF5000 cryomicrotome (Rose Scientific) and put on frosted slides for staining. Slides were fixed in 4% paraformaldehyde, incubated in 0.5% Triton X-100, and blocked in 0.1% bovine serum albumin, 5% goat serum, and rat anti-mouse CD16/CD32 (BD Pharmingen). Staining was performed using rabbit anti-glucagon mAb (Cell Signaling) and guinea pig anti-insulin polyclonal antibody (Dako) as primary antibodies, followed by washing and staining with AlexaFluor-647-conjuaged goat anti-rabbit antibody (Life Technologies) and AlexaFluor-555-conjugated anti-guinea pig antibody (Invitrogen). Hoechst 33342 (Molecular Probes) was used to stain DNA. Fluorescent images were obtained using a Leica TCS SP5 confocal microscopy under 10X magnification.

4.4 Supplementary Figures

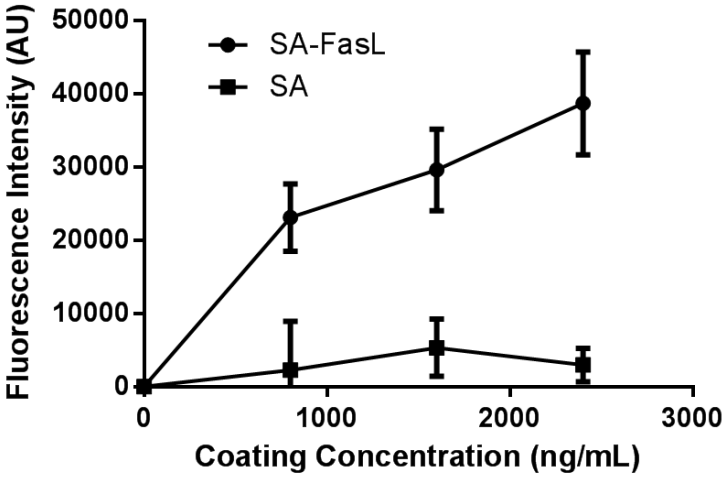

Figure 23. SA-FasL is tethered to biotinylated microgels in a dose-dependent manner. Biotinylated microgels (10^4) were suspended in 500 µL of SA-FasL or SA only solution at the concentrations indicated for 1 h. Microgels were then washed by centrifugation 10 times in 1% bovine serum albumin in PBS to remove unbound protein. Functionalized microgels were incubated with a 1:100 dilution of fluorescently labelled anti-FasL antibody for 1 h, followed by 10 washes by centrifugation. Washed microgels were placed in a 96 well plate and read on Perkin Elmer HTS 7000 plate reader, and background signal (empty well) was subtracted from all values (n=2, mean ± SEM).

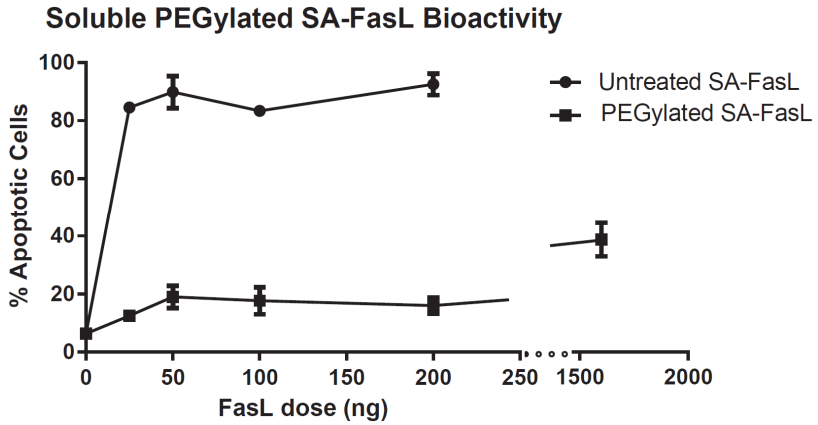

Figure 24. Direct tethering of SA-FasL to PEG-4MAL macromer reduces bioactivity. Various doses of SA-FasL were reacted with 10 µL of 10% PEG-4MAL macromer in solution for 1 h. Either untreated soluble SA-FasL or PEGylated SA-FasL was incubated with A20 cells overnight, and the number of apoptotic cells was determined by flow cytometry after staining with annexin V-APC and propidium iodide (n=2, mean ± SEM).

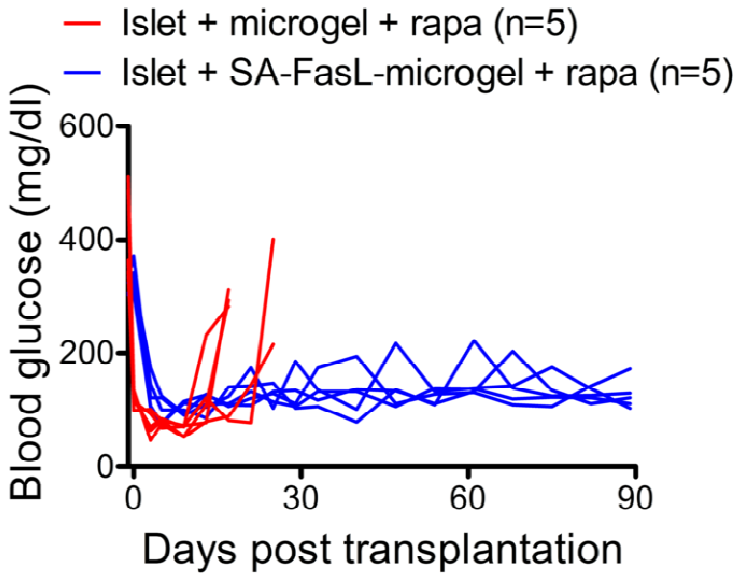

Figure 25. Blood glucose levels. Readings were taken on chemically diabetic C57BL/6 mice transplanted with microgels presenting SA-FasL (1 µg protein/1000 microgels) and naïve BALB/c islet grafts (500) under a short cover of rapamycin (administered i.p. daily at 0.2 mg/kg for 15 doses). Controls included mice subjected to the same regimen, except receiving microgels without SA-FasL protein.

CHAPTER 5: PARALLEL DROPLET MICROFLUIDICS FOR HIGH THROUGHPUT CELL ENCAPSULATION AND SYNTHETIC MICROGEL PRODUCTION

5.1 Abstract

Cells can microencapsulated in synthetic hydrogel microspheres (microgels) using droplet microfluidics, but microfluidic devices with a single droplet generating geometry have limited throughput, especially as microgel diameter decreases. Here we demonstrate the microencapsulation of human mesenchymal stem cells (hMSCs) in small (< 100 μm diameter) microgels, utilizing parallel droplet generators on a two-layer elastomer device, which has 600% increased throughput vs. single nozzle devices. Distribution of microgel diameters were compared between products of parallel vs single nozzle configurations for two different square nozzle widths, 35 μm and 100 μm. Microgels produced on parallel nozzles were equivalent to those produced on single nozzles, with no major increase in polydispersity noted. Microencapsulation of hMSCs was compared for parallel nozzle devices of each width. 35 μm wide nozzle devices could be operated at twice the cell concentration of 100 μm wide nozzle devices, but their volumetric throughput was only 12% of that for 100 μm nozzle devices and significantly more empty

microgels were produced than predicted by the Poisson distribution. 100 μm wide nozzle devices produced microgels as predicted by the Poisson distribution. Microgel size was impacted by the addition of cells, increasing on 35 μm nozzle devices but decreasing on 100 μm nozzle devices. Polydispersity of microgels did not increase with the addition of cells for either nozzle width. Viability of hMSCs encapsulated on 100 μm wide nozzle devices was >90% after encapsulation, but cells encapsulated on 35 μm wide nozzle devices had reduced viability of ~70%, suggesting nozzle size-dependent damage to cells.

5.2 Introduction

Delivery of encapsulated proteins and cells in hydrogel microspheres, or microgels, has emerged as a promising therapeutic strategy for the treatment of disease[202]. Some synthetic polymers, especially those utilizing bio-orthogonal click chemistry, provide tuneable release rates of encapsulated proteins which can be tailored based on hydrolytic or enzymatic degradation of microgels[149, 203]. These injectable microgels can be non-invasively implanted for extended local delivery of therapeutic proteins, such as growth factors and cytokines. Additionally, microgel delivery of proteins allows for ‘mosaic’ injections, in which multiple capsules with individually validated release profiles can be combined to provide more complex release profiles or multi-protein delivery. Encapsulation of cells in microgels provides several key benefits in transplantation settings. By controlling diffusivity properties of microgels, immune infiltration of transplanted cells can be mitigated while transport of oxygen and cellular waste products is

maintained. Because potential sources of therapeutic cells are often allogeneic or xenogeneic, this protection mechanism has been extensively investigated for reduction required immunosuppression for transplant acceptance. Microgels can also function to immobilize cells at a desired location by entrapping them in gels, an important consideration since many cell therapies currently rely on systemic administration of cells. In addition to isolating transplanted cells from the host, synthetic microgels permit engineering of encapsulated cell microenvironment, including matrix stiffness and adhesive ligand interactions, which are known to influence encapsulated cell health and function. Bulk hydrogel constructs can provide these benefits as well, but the microgel form factor enables applications for which bulk gels are not well suited, such as injection. Additionally, thick polymer coatings are a barrier to nutrients and oxygen, so hypoxic death is frequently observed with in cells at high concentration in bulk gels, and even in large microgels [204]. Therefore, microgel size should be minimized in order to maximize transport of oxygen to encapsulated cells, and to enable novel, minimally invasive transplantation schemes.

We have previously developed a microfluidic droplet strategy for generating size-controlled crosslinked synthetic microgels based on 4 arm poly(ethylene) glycol (PEG-4MAL) macromers which are terminated with maleimides [146]. Maleimides efficiently react with free thiols to form covalent bonds, allowing any cysteine containing peptide or thiolated ligand to be tethered to microgels. This versatile chemistry enables local sustained presentation of bioactive molecules in microgels, as well as enzyme-mediated active release of

therapeutic proteins when microgels are crosslinked with protease-sensitive crosslinks [203]. Crosslinking PEG-4MAL macromers can be accomplished with dithiol molecules and does not require free radical initiators, which are detrimental to encapsulated cell health [205]. Similar microfluidic schemes for producing microgels [166, 206, 207] and encapsulating cells [159, 208, 209] have recently been reported for widely varying applications, including wound healing, stem cell culture, and fundamental studies of cell biology.

Microfluidics can provide precise control of size and polydispersity of droplets [210], and can be used to generate microgels with polymers that are not amenable to extrusion processing [101]. Minimization of microgel diameter maximizes diffusion of oxygen and nutrients to encapsulated cells, enables applications for which larger microgels are not suited (such as injection), and potentially reduces transplant graft volume. Unfortunately, volumetric throughput of macromer decreases with the cube of droplet diameter, so volumetric throughput can be severely limited when very small microgels are being produced. Furthermore, cells suspended at high concentrations tend to aggregate, which can lead to incomplete cell encapsulation as well as increased microgel diameters. Therefore, to minimize cell-laden microgel diameter, a low concentration cell suspension must be used, resulting in a higher percentage of empty microgels. Microgels containing cells can be purified by sorting, or can be selectively crosslinked [211], but encapsulating clinically relevant numbers of cells in these very small microgels is highly challenging. Long processing times associated with encapsulation or sorting are likely to decrease cell viability, so

faster cell microencapsulation rates are desirable for therapeutic efficacy, not just convenience.

To maximize encapsulated cell production rate, both the concentration of cells in macromer and the volumetric throughput of macromer in microfluidic devices must be maximized. One way to increase flow rate of macromer in a microfluidic droplet generating device is to utilize a parallel flow focusing nozzle configuration. However, maintaining size control and low polydispersity of droplet diameter are very challenging when parallel nozzles are used, because coupled flows cause fluctuations to propagate between nozzles. Nonetheless, uniform droplet production has been shown on parallel droplet generators with a variety of configurations [212-216]. Parallel microfluidics have been used to produce microgels through light-initiated free-radical polymerization on single layer microfluidics, and the nature of crosstalk between parallel droplet generators has been studied in this context [217]. Furthermore, in an impressive display of microfluidic control, even uniform double emulsion polymerosomes were formed on parallel geometries [218, 219]. However, suspensions containing high density cell suspensions complicate fluid behaviour and may cause nonuniform distribution of fluid to focusing nozzles. Likely because of these hurdles, parallel droplet generators have not been utilized to date for suspension of cells in droplets, much less their encapsulation in polymer microspheres.

Here, we report a process for the high-throughput encapsulation of cells in sub-100 µm diameter microgels, which utilizes a novel two-layer microfluidic

device with six parallel flow focusing nozzles. This microfluidic device is capable of efficiently encapsulating high concentration cell suspensions, and enables a 600% increase in volumetric throughput rate over single nozzle configurations. Two different nozzle widths, 35 μm and 100 μm were developed, each with benefits and disadvantages. 35 μm wide nozzle devices produce smaller microgels than 100 μm wide nozzles and can uniformly break up droplets from precursors at higher operating cell densities as 100 μm-wide nozzle devices, which minimizes transplant graft volume. However, whereas hMSC viability is >90% after encapsulation on 100 μm wide nozzle devices , it is reduced to ~70% after encapsulation on 35 μm wide nozzle devices, and 100 μm wide nozzle devices also provide more than 8 times the volumetric throughput of 35 μm wide nozzle devices**.**

5.3 Experimental

5.3.1 Microfluidic fabrication

Photolithography was used to pattern microfluidic masters after spin coating SU-8 2050 photoresist (MicroChem) onto silicon wafers, then masters were developed and treated with vapor phase trichloro(1H,1H,2H,2H-perfluorooctyl)silane (Sigma) to reduce sticking. Devices with 35 μm and 100 μm wide nozzles had focusing layer patterns that were 35μm and 100 μm tall, respectively, and their corresponding top layer patterns were 80 μm and 140 μm tall. PDMS (Sylgard 184) was

mixed according to manufacturer specifications and was moulded on the SU-8 master to make microfluidic channel replicas (Figure 26A). After curing for 11 minutes at 110°C, crosslinker inlet and outlet holes were punched in the top layer, and inter-layer vias were punched in the bottom layer. Appropriate surfaces were exposed to air plasma for 20 seconds in a PlasmaPreen system, and layers were aligned and pressed together by hand before being cured at 110°C for 5 minutes. After PDMS to PDMS bond was stabilized, oil and macromer inlets were punched through both layers. These elastomer constructs were sonicated, along with glass substrates, in 200 proof ethanol and were dried with compressed nitrogen. Cleaned components were quickly treated with 12 seconds of plasma and PDMS was bonded to a glass slide, sealing the lower layer flow channels. Devices were cured overnight at 60°C before being used.

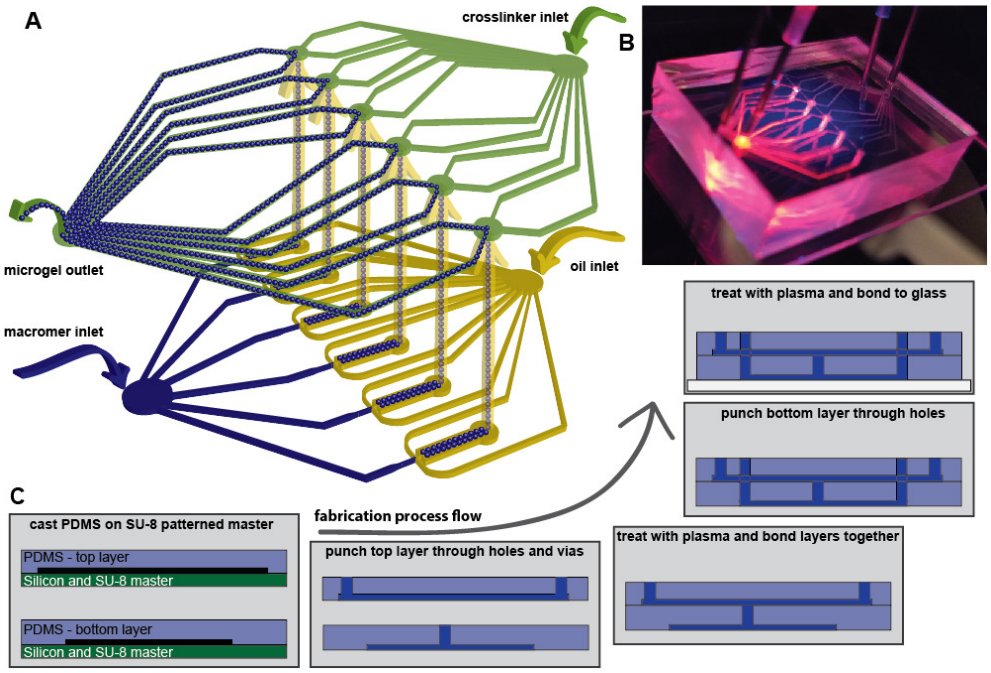

Figure 26. Schematic and representative images demonstrating parallel microfluidic device operation and fabrication are shown. (A) Droplets containing macromer precursor (and optionally cells) are emulsified in oil on the lower layer of the device when these immiscible fluids are co-flowed through a flow focusing geometry. The droplets produced on all 6 flow focusing nozzles are carried up to the top layer where they are exposed to crosslinker and are pooled before exiting the device at a single outlet. (B) Fluorescent label facilitates visualization of microfluidic device operation, as seen in this photograph of microgel generation in progress. (C) The two layer microfluidic device requires several steps for fabrication. First, PDMS is moulded from SU-8 and silicon masters, then holes that go through one layer only are punched. PDMS layers are exposed to air plasma, and are aligned and bonded to each other. Inlets for the bottom layer are

punched through both layers, and the device is completed by bonding the two layer PDMS construct to a glass substrate after plasma exposure.

5.3.2 Microgel synthesis and characterization

Microfluidic devices were primed with Light Mineral Oil (Sigma) containing 2% SPAN80 (Sigma) which was also used as the continuous phase fluid. The crosslinker emulsion was comprised of 30 mg/mL DTT (Sigma) emulsified at a 1:15 ratio in the continuous phase. The macromer solution consisted of 6.5% (w/v) PEG-4MAL (20 kDa, Laysan Bio), which had been reacted with a fluorescently labelled adhesive peptide (1.0 mM AlexaFluor594-conjugated GRGDSPC) for imaging and consistency with cell encapsulation experiments. Also motivated by consistency with subsequent cell encapsulation experiments, this reaction was performed in a buffer which had additives to address particular challenges associated with cell encapsulation. The buffer contained OptiPrep density gradient (Sigma) and PBS in a 1:4 ratio to match the density of cells and minimize settling of cells, and contained 0.1% Pluronic F108, which reduces cell sticking to glass or PDMS. After connecting the outlet and all inlets, fluid flows were driven at the flow rates prescribed in Table 1 by Hamilton gastight syringes on Harvard Apparatus Elite syringe pumps. To prevent unwanted gelation of polymer precursor on chip and to minimize polydispersity due to transient flows, first oil, then crosslinker fluid flows were initiated and allowed to stabilize. Only after flows stabilized was macromer precursor flow initiated. After at least 20 minutes of generation,

microgels were collected in phosphate buffered saline containing 2% bovine serum albumin (to reduce microgel sticking). Most of the oil was removed by aspiration after centrifugation (600*g* for 5 min), then microgels were washed 3 more times by centrifugation in a new 15 mL conical tube to remove any mineral oil residue from microgels. Microgels were imaged using a Nikon Ti-E microscope with Perfect Focus System and C2-Plus Confocal System, and diameter was determined using 'Analyze Particles' on binarized images in ImageJ. Output of 3 independent microgel generations were characterized for all 4 device designs tested, with a minimum of 163 microgels counted per device.

Table 1. Microfluidic devices with parallel nozzle configuration have 600% increased macromer throughput rate over single nozzle configurations. Flow rates shown were used for all experiments discussed herein.

		flow rate (µL/min)		
		macromer	oil	crosslinker
35µm width	single nozzle	0.2	1	2
	parallel nozzles	**1.2**	6	15
100µm width	single nozzle	1.67	12.5	15
	parallel nozzles	**10**	75	40

5.3.3 Human MSC microencapsulation and characterization

A similar protocol was used to encapsulate hMSCs, with a few modifications. First, hMSCs were trypsinized for 10 minutes in 0.25% trypsin/EDTA, which minimized cell clumping and homogenized cell morphology compared to shorter trypsinization times. A macromer solution was made containing twice the desired final concentrations – that is 13 wt% PEG-4MAL, 2.0 mM RGD, 0.2% Pluronic F108, in a buffer comprised of 1:2 OptiPrep in PBS. This precursor was mixed with an equal volume of cells suspended at twice their desired concentration. The resulting solution contained gel precursor concentrations consistent with those used for microgel synthesis, and contained the desired concentration of cells in suspension (2×10^7 cells/mL for 35 μm wide nozzle or 10^7 cells/mL for 100 μm wide nozzle). This suspension was mixed thoroughly by pipetting, and was used as quickly as possible to generate microgels in parallel nozzle microfluidic devices, using the same protocol described for empty microgels. Three independent encapsulations were performed on both the 35 μm and 100 μm wide nozzles for at least 20 minutes each, and the resulting microgels were washed with culture media 4 times by centrifugation. Live and dead cells were then stained with Calcein-AM and TOTO-3 iodide, respectively (ThermoFisher). Microgels containing cells were imaged on a confocal microscope and were measured in ImageJ. The number of cells per capsule was determined by manual counting due

to cell clustering. At least 425 capsules were characterized from each encapsulation.

5.3.4 Human MSC viability

Viability of microencapsulated hMSC was monitored over time for cells encapsulated on parallel microfluidic devices with both 35 μm and 100 μm wide nozzles. Cell viability on day 0 was calculated by dividing the number of Calcein-AM positive cells by the total number of cells counted. Some encapsulated cells were not stained on day 0, and were instead cultured with media changes every 3 days. On days 1, 3, and 7 post-encapsulation, encapsulated cells were removed from culture, and were stained and imaged to determine cell viability. As a control, viability was also determined over time for hMSCs grown on TC plastic. Day 0 viability of cells in microgels was compared for cells encapsulated on 35 μm vs 100 μm wide nozzle devices using Mann-Whitney test in GraphPad.

5.4 Results and Discussion

5.4.1 Microfluidic design and fabrication

The goals of our iterative design were to (1) maximize throughput of encapsulated cells while (2) minimizing microgel size and maintaining encapsulated cell health and function. During the course of preliminary experiments with devices comprised of single square nozzles, nozzle widths smaller than 30 μm did not consistently encapsulate cells, especially hMSCs, which are relatively large cells with heterogeneous morphology. Instead, due to an unknown mechanism, the product was frequently unencapsulated

cells mixed with empty microgels. Therefore, 35 μm wide nozzles were determined to be the smallest nozzle appropriate for high throughput encapsulation of hMSCs. Also during these preliminary experiments, we observed that cell viability was reduced in these very small microgels, which might limit their therapeutic potential. Cells encapsulated on 100 μm wide nozzles had higher viability, and therefore therapeutic potential, but they were still small enough that throughput limitations were a concern.

Therefore, several different two layer parallel nozzle flow focusing microfluidic devices were designed and fabricated (for both 35 μm and 100 μm widths) using soft lithography, in an iterative design process. Initial designs had flow focusers on the top layer, which worked for the 100 μm wide nozzle, but the higher pressure required for driving flow on the 35 μm wide focusing nozzles caused frequent device failure due to delamination of the PDMS to PDMS bond. Delamination was entirely eliminated by relocating oil and macromer supply and flow focusers to the bottom layer, with its stronger glass to PDMS bond. On the final design (Figure 1), all flow channels on the top layer are relatively large and open (80 μm tall for devices with 35 μm wide nozzles; 140 μm tall for devices with 100 μm wide nozzles), so they did not require pressures that instigated delamination. Devices which had more nozzles were also designed, but were more difficult to fabricate, and produced droplets with increased polydispersity. The 6 nozzle design represents a compromise, resulting in acceptable polydispersity as well as acceptable throughput, and being relatively robust to fabricate and operate, compared to other designs tested.

5.4.2 Parallel encapsulation allows for 600% increased throughput while maintaining size control of microgels

. A major benefit of synthesizing microgels with droplet microfluidics is the ability to precisely control microgel size and polydispersity. However, maintaining low polydispersity is challenging in parallel nozzle devices, because any variation in fluidic resistance between flow focusers (or respective distribution/collection channels) results in variation of droplet size produced at each nozzle. Additionally, pressure fluctuations tend to propagate through all the nozzles, producing droplets with heterogeneous diameters. Therefore, we synthesized PEG-4MAL microgels on both single and parallel nozzle devices in order to characterize any increase in polydispersity due to parallel synthesis (Figure 27). Three separate syntheses were performed on three separate devices of each design. Representative histograms of microgel size are shown for each synthesis (Figure 27A,B) along with representative fluorescent images of microgels. Although Kruskal-Wallis tests indicate differences in median microgel size across devices of the same design ($p<0.05$ for all 4 devices), this is likely due to the small variances and large sample sizes. No gross differences in size distribution were seen between microgels generated on multiple devices of the same design (Figure 27) and mean microgel size was highly consistent between devices of the same design (Table 2). For practical purposes, we conclude that microgel production is repeatable on all 4 microfluidic designs. Microgels analysed from all 3 encapsulations were pooled for each device so that comparisons could be made between single and parallel devices with the same nozzle size. For the 35

μm wide nozzle device, a t-test revealed statistical differences ($p=0.012$, Figure 27C) in mean diameter of microgels produced on parallel vs. single nozzles, but the magnitude of this difference was small (<1.8%) - average diameter was 65.1 ± 8.2 μm for parallel nozzle devices versus 64.0 ± 6.3 μm for single nozzle devices (Table 2). The mean diameter was equivalent for pooled microgels produced on 100 μm nozzles (104.5 μm), whether single or parallel configurations were used, and no differences in mean diameter were found ($p=0.97$). F-tests revealed differences in variance of microgel diameter for parallel vs. single nozzle production for both nozzle widths tested ($p<0.0001$ in each case). For 35 μm nozzle width, the parallel configuration resulted in higher standard deviations than the single configuration, as expected. Surprisingly, the single 100μm nozzle produced microgel diameters with higher standard deviations (± 9.6μm) than those produced on the parallel configuration (± 7.5μm). Whereas statistically significant differences were found between diameters of microgels produced on single versus parallel nozzle configurations, the differences are small and are unlikely to matter for practical applications. Taken together, these results demonstrate that our parallel microfluidic device is capable of increasing microgel production rate by 600%, while having minimal impact on the size or polydispersity of resulting microgels.

Table 2. Statistics for microgel populations produced on different microfluidic devices, with or without cells. Results are shown for three independent syntheses for each process. Measured values from all 3 syntheses are pooled in the right most column to facilitate comparison between designs.

			device 1	device 2	device 3	pooled microgels
35µm nozzle	single nozzle (-cell)	mean diameter (µm)	64.2	62.9	64.7	64.0
		±SD (µm)	6.0	5.3	6.8	6.3
		CV (%)	9.3	8.4	10.6	9.9
	parallel nozzles (-cell)	mean diameter (µm)	65.6	65.1	64.2	65.1
		±SD (µm)	7.9	8.5	8.8	8.2
		CV (%)	12.1	13.0	13.7	12.7
	parallel nozzles (+cell)	mean diameter (µm)	77.2	76.4	75.9	76.5
		±SD (µm)	6.3	5.7	7.5	6.6
		CV (%)	8.2	7.5	9.9	8.6
100µm nozzle	single nozzle (-cell)	mean diameter (µm)	106.0	102.0	105.5	104.5
		±SD (µm)	12.2	12.7	8.4	10.1
		CV (%)	11.5	12.5	7.9	9.6
	parallel nozzles (-cell)	mean diameter (µm)	103.6	104.0	107.1	104.5
		±SD (µm)	7.0	6.6	7.3	7.9
		CV (%)	6.7	6.3	6.8	7.5
	parallel nozzles (+cell)	mean diameter (µm)	97.8	98.1	98.3	98.1
		±SD (µm)	7.6	7.2	6.6	7.1
		CV (%)	7.8	7.3	6.7	7.3

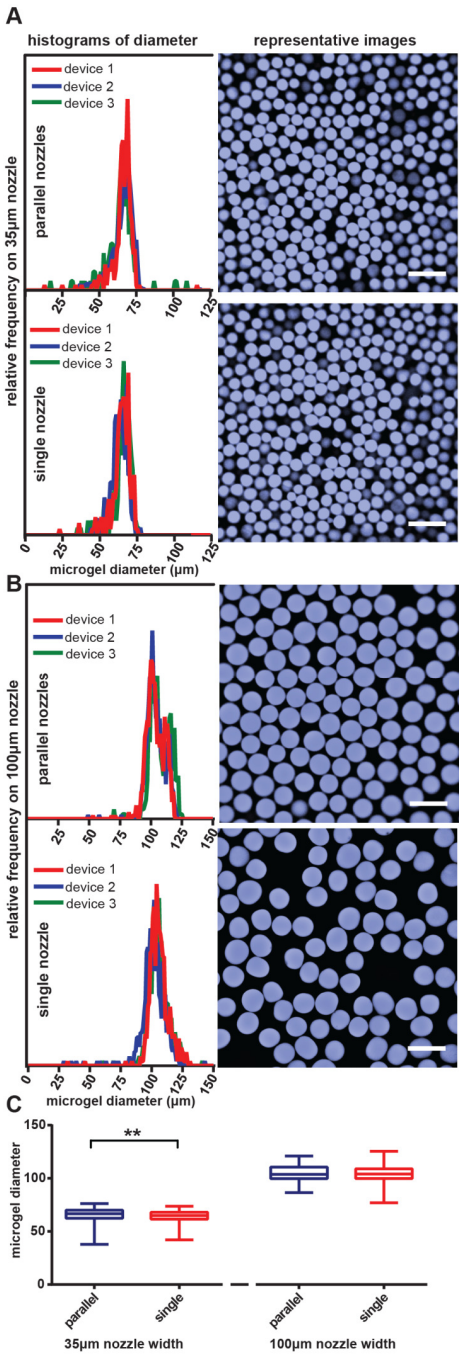

Figure 27. Microfluidic devices with parallel nozzles can produce microgels with controlled size, and with polydispersities comparable to microgels produced on a single nozzle. (A,B) Representative histograms of microgel diameter frequency and representative fluorescent images of microgels show similar output from

single and parallel nozzles for both nozzle widths tested. (C) Consistency in diameter distribution is further demonstrated by comparing pooled microgels produced from each device. Significant differences were found between parallel and single configurations of 35μm nozzles (p=.0012) , but the magnitude of differences was not practically relevant. 100μm nozzles did not produce different sized microgels with parallel vs. single configurations (p=0.97).

5.4.3 Human MSCs can be encapsulated on parallel nozzle microfluidic device with high loading density.

The design criteria of maximum cell throughput and the desire for reduced transplant graft volume and microgel size both motivate a minimization of empty microgels and maximization of cell loading in each microgel. Increasing the cell concentration in macromer solution exacerbates several challenges that may prevent successful encapsulation. High concentration of hMSCs tend to aggregate in solution, which often results in many empty microgels and a relatively few, large microgels that contain clusters of cells. The tendency of hMSCs to aggregate was be reduced by increasing trypsin exposure from 5 minutes to 10 minutes while harvesting cells, without notable deleterious effects on cell viability. Cells, especially when aggregating, tended to stick in microfluidic channels, forming sieves that prevent successful encapsulation. The addition of 0.1% Pluronic F108 eliminated this problem, along with further reducing cell aggregation.

Cells also tended to settle in microfluidic tubing because their density is higher than a 6.5% PEG-4MAL solution in PBS, which results in increased cell aggregation and many empty microgels. After adding the cytocompatible density gradient media OptiPrep at a 1:4 ratio in cell suspensions, encapsulations up to 30 minutes were completed without noticeable cell settling. These three process improvements enabled microencapsulation of hMSCs with relatively high loading densities, as shown by fluorescent images in

Figure **28**A. In these images, green indicates live cells (stained with Calcein-AM), red indicates dead cells (stained with TOTO-3 iodide), and blue indicates the outline of microgels (obtained using 'Find Edges' in ImageJ). In our hands, maximum cell concentrations for robust encapsulation were determined to be $2x10^7$ cells/mL for 35 μm wide nozzle devices and 10^7 cells/mL for 100 μm wide nozzle devices. Histograms showing the frequency of capsules containing a given number of cells are shown in

Figure 28B, along with the frequencies predicted by the Poisson distribution, using the measured average value as used as expected value. Measured frequencies for number of cells per microgel closely matched those predicted by the Poisson distribution for microencapsulation on both 35 μm and 100 μm wide nozzles, except that approximately two times more empty microgels are produced than expected on 35 μm wide nozzles. Fewer empty microgels are produced when 100 μm wide nozzles are used rather than 35 μm wide nozzles ($p=0.02$,

Figure **28**C), which may lead to more uniform cell spacing in packed microgel arrays.

The diameters of microgels which encapsulate hMSCs were measured from 3 separate parallel microfluidic devices for both 35 μm and 100 μm nozzle widths (Table 2). Cell-laden microgels produced on 100 μm wide nozzles had significantly smaller diameter than cell-free microgels, with a modest decrease in mean diameter of 6.4 μm, or 6.1%. Microgels produced on 35 μm wide nozzles were significantly larger when they contained cells than when no cells were present ($p<0.0001$), with an increase in mean diameter of 11.4 μm, or 18%. Whereas aggregation of cells could explain the larger size of capsules produced on 35 μm wide nozzles, increased polydispersity would be expected if this was the case. Surprisingly, the addition of cells decreased microgel polydispersity when compared to microgels with no cells, as seen by the lower coefficient of variation on 35 μm wide nozzles when cells were present. The presence of cells did not meaningfully impact polydispersity of microgels from 100 μm wide nozzles, although the F-test shows statistically significant differences in variance between cell-laden and cell-free microgels ($p<0.0001$ for both nozzle sizes).

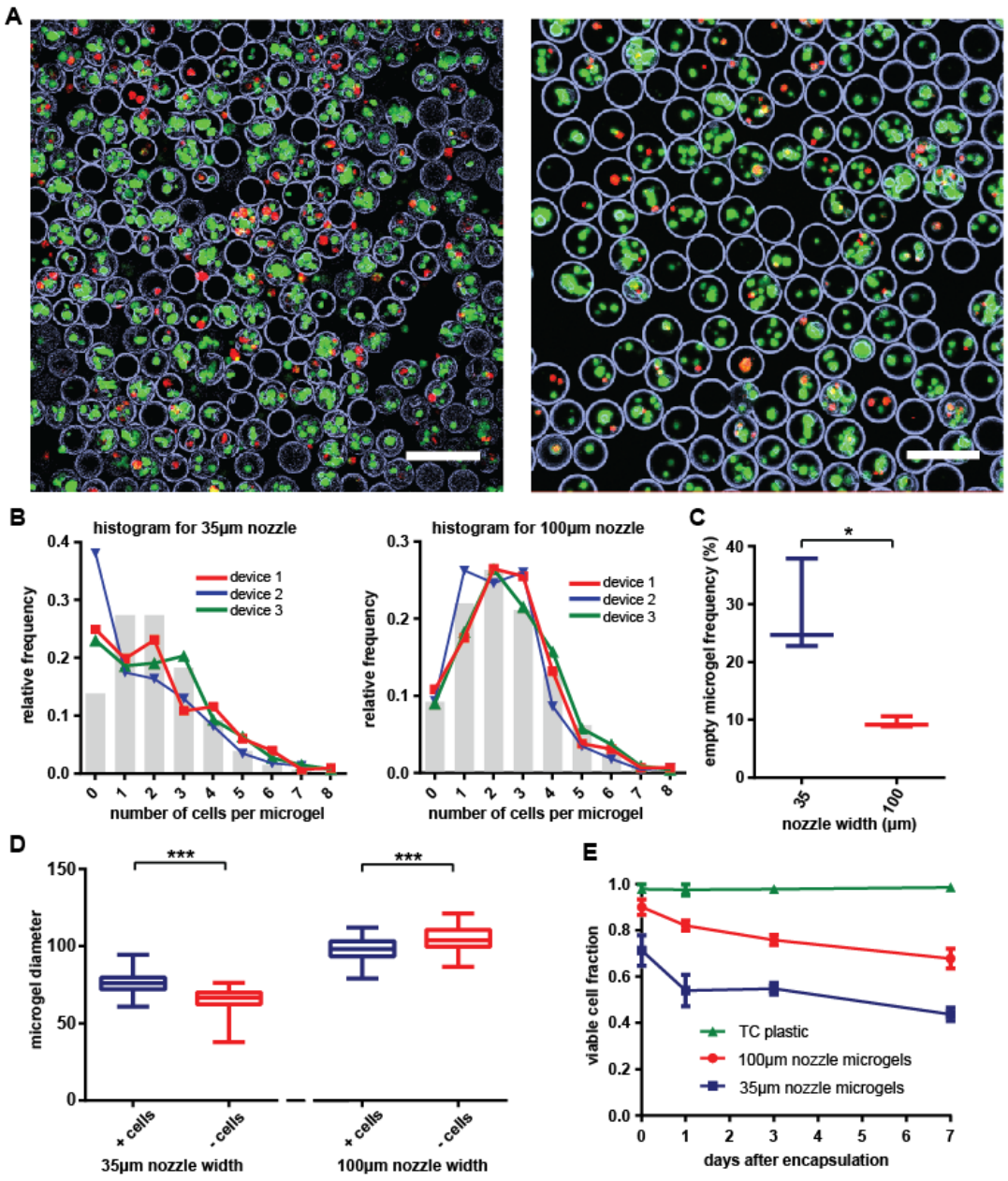

Figure 28. Parallel nozzle microfluidic devices can be used for high throughput encapsulation of hMSCs with high loading density, and resulting microgels support hMSC viability. (A) Representative images are shown for cells microencapsulated on both 35 µm (left) and 100 µm (right) nozzle widths.

Microgels encapsulating hMSCs were functionalized with a fluorescently labelled peptide containing the cell adhesive sequence RGD in order to support cell health and aid microgel visualization (outline of microgels was traced in blue using ImageJ). Live cells were stained with Calcein-AM (green) and dead cells with TOTO-3 iodide (red). (B) The number of cells per microgel was recorded for 3 independent encapsulations for each size nozzle, and their relative frequencies were plotted on histograms, along with the frequencies predicted by the Poisson distribution (grey bars). Number of cells in microgels produced on 100 μm wide nozzles closely matched the frequencies predicted by the Poisson distribution, but microgels produced on 35 μm wide nozzle devices contained more empty microgels than predicted. (C) Microencapsulation on 100 μm wide nozzles produces significantly fewer empty microgels than devices with 35 μm wide nozzles ($p=0.02$). (D) Addition of cells has significant effects on distributions of microgel diameter vs. cell-free microgels for both 35 μm width, where average microgel size increases, and 100 μm width, where average microgel size is decreases ($p<0.0001$ for both widths). (E) Viable cell fraction was determined over time in culture to measure the ability of microgels produced on each nozzle width to support hMSC health. Cells encapsulated on 100 μm wide nozzles had good viability on the day of encapsulation, and microgels reasonably supported their health for 7 days in culture. Cells encapsulated on 35 μm wide nozzles had significantly reduced viability on the day of encapsulation versus cells encapsulated on 100 μm wide nozzles ($p=0.01$), but after this initial loss of

viability, cell viability decreased at similar rates to cells encapsulated on 100 μm wide nozzles.

5.4.4 Microgels support hMSC viability, but the microencapsulation process reduces cell viability in a nozzle size-dependent fashion

Human MSCs were encapsulated in microgels utilizing 3 separate devices in independent encapsulations, for both 35 μm and 100 μm nozzle widths with parallel configurations. These microgels were functionalized with a peptide that contained the cell adhesive sequence RGD to support adhesive signalling of encapsulated cells. On days 0, 1, 3, and 7 after encapsulation, live and dead cells were labelled with Calcein-AM and TOTO-3 iodide, respectively, before being imaged, and viable cell fractions were calculated as the fraction of live cells over the total number of cells counted for each sample (Figure 3E). Cells encapsulated on 100 μm wide nozzles had excellent initial viability of <90% on the day of encapsulation, and viability was remained high (<75%) on day 3 post-encapsulation, indicating that microgels support cell health. In contrast, cells encapsulated on 35 μm wide nozzles average only 71% viability on the day of encapsulation, implicating the smaller dimensions of the device as damaging to cells. This damage could be due to increased probability of cells being exposed to membrane-disrupting mineral oil during encapsulation, which has been shown to decrease encapsulated cell viability [220]. After the initial loss of viability due to encapsulation, cells encapsulated on 35 μm wide nozzles died at about the same rate as cells encapsulated on 100 μm wide devices, showing that microgels of either size support cell survival equally.

5.5 Conclusions

Synthetic hydrogels used to deliver cells *in vivo* can be engineered to provide important biochemical signals to encapsulated cells and host tissue, and tuneable pore size allows for immuno-isolation of encapsulated cells from host tissue. Bulk hydrogel constructs limit mass transport around encapsulated cells and are often prohibitively large when many cells are required. Microencapsulation, or the encapsulation of cells in microgels, can reduce mass transport limitations and large graft sizes associated with bulk encapsulation of cells, and enables injectable delivery of cells within controlled microenvironments. All of these benefits are enhanced as microgel diameter is decreased, but volumetric throughput decreases with the cube of nozzle width, so it can be difficult to encapsulate clinically relevant numbers of cells in very small microgels. The parallel microfluidic device presented here increases microgel throughput 6-fold with minimal change in polydispersity, for faster encapsulation of clinically relevant numbers of cells. Microencapsulation on 35 μm wide nozzle devices can be done at very high cell loading ($2*10^7$ cells/mL), which results in relatively small microgels (76.5 ± 6.6 μm), minimizing graft volume and transport limitations. Unfortunately, encapsulation on 35 μm wide nozzle devices reduced cell viability to ~70%, and even on parallel nozzles, macromer throughput was only 1.2 μL/min – 12% of the 100 μm wide nozzle device throughput. In addition to higher throughput, microencapsulation of hMSCs on 100 μm wide nozzles resulted in excellent viability of <90%. The lower cell densities required to maintain uniform droplet breakup on 100 μm wide

nozzles would result in increased graft volumes, but associated increases in cell viability and throughput may outweigh these concerns. Each nozzle width has been designed prioritizing differently the particular challenges associated with high throughput cell encapsulation in small microgels, but both of these devices utilize similar, novel approaches to solve limited cell throughput. By using high concentration cell suspensions and parallel flow focusing nozzles, clinically relevant cell numbers can be rapidly encapsulated in small microgels.

This work was funded by NIH (R21EB020107) and the Juvenile Diabetes Research Foundation (2-SRA-2014-287-Q-R).

CHAPTER 6: CONCLUSIONS AND FUTURE DIRECTIONS

Mitigating host rejection of transplanted cells without systemic immunosuppression is a major goal of transplant research, and new tools are needed to empower innovative intervention strategies. Biomaterials which microencapsulate therapeutic cells in perm-selective membranes have been utilized for passive immunoprotection. Specifically, pancreatic islets have been encapsulated in alginate-PLL microgels with tightly controlled permeability, and immune rejection of these islets was often reduced. Unlike alginate, some synthetic hydrogels can use click chemistry for facile functionalization with diverse bioactive molecules, including cell adhesive peptides for maintaining encapsulated cell function and immunomodulatory proteins for further mitigating host immune rejection. Unfortunately, the extrusion processing used for alginate microencapsulation is not suited to synthetic microgel production, so new strategies were needed to microencapsulate cells in synthetic hydrogels.

In aim 1, which was published in *Advanced Materials* [146], one such strategy was devised and characterized. A novel microfluidic device that was capable of cell and islet encapsulation in PEG-4MAL microgels was designed and fabricated. The relationship between flow rates and resulting microgel size and polydispersity was investigated. Additionally, the permeability of 5% PEG-

4MAL microgels was characterized, revealing that diffusion of insulin and glucose is relatively unaffected, while diffusion of IgG antibodies is grossly limited. This suggests that PEG-4MAL microgels will act as effective immuno-isolation devices. Finally, human pancreatic islets and mesenchymal stem cells were encapsulated in PEG-4MAL microgels with no major reduction in viability or function, demonstrating the cyto-compatibility of the microencapsulation process. The approaches established in this aim were refined and applied for immunoprotection and immunomodulation of encapsulated islets in rodent models of T1D using two different strategies as presented in aims 2 and 3. In another refinement, novel two-layer microfluidic chips with parallel flow focusing geometry were used to microencapsulate immunomodulatory hMSCs with high throughput, as discussed in chapter 5.

In aim 2, islet microencapsulation in PEG-4MAL hydrogels was optimized, first *in vitro* and later in syngeneic diabetic recipients. First, bulk hydrogel encapsulation was used to determine the best available adhesive peptide sequence for supporting islet function and survey the effects of different crosslinkers on encapsulated islets. Islets encapsulated in RGD functionalized PEG-4MAL containing degradable crosslinks performed the best, but this material would not be suitable for long-term immunoisolation applications. Therefore, nondegradable DTT crosslinked hydrogels were preferred for their stability, since they supported adequate islet function, comparable to alginate. Islets microencapsulated in microgels with optimized hydrogel composition using

microfluidics had only slightly reduced viability compared to unencapsulated control islets, and their glucose responsiveness was not reduced or delayed measurably by microencapsulation. These same nondegradable PEG-4MAL microgels supported function of single-donor islet mass to the EFP of syngeneic diabetic recipients, when delivered within a vasculogenic bulk hydrogel. Restoration of glycemic control in with PEG-4MAL microencapsulated islets was similar to seen with unencapsulated control islets delivered to the EFP in vasculogenic bulk gels, since similar proportions of grafts restored euglycemia at similar rates in both groups, . In contrast, islets microencapsulated in larger, alginate microgels did not restore euglycemia when delivered to the EFP in vasculogenic bulk hydrogels (n=5). The relatively larger size of alginate microgels may provide a large enough diffusional barrier to reduce islet function, possibly inducing hypoxia. Even though PEG-4MAL microencapsulated islets were not directly connected with host circulation as was seen with unencapsulated islets, induced vasculature surrounded microgels, and therefore smaller microgels resulted in less distance between islets and host blood supply. Delivering alginate microencapsulated single donor islet mass IP results in rapid reduction in blood glucose, but gradual loss of islet function is seen by increasing fluctuations in daily blood glucose and eventually by graft failure in some cases. This decline in function could be explained by hypoxia due to poor proximity of islets to host circulation. In this aim, we successfully optimized a hydrogel delivery strategy which minimizes mass transport limitations associated with microencapsulation *in* vivo, by both decreasing microgel size and by inducing

dense vascularization between microgels. This strategy was shown to be effective at maintaining islet function in syngeneic models, and is currently being tested for immuno-isolation potential in allogeneic murine models.

As shown by the results of aim 3, which is in preparation for publication, microgels presenting immunomodulatory SA-FasL conferred graft acceptance to co-transplanted islets in a murine model of T1D. Biotinylated microgels were produced by pre-reacting PEG-4MAL macromer with biotin-PEG-thiol, and these biotinylated microgels were shown to bind and display bioactive SA-FasL in a dose-dependent fashion. SA-FasL is an engineered immunomodulatory protein that has previously been captured on modified cells, resulting in graft acceptance without the need for long term immunosuppression. Likewise, SA-FasL modified microgels transplanted with allogeneic islets under the kidney capsule of diabetic mice resulted in long term (200 day) graft acceptance with only transient (14 day) administration of systemic immunosuppression. This graft acceptance was found to be correlated with an increase in the ratio of Treg:Teff cells in transplanted kidneys, demonstrating active immunomodulation due to SA-FasL presenting microgels. Notably, this immunoprivileged status was localized to the graft, and systemic immune response was not affected by SA-FasL presenting microgels. This approach demonstrates the efficacy of active immunomodulation, which is sufficient to confer graft tolerance, even when no physical barrier is placed between donor islets and host immune system. Because simple mixing of SA-FasL presenting microgels with unmodified donor islets mitigates the host

immune reaction, this approach is amenable to widespread clinical deployment as an off-the-shelf product. Because of the clinical significance of this strategy, along with promising preliminary results in rodents, efficacy of SA-FasL codelivery with allogeneic islets in diabetic nonhuman primates will be evaluated in upcoming studies. If these studies are successful, rapid transition to clinical trials should be undertaken as quickly as possible so that diabetic human patients can benefit. If immunoprotective deficiencies are found in nonhuman primate studies, the approach can be modified in two ways. First, other engineered immunomodulatory proteins chimeric with SA, such as SA-PD-L1, may be more effective at conferring graft acceptance than SA-FasL due to increased immunomodulatory efficacy. Therefore, identification, production, and testing of these immunomodulatory proteins should be a priority. Second, rather than mixing SA-FasL microgels with unmodified islets, islets could be microencapsulated in biotinylated microgels onto which SA-FasL is captured before transplantation. Microencapsulation adds the immunoprotective benefits of permselectivity but would complicate the clinical deployment of resulting interventions.

Chapter 5 presents the design and optimization of a novel two-layer microfluidic device with parallel flow focusing nozzles for high throughput cell encapsulation. This parallel configuration increases the throughput of microgels by 600% without major increases in polydispersity for devices with 35μm or 100μm square nozzles. These devices can both microencapsulate cells in

synthetic microgels under 100μm diameter with uniform size and can be operated with high cell loading density to reduce graft volume and facilitate injection of encapsulated cells. 100μm nozzle microencapsulation results in 90% post-encapsulation viability with hMSCs, and has very high macromer volumetric throughput of 10μL/min. 35μm nozzle microencapsulation results in reduced post-encapsulation viability of 71% with hMSCs and utilizes a reduced macromer volumetric throughput of 1.2μL/min, but the smaller nozzles can make uniform droplets with cell suspensions twice as dense as those used for 100μm nozzle microencapsulation and smaller nozzles produce smaller microgels which may be advantageous for some applications. This technology was developed to encapsulate clinically relevant numbers of MSCs very small microgels which were to be infused into coronary circulation where they would lodge and secrete angiogenic and other pro-healing factors. Dosing studies were performed in pigs to determine how many microgels produced on 35μm nozzles could be infused without reduction in cardiac function (data not shown). However, post-encapsulation viability was poor for these MSCs, so therapeutic efficacy of this approach is doubtful with current encapsulation methods. It is likely that cell viability in microgels produced on 35μm nozzles is reduced due to exposure to membrane-disrupting mineral oil when droplets are being produced. Therefore, one approach to increase viability of microencapsulated cells is to use a cyto-compatible continuous phase, such as a perfluorinated hydrocarbon continuous phase, stabilized with fluorinated surfactants with non-ionic head groups. This approach will not allow for emulsion of aqueous DTT solution, so an alternative

mechanism of crosslinking is required. Photocrosslinkable norbornene-functionalized 4-arm PEG macromers may enable use of cyto-compatible continuous phases without drastic changes to microgel properties. Although viability concerns preclude the use of cells encapsulated on 35μm nozzles with mineral oil for therapeutic applications, microgels containing cells encapsulated on 100μm nozzles are only around 30% larger in diameter than those produced on 35μm nozzles and have good post-encapsulation viability. These cell-laden microgels, which can act as engineered stem cell niches when appropriate cell-instructive cues included, can be injected in minimally invasive transplant procedures. The applications of this technology - including injectable delivery of MSCs for immunomodulation and healing, and mixing of microgels with various payloads in a ‘bottom up’ approach – are numerous, and this powerful tool should be considered when designing cell or protein delivery strategies.

REFERENCES

1. Daneman, D., *Type 1 diabetes.* Lancet, 2006. **367**(9513): p. 847-58.
2. Onkamo, P., et al., *Worldwide increase in incidence of Type I diabetes - the analysis of the data on published incidence trends.* Diabetologia, 1999. **42**(12): p. 1395-1403.
3. Aanstoot, H.J., et al., *The global burden of youth diabetes: perspectives and potential.* Pediatr Diabetes, 2007. **8 Suppl 8**: p. 1-44.
4. Dabelea, D., et al., *Prevalence of type 1 and type 2 diabetes among children and adolescents from 2001 to 2009.* Jama, 2014. **311**(17): p. 1778-86.
5. JDRF. *Type 1 Diabetes Facts*. 2016 [cited 2016 11/15]; Available from: http://www.jdrf.org/about/fact-sheets/type-1-diabetes-facts/.
6. Malik, F.S. and C.E. Taplin, *Insulin Therapy in Children and Adolescents with Type 1 Diabetes.* Paediatr Drugs, 2014.
7. NIDDK. *Pancreatic Islet Transplantation*. [cited 2017 Jan 11]; Available from: https://www.niddk.nih.gov/health-information/diabetes/overview/insulin-medicines-treatments/pancreatic-islet-transplantation.
8. Ryan, E.A., et al., *Clinical outcomes and insulin secretion after islet transplantation with the edmonton protocol.* Diabetes, 2001. **50**(4): p. 710-719.
9. Shapiro, A.M.J., et al., *Islet transplantation in seven patients with type 1 diabetes mellitus using a glucocorticoid-free immunosuppressive regimen.* New England Journal of Medicine, 2000. **343**(4): p. 230-238.
10. Scharp, D.W., et al., *Insulin Independence After Islet Transplantation Into Type I Diabetic Patient.* Diabetes, 1990. **39**(4): p. 515-518.
11. Boggi, U., et al., *Long-term (5 years) efficacy and safety of pancreas transplantation alone in type 1 diabetic patients.* Transplantation, 2012. **93**(8): p. 842-6.
12. Vardanyan, M., et al., *Pancreas vs. islet transplantation: a call on the future.* Curr Opin Organ Transplant, 2010. **15**(1): p. 124-30.
13. Shapiro, A.M.J., et al., *International trial of the edmonton protocol for islet transplantation.* New England Journal of Medicine, 2006. **355**(13): p. 1318-1330.
14. Jaeckel, E. and F. Lehner, *Pancreas and islet transplantation.* Internist, 2009. **50**(5): p. 536-+.
15. Barton, F.B., et al., *Improvement in outcomes of clinical islet transplantation: 1999–2010.* Diabetes care, 2012. **35**(7): p. 1436-1445.
16. Brooks, A., et al., *Attainment of metabolic goals in the integrated UK islet transplant program with locally isolated and transported preparations.* American Journal of Transplantation, 2013. **13**(12): p. 3236-3243.
17. Vantyghem, M.-C., et al., *Primary graft function, metabolic control, and graft survival after islet transplantation.* Diabetes Care, 2009. **32**(8): p. 1473-1478.
18. Lablanche, S., et al., *Five-year metabolic, functional, and safety results of patients with type 1 diabetes transplanted with allogenic islets within the Swiss-French GRAGIL network.* Diabetes Care, 2015. **38**(9): p. 1714-1722.
19. Bellin, M.D., et al., *Potent Induction Immunotherapy Promotes Long-Term Insulin Independence After Islet Transplantation in Type 1 Diabetes.* American Journal of Transplantation, 2012. **12**(6): p. 1576-1583.
20. Amrani, A., et al., *Progression of autoimmune diabetes driven by avidity maturation of a T-cell population.* Nature, 2000. **406**(6797): p. 739-742.

21. Yoon, J.W., H.S. Jun, and P. Santamaria, *Cellular and molecular mechanisms for the initiation and progression of beta cell destruction resulting from the collaboration between macrophages and T cells.* Autoimmunity, 1998. **27**(2): p. 109-22.
22. Lee, K.U., K. Amano, and J.W. Yoon, *Evidence for initial involvement of macrophage in development of insulitis in NOD mice.* Diabetes, 1988. **37**(7): p. 989-91.
23. Katz, J.D., C. Benoist, and D. Mathis, *T helper cell subsets in insulin-dependent diabetes.* Science, 1995. **268**(5214): p. 1185-8.
24. Yoon, J.W. and H.S. Jun, *Cellular and molecular pathogenic mechanisms of insulin-dependent diabetes mellitus.* Ann N Y Acad Sci, 2001. **928**: p. 200-11.
25. Atkinson, M.A. and G.S. Eisenbarth, *Type 1 diabetes: new perspectives on disease pathogenesis and treatment.* Lancet, 2001. **358**(9277): p. 221-9.
26. Nakayama, M., et al., *Prime role for an insulin epitope in the development of type 1 diabetes in NOD mice.* Nature, 2005. **435**(7039): p. 220-3.
27. von Herrath, M., S. Sanda, and K. Herold, *Type 1 diabetes as a relapsing-remitting disease?* Nat Rev Immunol, 2007. **7**(12): p. 988-94.
28. Pearl-Yafe, M., et al., *Pancreatic islets under attack: cellular and molecular effectors.* Curr Pharm Des, 2007. **13**(7): p. 749-60.
29. Finegood, D.T., L. Scaglia, and S. Bonner-Weir, *Dynamics of beta-cell mass in the growing rat pancreas. Estimation with a simple mathematical model.* Diabetes, 1995. **44**(3): p. 249-56.
30. Faustman, D.L., et al., *Prevention of rejection of murine islet allografts by pretreatment with anti-dendritic cell antibody.* Proc Natl Acad Sci U S A, 1984. **81**(12): p. 3864-8.
31. Ionescu-Tirgoviste, C., et al., *A 3D map of the islet routes throughout the healthy human pancreas.* Sci Rep, 2015. **5**: p. 14634.
32. Jansson, L., et al., *Pancreatic islet blood flow and its measurement.* Upsala journal of medical sciences, 2016: p. 1-15.
33. Bonner-Weir, S., *The microvasculature of the pancreas, with emphasis on that of the islets of Langerhans.* The pancreas: biology, pathobiology, and disease. Vay Liang W. Go, editor. Raven Press. New York, New York, USA, 1993: p. 759-768.
34. Jansson, L., *The regulation of pancreatic islet blood flow.* Diabetes/metabolism reviews, 1994. **10**(4): p. 407-416.
35. Henderson, J. and M. Moss, *A morphometric study of the endocrine and exocrine capillaries of the pancreas.* Quarterly Journal of Experimental Physiology, 1985. **70**(3): p. 347-356.
36. Gilon, P. and J.-C. Henquin, *Mechanisms and physiological significance of the cholinergic control of pancreatic β-cell function.* Endocrine reviews, 2001. **22**(5): p. 565-604.
37. Gautam, D., et al., *Role of the M3 muscarinic acetylcholine receptor in β-cell function and glucose homeostasis.* Diabetes, Obesity and Metabolism, 2007. **9**(s2): p. 158-169.
38. Rodriguez-Diaz, R., et al., *Autonomic axons in the human endocrine pancreas show unique innervation patterns.* Cell metabolism, 2011. **14**(1): p. 45.
39. Rodriguez-Diaz, R., et al., *Alpha cells secrete acetylcholine as a non-neuronal paracrine signal priming beta cell function in humans.* Nature medicine, 2011. **17**(7): p. 888-892.
40. Korpos, E., et al., *The peri-islet basement membrane, a barrier to infiltrating leukocytes in type 1 diabetes in mouse and human.* Diabetes, 2013. **62**(2): p. 531-42.
41. Virtanen, I., et al., *Blood vessels of human islets of Langerhans are surrounded by a double basement membrane.* Diabetologia, 2008. **51**(7): p. 1181-91.

42. Irving-Rodgers, H.F., et al., *Molecular composition of the peri-islet basement membrane in NOD mice: a barrier against destructive insulitis.* Diabetologia, 2008. **51**(9): p. 1680-8.
43. Thomas, F.T., et al., *Anoikis, extracellular matrix, and apoptosis factors in isolated cell transplantation.* Surgery, 1999. **126**(2): p. 299-304.
44. Wang, R.N. and L. Rosenberg, *Maintenance of beta-cell function and survival following islet isolation requires re-establishment of the islet-matrix relationship.* Journal of Endocrinology, 1999. **163**(2): p. 181-190.
45. Weber, L.M., et al., *The effects of cell-matrix interactions on encapsulated beta-cell function within hydrogels functionalized with matrix-derived adhesive peptides.* Biomaterials, 2007. **28**(19): p. 3004-3011.
46. Yap, W.T., et al., *Collagen IV-Modified Scaffolds Improve Islet Survival and Function and Reduce Time to Euglycemia.* Tissue engineering. Part A, 2013. **19**(21-22): p. 2361-72.
47. Bruni, A., et al., *Islet cell transplantation for the treatment of type 1 diabetes: recent advances and future challenges.* Diabetes, metabolic syndrome and obesity: targets and therapy, 2014. **7**: p. 211.
48. Bellin, M.D., D.E. Sutherland, and R.P. Robertson, *Pancreatectomy and autologous islet transplantation for painful chronic pancreatitis: indications and outcomes.* Hospital practice, 2012. **40**(3): p. 80-87.
49. Balamurugan, A. and T.L. Pruett, *Trying to Prevent the Clogged Drain: Optimizing the Yield and Function of Portal Vein-Infused Islets.* Digestive diseases and sciences, 2013. **58**(5): p. 1170.
50. Kaufman, D.B., et al., *Effect of 15-deoxyspergualin on immediate function and long-term survival of transplanted islets in murine recipients of a marginal islet mass.* Diabetes, 1994. **43**(6): p. 778-783.
51. Bottino, R., et al., *Transplantation of allogeneic islets of Langerhans in the rat liver: effects of macrophage depletion on graft survival and microenvironment activation.* Diabetes, 1998. **47**(3): p. 316-323.
52. Kenyon, N.S., et al., *Long-term survival and function of intrahepatic islet allografts in baboons treated with humanized anti-CD154.* Diabetes, 1999. **48**(7): p. 1473-1481.
53. Biarnés, M., et al., *β-cell death and mass in syngeneically transplanted islets exposed to short-and long-term hyperglycemia.* Diabetes, 2002. **51**(1): p. 66-72.
54. Johnson, J.D., et al., *Different Effects of FK506, Rapamycin, and Mycophenolate Mofetil on Glucose-Stimulated Insulin Release and Apoptosis in Human Islets.* Cell Transplantation, 2009. **18**(8): p. 833-845.
55. Vaithilingam, V., G. Sundaram, and B.E. Tuch, *Islet cell transplantation.* Current Opinion in Organ Transplantation, 2008. **13**(6): p. 633-638.
56. Lakey, J.R., M. Mirbolooki, and A.M. Shapiro, *Current status of clinical islet cell transplantation.* Methods Mol Biol, 2006. **333**: p. 47-104.
57. Shapiro, A.M.J., *Strategies toward single-donor islets of Langerhans transplantation.* Current Opinion in Organ Transplantation, 2011. **16**(6): p. 627-631.
58. Veriter, S., et al., *Improvement of subcutaneous bioartificial pancreas vascularization and function by coencapsulation of pig islets and mesenchymal stem cells in primates.* Cell Transplant, 2014. **23**(11): p. 1349-64.
59. Kim, M.S., et al., *An in vivo study of the host tissue response to subcutaneous implantation of PLGA-and/or porcine small intestinal submucosa-based scaffolds.* Biomaterials, 2007. **28**(34): p. 5137-5143.

60. Pepper, A.R., et al., *A prevascularized subcutaneous device-less site for islet and cellular transplantation.* Nature biotechnology, 2015.
61. Pileggi, A., et al., *Reversal of diabetes by pancreatic islet transplantation into a subcutaneous, neovascularized device.* Transplantation, 2006. **81**(9): p. 1318-1324.
62. Kemp, C., et al., *Effect of transplantation site on the results of pancreatic islet isografts in diabetic rats.* Diabetologia, 1973. **9**(6): p. 486-491.
63. Phelps, E.A., et al., *Vasculogenic bio-synthetic hydrogel for enhancement of pancreatic islet engraftment and function in type 1 diabetes.* Biomaterials, 2013. **34**(19): p. 4602-4611.
64. Gaber, A.O., et al., *Insulin independence achieved using the transmesenteric approach to the portal vein for islet transplantation.* Transplantation, 2004. **77**(2): p. 309-311.
65. Kin, T., G.S. Korbutt, and R.V. Rajotte, *Survival and metabolic function of syngeneic rat islet grafts transplanted in the omental pouch.* American Journal of Transplantation, 2003. **3**(3): p. 281-285.
66. Yasunami, Y., P.E. Lacy, and E.H. Finke, *A new site for islet transplantation--a peritoneal-omental pouch.* Transplantation, 1983. **36**(2): p. 181-182.
67. Merani, S., et al., *Optimal implantation site for pancreatic islet transplantation.* British Journal of Surgery, 2008. **95**(12): p. 1449-1461.
68. Berman, D.M., et al., *Long-Term Survival of Nonhuman Primate Islets Implanted in an Omental Pouch on a Biodegradable Scaffold.* American Journal of Transplantation, 2009. **9**(1): p. 91-104.
69. Rajab, A., *Islet transplantation: alternative sites.* Current diabetes reports, 2010. **10**(5): p. 332-337.
70. van der Windt, D.J., et al., *The choice of anatomical site for islet transplantation.* Cell transplantation, 2008. **17**(9): p. 1005-1014.
71. Robertson, R.P., *Islet transplantation as a treatment for diabetes—a work in progress.* New England Journal of Medicine, 2004. **350**(7): p. 694-705.
72. Andersson, A., O. Korsgren, and L. Jansson, *Intraportally transplanted pancreatic islets revascularized from hepatic arterial system.* Diabetes, 1989. **38 Suppl 1**: p. 192-5.
73. Hart, T.K. and R.M. Pino, *Pseudoislet vascularization. Induction of diaphragm-fenestrated endothelia from the hepatic sinusoids.* Lab Invest, 1986. **54**(3): p. 304-13.
74. Brissova, M. and A.C. Powers, *Revascularization of transplanted islets: can it be improved?* Diabetes, 2008. **57**(9): p. 2269-71.
75. Carlsson, P.O., et al., *Markedly decreased oxygen tension in transplanted rat pancreatic islets irrespective of the implantation site.* Diabetes, 2001. **50**(3): p. 489-95.
76. Mattsson, G., L. Jansson, and P.O. Carlsson, *Decreased vascular density in mouse pancreatic islets after transplantation.* Diabetes, 2002. **51**(5): p. 1362-6.
77. Barshes, N.R., S. Wyllie, and J.A. Goss, *Inflammation-mediated dysfunction and apoptosis in pancreatic islet transplantation: implications for intrahepatic grafts.* J Leukoc.Biol, 2005. **77**(5): p. 587-597.
78. Emamaullee, J.A. and A.M. Shapiro, *Factors influencing the loss of beta-cell mass in islet transplantation.* Cell Transplant., 2007. **16**(1): p. 1-8.
79. Linn, T., et al., *Ischaemia is linked to inflammation and induction of angiogenesis in pancreatic islets.* Clin.Exp.Immunol., 2006. **144**(2): p. 179-187.
80. Cheng, K., et al., *Adenovirus-based vascular endothelial growth factor gene delivery to human pancreatic islets.* Gene Ther., 2004. **11**(14): p. 1105-1116.

81. Narang, A.S., et al., *Vascular endothelial growth factor gene delivery for revascularization in transplanted human islets.* Pharm Res, 2004. **21**(1): p. 15-25.
82. Sigrist, S., et al., *Influence of VEGF on the viability of encapsulated pancreatic rat islets after transplantation in diabetic mice.* Cell Transplant., 2003. **12**(6): p. 627-635.
83. Zhang, N., et al., *Elevated vascular endothelial growth factor production in islets improves islet graft vascularization.* Diabetes, 2004. **53**(4): p. 963-70.
84. Stendahl, J.C., et al., *Growth factor delivery from self-assembling nanofibers to facilitate islet transplantation.* Transplantation, 2008. **86**(3): p. 478-81.
85. Brady, A.C., et al., *Pro-Angiogenic Hydrogels within Macroporous Scaffolds Enhances Islet Engraftment in an Extrahepatic Site.* Tissue Eng Part A, 2013.
86. Najjar, M., et al., *Fibrin gels engineered with pro-angiogenic growth factors promote engraftment of pancreatic islets in extrahepatic sites in mice.* Biotechnology and bioengineering, 2015. **112**(9): p. 1916-1926.
87. Vos, P.d., et al., *Advances and barriers in mammalian cell encapsulation for treatment of diabetes.* Immunology, Endocrine & Metabolic Agents in Medicinal Chemistry (Formerly Current Medicinal Chemistry-Immunology, Endocrine and Metabolic Agents), 2006. **6**(2): p. 139-153.
88. Lacík, I., *Polymer chemistry in diabetes treatment by encapsulated islets of Langerhans: review to 2006.* Australian journal of chemistry, 2006. **59**(8): p. 508-524.
89. TheraCyte. [cited 2017 Jan 11]; Available from: http://www.theracyte.com/TechnologyProducts.htm.
90. Li, R.H., *Materials for immunoisolated cell transplantation.* Advanced Drug Delivery Reviews, 1998. **33**(1): p. 87-109.
91. Lum, Z.-P., et al., *XENOGRAFTS OF RAT ISLETS INTO DIABETIC MICE: AN EVALUATION OF NEW SMALLER CAPSULES.* Transplantation, 1992. **53**(6): p. 1180-1183.
92. Teramura, Y., Y. Kaneda, and H. Iwata, *Islet-encapsulation in ultra-thin layer-by-layer membranes of poly (vinyl alcohol) anchored to poly (ethylene glycol)–lipids in the cell membrane.* Biomaterials, 2007. **28**(32): p. 4818-4825.
93. Teramura, Y. and H. Iwata, *Bioartificial pancreas: microencapsulation and conformal coating of islet of Langerhans.* Advanced drug delivery reviews, 2010. **62**(7): p. 827-840.
94. Teramura, Y., et al., *Behavior of synthetic polymers immobilized on a cell membrane.* Biomaterials, 2008. **29**(10): p. 1345-1355.
95. Peppas, N.A., et al., *Hydrogels in biology and medicine: from molecular principles to bionanotechnology.* Advanced Materials, 2006. **18**(11): p. 1345-1360.
96. Nicodemus, G.D. and S.J. Bryant, *Cell encapsulation in biodegradable hydrogels for tissue engineering applications.* Tissue Engineering Part B: Reviews, 2008. **14**(2): p. 149-165.
97. Tatarkiewicz, K., et al., *Reversal of hyperglycemia in streptozotocin diabetic mice by xenotransplantation of microencapsulated rat islets.* Annals of transplantation: quarterly of the Polish Transplantation Society, 1996. **2**(2): p. 20-23.
98. Sakai, S., et al., *Development of mammalian cell-enclosing subsieve-size agarose capsules (< 100 μm) for cell therapy.* Biomaterials, 2005. **26**(23): p. 4786-4792.
99. Smidsrød, O. and G. Skja, *Alginate as immobilization matrix for cells.* Trends in biotechnology, 1990. **8**: p. 71-78.
100. Tam, S.K., et al., *Impact of residual contamination on the biofunctional properties of purified alginates used for cell encapsulation.* Biomaterials, 2006. **27**(8): p. 1296-1305.
101. Lim, F. and A.M. Sun, *MICROENCAPSULATED ISLETS AS BIOARTIFICIAL ENDOCRINE PANCREAS.* Science, 1980. **210**(4472): p. 908-910.

102. HUNKELER, #160, and D., *Polymers for bioartificial organs*. Vol. 5. 1997, Cambridge, ROYAUME-UNI: Elsevier.
103. Strand, B.L., et al., *Poly-L-lysine induces fibrosis on alginate microcapsules via the induction of cytokines.* Cell transplantation, 2001. **10**(3): p. 263-275.
104. Vegas, A.J., et al., *Long-term glycemic control using polymer-encapsulated human stem cell-derived beta cells in immune-competent mice.* Nat Med, 2016. **22**(3): p. 306-311.
105. Vegas, A.J., et al., *Combinatorial hydrogel library enables identification of materials that mitigate the foreign body response in primates.* Nat Biotech, 2016. **34**(3): p. 345-352.
106. Zhu, J. and R.E. Marchant, *Design properties of hydrogel tissue-engineering scaffolds.* Expert Rev Med Devices, 2011. **8**(5): p. 607-26.
107. Rizzi, S.C., et al., *Recombinant protein-co-PEG networks as cell-adhesive and proteolytically degradable hydrogel matrixes. Part II: biofunctional characteristics.* Biomacromolecules, 2006. **7**(11): p. 3019-29.
108. Rizzi, S.C. and J.A. Hubbell, *Recombinant protein-co-PEG networks as cell-adhesive and proteolytically degradable hydrogel matrixes. Part I: Development and physicochemical characteristics.* Biomacromolecules, 2005. **6**(3): p. 1226-38.
109. Metters, A. and J. Hubbell, *Network formation and degradation behavior of hydrogels formed by Michael-type addition reactions.* Biomacromolecules, 2005. **6**(1): p. 290-301.
110. Lutolf, M.P. and J.A. Hubbell, *Synthesis and physicochemical characterization of end-linked poly(ethylene glycol)-co-peptide hydrogels formed by Michael-type addition.* Biomacromolecules, 2003. **4**(3): p. 713-22.
111. Hiemstra, C., et al., *Rapidly in situ-forming degradable hydrogels from dextran thiols through Michael addition.* Biomacromolecules, 2007. **8**(5): p. 1548-56.
112. Alge, D.L., et al., *Synthetically tractable click hydrogels for three-dimensional cell culture formed using tetrazine-norbornene chemistry.* Biomacromolecules, 2013. **14**(4): p. 949-53.
113. Phelps, E.A., et al., *Maleimide Cross-Linked Bioactive PEG Hydrogel Exhibits Improved Reaction Kinetics and Cross-Linking for Cell Encapsulation and In Situ Delivery.* Advanced Materials, 2012. **24**(1): p. 64-+.
114. Lin, C.C. and K.S. Anseth, *Cell-cell communication mimicry with poly(ethylene glycol) hydrogels for enhancing beta-cell function.* Proceedings of the National Academy of Sciences of the United States of America, 2011. **108**(16): p. 6380-6385.
115. Raeber, G., M. Lutolf, and J. Hubbell, *Molecularly engineered PEG hydrogels: a novel model system for proteolytically mediated cell migration.* Biophysical journal, 2005. **89**(2): p. 1374-1388.
116. Patterson, J. and J.A. Hubbell, *Enhanced proteolytic degradation of molecularly engineered PEG hydrogels in response to MMP-1 and MMP-2.* Biomaterials, 2010. **31**(30): p. 7836-7845.
117. Zhao, C.X., *Multiphase flow microfluidics for the production of single or multiple emulsions for drug delivery.* Advanced Drug Delivery Reviews, 2013. **65**(11-12): p. 1420-1446.
118. Chu, L.Y., et al., *Controllable monodisperse multiple emulsions.* Angewandte Chemie International Edition, 2007. **46**(47): p. 8970-8974.
119. Shui, L., J.C. Eijkel, and A. van den Berg, *Multiphase flow in microfluidic systems–Control and applications of droplets and interfaces.* Advances in colloid and interface science, 2007. **133**(1): p. 35-49.

120. Sakai, S., et al., *Biocompatibility of subsieve-size capsules versus conventional-size microcapsules.* Journal of Biomedical Materials Research Part A, 2006. **78**(2): p. 394-398.
121. Zhang, H., et al., *Microfluidic production of biopolymer microcapsules with controlled morphology.* J Am Chem Soc, 2006. **128**(37): p. 12205-10.
122. Panda, P., et al., *Stop-flow lithography to generate cell-laden microgel particles.* Lab Chip, 2008. **8**(7): p. 1056-61.
123. Shepherd, R.F., et al., *Microfluidic Assembly of Homogeneous and Janus Colloid-Filled Hydrogel Granules.* Langmuir, 2006. **22**(21): p. 8618-8622.
124. Kim, J.-W., et al., *Fabrication of Monodisperse Gel Shells and Functional Microgels in Microfluidic Devices.* Angewandte Chemie International Edition, 2007. **46**(11): p. 1819-1822.
125. De Geest, B.G., et al., *Synthesis of Monodisperse Biodegradable Microgels in Microfluidic Devices.* Langmuir, 2005. **21**(23): p. 10275-10279.
126. Sugiura, S., et al., *Size control of calcium alginate beads containing living cells using micro-nozzle array.* Biomaterials, 2005. **26**(16): p. 3327-3331.
127. Gugerli, R., et al., *Quantitative study of the production and properties of alginate/poly-L-lysine microcapsules.* Journal of microencapsulation, 2002. **19**(5): p. 571-590.
128. Cobbold, S.P. and H. Waldmann, *Regulatory cells and transplantation tolerance.* Cold Spring Harbor perspectives in medicine, 2013. **3**(6): p. a015545.
129. Kendal, A.R., et al., *Sustained suppression by Foxp3+ regulatory T cells is vital for infectious transplantation tolerance.* J Exp Med, 2011. **208**(10): p. 2043-53.
130. Mundra, V., I.C. Gerling, and R.I. Mahato, *Mesenchymal Stem Cell-Based Therapy.* Molecular Pharmaceutics, 2013. **10**(1): p. 77-89.
131. Bartholomew, A., et al., *Mesenchymal stem cells suppress lymphocyte proliferation in vitro and prolong skin graft survival in vivo.* Experimental hematology, 2002. **30**(1): p. 42-48.
132. Uccelli, A., L. Moretta, and V. Pistoia, *Mesenchymal stem cells in health and disease.* Nature Reviews Immunology, 2008. **8**(9): p. 726-736.
133. Prevosto, C., et al., *Generation of CD4+ or CD8+ regulatory T cells upon mesenchymal stem cell-lymphocyte interaction.* Haematologica, 2007. **92**(7): p. 881-8.
134. Beyth, S., et al., *Human mesenchymal stem cells alter antigen-presenting cell maturation and induce T-cell unresponsiveness.* Blood, 2005. **105**(5): p. 2214-9.
135. Aggarwal, S. and M.F. Pittenger, *Human mesenchymal stem cells modulate allogeneic immune cell responses.* Blood, 2005. **105**(4): p. 1815-22.
136. Corcione, A., et al., *Human mesenchymal stem cells modulate B-cell functions.* Blood, 2006. **107**(1): p. 367-72.
137. Berman, D.M., et al., *Mesenchymal stem cells enhance allogeneic islet engraftment in nonhuman primates.* Diabetes, 2010. **59**(10): p. 2558-68.
138. Peng, Y., et al., *TGF-β regulates in vivo expansion of Foxp3-expressing CD4+ CD25+ regulatory T cells responsible for protection against diabetes.* Proceedings of the National Academy of Sciences of the United States of America, 2004. **101**(13): p. 4572-4577.
139. Hughes, P.D., et al., *Apoptosis regulators Fas and Bim cooperate in shutdown of chronic immune responses and prevention of autoimmunity.* Immunity, 2008. **28**(2): p. 197-205.
140. Strasser, A., P.J. Jost, and S. Nagata, *The many roles of FAS receptor signaling in the immune system.* Immunity, 2009. **30**(2): p. 180-192.

141. Min, W.-P., et al., *Dendritic cells genetically engineered to express Fas ligand induce donor-specific hyporesponsiveness and prolong allograft survival.* The Journal of Immunology, 2000. **164**(1): p. 161-167.
142. Swenson, K.M., et al., *Fas ligand gene transfer to renal allografts in rats: effects on allograft survival.* Transplantation, 1998. **65**(2): p. 155-60.
143. Phelps, E.A., et al., *Maleimide cross-linked bioactive PEG hydrogel exhibits improved reaction kinetics and cross-linking for cell encapsulation and in situ delivery.* Adv Mater, 2012. **24**(1): p. 64-70, 2.
144. Salimath, A.S., et al., *Dual delivery of hepatocyte and vascular endothelial growth factors via a protease-degradable hydrogel improves cardiac function in rats.* PLoS One, 2012. **7**(11): p. e50980.
145. Phelps, E.A., et al., *Bioartificial matrices for therapeutic vascularization.* Proc Natl Acad Sci U S A, 2010. **107**(8): p. 3323-8.
146. Headen, D.M., et al., *Microfluidic-Based Generation of Size-Controlled, Biofunctionalized Synthetic Polymer Microgels for Cell Encapsulation.* Advanced Materials, 2014. **26**(19): p. 3003-3008.
147. Wang, T., et al., *An encapsulation system for the immunoisolation of pancreatic islets.* Nature Biotechnology, 1997. **15**(4): p. 358-362.
148. Santos, E., et al., *Therapeutic cell encapsulation: Ten steps towards clinical translation.* Journal of Controlled Release, 2013. **170**(1): p. 1-14.
149. Lutolf, M.P. and J.A. Hubbell, *Synthetic biomaterials as instructive extracellular microenvironments for morphogenesis in tissue engineering.* Nat Biotechnol, 2005. **23**(1): p. 47-55.
150. Peppas, N.A. and R. Langer, *NEW CHALLENGES IN BIOMATERIALS.* Science, 1994. **263**(5154): p. 1715-1720.
151. Langer, R. and D.A. Tirrell, *Designing materials for biology and medicine.* Nature, 2004. **428**(6982): p. 487-492.
152. Onoe, H., et al., *Metre-long cell-laden microfibres exhibit tissue morphologies and functions.* Nature Materials, 2013. **12**(6): p. 584-590.
153. Jun, Y., et al., *Microfluidics-generated pancreatic islet microfibers for enhanced immunoprotection.* Biomaterials, 2013. **34**(33): p. 8122-30.
154. Goosen, M.F.A., et al., *Electrostatic droplet generation for encapsulation of somatic tissue: Assessment of high-voltage power supply.* Biotechnology Progress, 1997. **13**(4): p. 497-502.
155. Choi, C.-H., et al., *Generation of monodisperse alginate microbeads and in situ encapsulation of cell in microfluidic device.* Biomedical Microdevices, 2007. **9**(6): p. 855-862.
156. Tan, W.H. and S. Takeuchi, *Monodisperse Alginate Hydrogel Microbeads for Cell Encapsulation.* Advanced Materials, 2007. **19**(18): p. 2696-2701.
157. Um, E., et al., *Continuous generation of hydrogel beads and encapsulation of biological materials using a microfluidic droplet-merging channel.* Microfluidics and Nanofluidics, 2008. **5**(4): p. 541-549.
158. Rossow, T., et al., *Controlled Synthesis of Cell-Laden Microgels by Radical-Free Gelation in Droplet Microfluidics.* Journal of the American Chemical Society, 2012. **134**(10): p. 4983-4989.
159. Velasco, D., E. Tumarkin, and E. Kumacheva, *Microfluidic Encapsulation of Cells in Polymer Microgels.* Small, 2012. **8**(11): p. 1633-1642.

160. Allazetta, S., T.C. Hausherr, and M.P. Lutolf, *Microfluidic synthesis of cell-type-specific artificial extracellular matrix hydrogels.* Biomacromolecules, 2013. **14**(4): p. 1122-31.
161. Chung, S.E., et al., *Optofluidic maskless lithography system for real-time synthesis of photopolymerized microstructures in microfluidic channels.* Applied Physics Letters, 2007. **91**(4): p. 041106.
162. Thorsen, T., et al., *Dynamic pattern formation in a vesicle-generating microfluidic device.* Phys Rev Lett, 2001. **86**(18): p. 4163-6.
163. Anna, S.L., N. Bontoux, and H.A. Stone, *Formation of dispersions using ``flow focusing'' in microchannels.* Applied Physics Letters, 2003. **82**(3): p. 364-366.
164. Wan, J., et al., *Microfluidic Generation of Droplets with a High Loading of Nanoparticles.* Langmuir, 2012. **28**(37): p. 13143-13148.
165. Koster, S., et al., *Drop-based microfluidic devices for encapsulation of single cells.* Lab Chip, 2008. **8**(7): p. 1110-5.
166. Kesselman, L.R.B., et al., *Synthesis of Monodisperse, Covalently Cross-Linked, Degradable "Smart" Microgels Using Microfluidics.* Small, 2012. **8**(7): p. 1092-1098.
167. Tumarkin, E. and E. Kumacheva, *Microfluidic generation of microgels from synthetic and natural polymers.* Chemical Society Reviews, 2009. **38**(8): p. 2161-2168.
168. Blasi, P., et al., *Conformal polymer coatings for pancreatic islets transplantation.* International Journal of Pharmaceutics, 2013. **440**(2): p. 141-147.
169. Teramura, Y., et al., *Microencapsulation of cells, including islets, within stable ultra-thin membranes of maleimide-conjugated PEG-lipid with multifunctional crosslinkers.* Biomaterials, 2013. **34**(11): p. 2683-2693.
170. Ranganath, Sudhir H., et al., *Harnessing the Mesenchymal Stem Cell Secretome for the Treatment of Cardiovascular Disease.* Cell Stem Cell, 2012. **10**(3): p. 244-258.
171. Lutolf, M.P., P.M. Gilbert, and H.M. Blau, *Designing materials to direct stem-cell fate.* Nature, 2009. **462**(7272): p. 433-441.
172. Lienemann, P.S., et al., *A Versatile Approach to Engineering Biomolecule-Presenting Cellular Microenvironments.* Advanced Healthcare Materials, 2013. **2**(2): p. 292-296.
173. Nakayama, M., et al., *Priming and effector dependence on insulin B : 9-23 peptide in NOD islet autoimmunity.* Journal of Clinical Investigation, 2007. **117**(7): p. 1835-1843.
174. Roep, B.O., et al., *T-cell clones from a type-1 diabetes patient respond to insulin secretory granule proteins.* Nature, 1990. **345**(6276): p. 632-634.
175. Yoon, J.W., et al., *Control of autoimmune diabetes in NOD mice by CAD expression or suppression in beta cells.* Science, 1999. **284**(5417): p. 1183-1187.
176. Alejandro, R., et al., *Long-term function (6 years) of islet allografts in type 1 diabetes.* Diabetes, 1997. **46**(12): p. 1983-1989.
177. Radu, R.G., et al., *Tacrolimus suppresses glucose-induced insulin release from pancreatic islets by reducing glucokinase activity.* American Journal of Physiology-Endocrinology and Metabolism, 2005. **288**(2): p. E365-E371.
178. Hernandez-Fisac, I., et al., *Tacrolimus-induced diabetes in rats courses with suppressed insulin gene expression in pancreatic islets.* American Journal of Transplantation, 2007. **7**(11): p. 2455-2462.
179. Haskins, K. and M. McDuffie, *Acceleration of diabetes in young NOD mice with a CD4+ islet-specific T-cell clone.* Science, 1990. **249**(4975): p. 1433-1436.
180. Roep, B.O., et al., *Auto- and alloimmune reactivity to human islet allografts transplanted into type 1 diabetic patients.* Diabetes, 1999. **48**(3): p. 484-490.

181. Yolcu, E.S., et al., *Apoptosis as a mechanism of T-regulatory cell homeostasis and suppression.* Immunology and Cell Biology, 2008. **86**(8): p. 650-658.
182. Ju, S.T., et al., *Fas(CD95) FasL interactions required for programmed cell-death after T-cell activation.* Nature, 1995. **373**(6513): p. 444-448.
183. Brunner, T., et al., *Cell-autonomous Fas (CD95) Fas-ligand interaction mediates activation-induced apoptosis in T-cell hybridomas.* Nature, 1995. **373**(6513): p. 441-444.
184. Arai, H., et al., *Inhibition of the alloantibody response by CD95 ligand.* Nature Medicine, 1997. **3**(8): p. 843-848.
185. Lau, H.T., et al., *Prevention of islet allograft rejection with engineered myoblasts expressing FasL in mice.* Science, 1996. **273**(5271): p. 109-112.
186. Matsue, H., et al., *Induction of antigen-specific immunosuppression by CD95L cDNA-transfected 'killer' dendritic cells.* Nature Medicine, 1999. **5**(8): p. 930-937.
187. Min, W.P., et al., *Dendritic cells genetically engineered to express Fas ligand induce donor-specific hyporesponsiveness and prolong allograft survival.* Journal of Immunology, 2000. **164**(1): p. 161-167.
188. Tourneur, U., et al., *Transgenic expression of CD95 ligand on thyroid follicular cells confers immune privilege upon thyroid allografts.* Journal of Immunology, 2001. **167**(3): p. 1338-1346.
189. LA, O.R., et al., *Membrane-bound Fas ligand only is essential for Fas-induced apoptosis.* Nature, 2009. **461**(7264): p. 659-63.
190. Ottonello, L., et al., *Soluble Fas ligand is chemotactic for human neutrophilic polymorphonuclear leukocytes.* Journal of Immunology, 1999. **162**(6): p. 3601-3606.
191. Yolcu, E.S., et al., *Cell membrane modification for rapid display of proteins as a novel means of immunomodulation: FasL-decorated cells prevent islet graft rejection.* Immunity, 2002. **17**(6): p. 795-808.
192. Yolcu, E.S., et al., *Pancreatic islets engineered with SA-FasL protein establish robust localized tolerance by inducing regulatory T cells in mice.* J Immunol, 2011. **187**(11): p. 5901-9.
193. Lau, H.T., et al., *Prevention of islet allograft rejection with engineered myoblasts expressing FasL in mice.* Science, 1996. **273**: p. 109-112.
194. Bunnag, S., et al., *FOXP3 expression in human kidney transplant biopsies is associated with rejection and time post transplant but not with favorable outcomes.* Am J Transplant, 2008. **8**(7): p. 1423-33.
195. Yapici, U., et al., *Intragraft FOXP3 protein or mRNA during acute renal allograft rejection correlates with inflammation, fibrosis, and poor renal outcome.* Transplantation, 2009. **87**(9): p. 1377-80.
196. Stuart, P.M., et al., *CD95 ligand (FasL)-induced apoptosis is necessary for corneal allograft survival.* J Clin Invest, 1997. **99**(3): p. 396-402.
197. Griffith, T.S., et al., *Fas ligand-induced apoptosis as a mechanism of immune privilege.* Science, 1995. **270**(5239): p. 1189-1192.
198. Takeda, Y., et al., *Protection of islet allografts transplanted together with Fas ligand expressing testicular allografts.* Diabetologia, 1998. **41**(3): p. 315-21.
199. Yolcu, E.S., et al., *Pancreatic Islets Engineered with SA-FasL Protein Establish Robust Localized Tolerance by Inducing Regulatory T Cells in Mice.* Journal of Immunology, 2011. **187**(11): p. 5901-5909.
200. Kang, S.M., et al., *Fas ligand expression in islets of Langerhans does not confer immune privilege and instead targets them for rapid destruction.* Nat Med, 1997. **3**(7): p. 738-43.

201. Ogasawara, J., et al., *Lethal effect of the anti-Fas antibody in mice.* Nature, 1993. **364**(6440): p. 806-9.
202. Liu, A.L. and A.J. Garcia, *Methods for Generating Hydrogel Particles for Protein Delivery.* Ann Biomed Eng, 2016. **44**(6): p. 1946-58.
203. Foster, G.A., et al., *Protease-degradable microgels for protein delivery for vascularization.* Biomaterials, 2017. **113**: p. 170-175.
204. Johnson, A.S., et al., *Quantitative Assessment of Islets of Langerhans Encapsulated in Alginate.* Tissue Engineering Part C-Methods, 2011. **17**(4): p. 435-449.
205. Williams, C.G., et al., *Variable cytocompatibility of six cell lines with photoinitiators used for polymerizing hydrogels and cell encapsulation.* Biomaterials, 2005. **26**(11): p. 1211-1218.
206. Allazetta, S., T.C. Hausherr, and M.P. Lutolf, *Microfluidic Synthesis of Cell-Type-Specific Artificial Extracellular Matrix Hydrogels.* Biomacromolecules, 2013. **14**(4): p. 1122-1131.
207. Griffin, D.R., et al., *Accelerated wound healing by injectable microporous gel scaffolds assembled from annealed building blocks.* Nat Mater, 2015. **14**(7): p. 737-44.
208. Allazetta, S., et al., *Cell-Instructive Microgels with Tailor-Made Physicochemical Properties.* Small, 2015. **11**(42): p. 5647-5656.
209. Siltanen, C., et al., *Microfluidic fabrication of bioactive microgels for rapid formation and enhanced differentiation of stem cell spheroids.* Acta Biomaterialia, 2016. **34**: p. 125-132.
210. Anna, S.L., N. Bontoux, and H.A. Stone, *Formation of dispersions using "flow focusing" in microchannels.* Applied Physics Letters, 2003. **82**(3): p. 364-366.
211. Mao, A.S., et al., *Deterministic encapsulation of single cells in thin tunable microgels for niche modelling and therapeutic delivery.* Nat Mater, 2016. **advance online publication**.
212. Tetradis-Meris, G., et al., *Novel Parallel Integration of Microfluidic Device Network for Emulsion Formation.* Industrial & Engineering Chemistry Research, 2009. **48**(19): p. 8881-8889.
213. Bardin, D., et al., *Parallel generation of uniform fine droplets at hundreds of kilohertz in a flow-focusing module.* Biomicrofluidics, 2013. **7**(3): p. 13.
214. Jeong, H.-H., et al., *Kilo-scale droplet generation in three-dimensional monolithic elastomer device (3D MED).* Lab on a Chip, 2015. **15**(23): p. 4387-4392.
215. Mulligan, M.K. and J.P. Rothstein, *Scale-up and control of droplet production in coupled microfluidic flow-focusing geometries.* Microfluidics and Nanofluidics, 2012. **13**(1): p. 65-73.
216. Muluneh, M. and D. Issadore, *Hybrid soft-lithography/laser machined microchips for the parallel generation of droplets.* Lab on a Chip, 2013. **13**(24): p. 4750-4754.
217. Li, W., et al., *Multiple modular microfluidic (M 3) reactors for the synthesis of polymer particles.* Lab on a Chip, 2009. **9**(18): p. 2715-2721.
218. Kim, S.H., et al., *Enhanced-throughput production of polymersomes using a parallelized capillary microfluidic device.* Microfluidics and Nanofluidics, 2013. **14**(3-4): p. 509-514.
219. Romanowsky, M.B., et al., *High throughput production of single core double emulsions in a parallelized microfluidic device.* Lab on a Chip, 2012. **12**(4): p. 802-807.
220. Kim, S., J. Oh, and C. Cha, *Enhancing the biocompatibility of microfluidics-assisted fabrication of cell-laden microgels with channel geometry.* Colloids and Surfaces B: Biointerfaces, 2016. **147**: p. 1-8.